

Onon Otgonzul, M.Sc.

**BIOACTIVE POLYMERIC SYSTEMS**  
**FOR FOOD AND MEDICAL PACKAGING APPLICATIONS**

DOCTORAL THESIS

Program: P2901 Chemistry and food technology

Course: 2901V013 Food technology

Supervisor: Prof. Ing. Petr Sáha, CSc.

Consultant: Ing. Vladimír Sedlařík, Ph.D.

Zlín, Czech Republic-2010

<b>ACKNOWLEDGEMENTS</b>	3
<b>ABSTRACT</b>	4
<b>ABSTRAKT</b>	5
<b>Table of Contents</b>	
<b>INTRODUCTION</b>	6
<b>1. THEORITICAL PART:</b>	8
<b>1.1 BIOACTIVE POLYMER SYSTEMS</b>	8
1.1.1 Food and pharmaceutical packaging	8
1.1.2 Introduction to bioactive polymer systems	11
1.1.3 Non-migratory bioactive polymer systems	12
1.1.4 Migratory bioactive polymer systems	16
1.1.5 Biodegradable polymer systems	21
1.1.6 Bioactive agents	26
1.1.7 Applications of bioactive polymer systems	30
<b>1.2 POLYMER BLEND</b>	33
1.2.1 Introduction to polymer blend	33
1.2.2 Compatibilization of polymer blend	39
1.2.3 Controlled morphology	42
<b>AIMS OF WORK</b>	47
<b>2. EXPERIMENTAL PART:</b>	49
<b>2.1 MATERIALS AND SAMPLE PREPARATION</b>	49
<b>2.2 CHARACTERIZATION METHODS</b>	53
Microscopic analysis	53
Mechanical test	54
Thermal analysis	56
Spectroscopic analysis	58
Rheological analysis	59
Release testing	59
Water uptake testing	60
<b>3. RESULTS AND DISCUSSIONS:</b>	61
3.1 Correlation of morphology and viscoelastic properties of the PA6/BioFlex polymeric blends in molten state	61
3.2 The effect of morphological organization on mechanical and thermal properties of the PA6/BioFlex polymeric blends	84
3.3 Time dependent release of model bioactive component from the PA6/BioFlex polymeric blends with various morphology. Effect of bioactive agent into the polymer blends	101
<b>CONCLUSIONS</b>	109
<b>CONTRIBUTIONS TO SCIENCE AND PRACTICE</b>	113
<b>REFERENCES</b>	114
<b>LIST OF FIGURES</b>	124
<b>LIST OF TABLES</b>	125
<b>LIST OF ABBREVIATIONS</b>	127
<b>CURRICULUM VITAE</b>	128

## **ACKNOWLEDGEMENTS**

I would like to thank all people who helped this thesis is possible.

First of all, I would like to express my sincere gratitude to my supervisor Prof. Petr Sába, for giving me the opportunity to join Polymer Centre, and for creating very good conditions for my research activities.

I am deeply grateful to my consultant, Dr. Vladimír Sedlařík, who guided me through my studies with kindness and huge encouragement.

My special thanks belong to staff of Polymer Centre and University Institute for friendly working environment.

Apart from my colleagues and friends, I owe my deepest gratitude to my whole family for their unconditional love and support.

## **ABSTRACT**

The presented work summarizes the current state of the art in the field of bioactive polymer packaging technology and polymer blending and the already reported knowledge is applied on the developed system based on polyamide 6 and biodegradable co-polyester of polylactide (BioFlex). The main attention is paid to the detailed description of co-continuity formation phenomenon and its occurrence prediction. Moreover, the correlations between morphological arrangement and material properties such as mechanical, rheological, thermal and structural properties are the subsequent goals of this PhD work. To verify the hypothesis of co-continuous morphologies capability to be used in bioactive packaging the time dependent release of model component from the blends having various morphologies is the object the detailed investigation to complete the assignment of this thesis, finally. The release studies were done by using a bioactive model compound (crystal violet), which was incorporated into a polymer blend. The release kinetic profile into various liquid media was observed in dependence on morphology of the polymer blends.

**Keywords:** bioactive packaging, polymer blends, co-continuous morphology, polyamide, polylactide acid co-polyester

## ABSTRAKT

Předkládaná práce poskytuje komplexní shrnutí dosavadního stavu poznání v oblasti bioaktivních polymerních obalových materiálů a polymerních směsí. Tento přehled doposud známých skutečností byl aplikován na konkrétní binární polymerní systém na bázi polyamid 6 – BioFlex (biorozložitelný kopolyester na bázi polymeru kyseliny mléčné). Hlavní pozornost je věnována popisu fenoménu tvorby takzvané ko-kontinuální struktury a její korelaci s experimentálními daty získanými pomocí sledování mechanických, reologických, termálních a strukturních vlastností a semi-empirickými modely vyvinutými za účelem předpovědi její přítomnosti v daném systému. Za účelem ověření hypotézy použitelnosti systémů s ko-kontinuální morfologií pro bioaktivní obaly byly připraveny směsi obsahující modelovou bioaktivní sloučeninu – krystalovou violet'. Kinetika uvolňování této látky ze systémů vyznačujících se rozdílnou morfologií byla sledována a porovnávána v různých kapalných médiích.

**Klíčová slova:** bioaktivní obaly, polymerní směsi, ko-kontinuální morfologie, polyamid, kopolyester polylaktidu

## **Introduction**

For a long time, food and pharmaceutical packaging has been used in order to protect the quality, freshness and safety of food and pharmaceuticals. The main goal of the food and pharmaceutical packaging is to store products in a cost-effective way that is suitable for both industry requirements and consumer desires, maintains safety and possibly minimizes the environmental impact. The type of material used in packaging is important. A correct selection of packaging material can support the quality and shelf life of a product. Traditionally, glass, metals (aluminium foils and laminates, tinplate and tin-free steel), paper and paperboards and plastics are applied. Moreover, these materials, especially plastics are modified and designed for the advanced properties such as antimicrobial, antioxidant releasing packaging, moisture and gas control packaging as well as controlled drug delivery [1].

Generally, foods and pharmaceuticals are sensitive and their shelf life is limited by the interactions of intrinsic factors such as water activity, pH, added preservatives and extrinsic factors including temperature, relative humidity, light and gas composition [2]. One of the major possibilities to extend the shelf life of products is to develop packaging material with specific properties. It can be called bioactive packaging materials and can be used to improve the quality and to extend the shelf life. In food packaging, the goal is to use bioactive materials to get desirable response, for example the inhibition of microbial growth, adjusting barrier materials, indicating and sensing materials as well as flavour maintenance and enhancing materials [3]. Furthermore, bioactive polymers may help to support the consumers' health due to its unique role of enhancing the food impact [4].

Bioactive polymer materials can be formed by direct incorporation of bioactive agent into a polymer matrix, immobilization and coating techniques.

For the application, modern packaging techniques can be applied including active, intelligent or smart, bioactive and green packaging.

In order to create an ideal bioactive polymer system, the one of the possibilities is to obtain partially biodegradable polymer blends with improved mechanical properties in which bioactive agents can be incorporated into its biodegradable phase for the purpose of releasing bioactive agents concomitantly with biodegradation. In addition, the blending of different polymers is an attractive way of adding new properties to a product. By controlling the blend morphology during processing, it is possible to impart unique properties to the mixture [1].

# **1. THEORITICAL PART**

## **1.1 BIOACTIVE POLYMER SYSTEMS**

### **1.1.1 Food and pharmaceutical packaging**

Packaging is the most important process aimed at providing stable quality of food and pharmaceutical products for their storage, transportation, distribution and end-use. The basic functions of packaging are protection from mechanical damage and prevention or inhibition of chemical changes, biochemical changes and microbiological spoilage. Moreover, packaging plays number of significant roles: to give information about products, to present material type, shape, size and colour as well as suitability [1].

The quality of the packaged product is a combination of attributes which is highly appreciated by consumers. The quality factors such as appearance (freshness, colour and defects), texture (crispness, toughness and tissue integrity), flavour (taste and smell), nutritive value (vitamins, minerals and dietary fibers), and safety (no microbial contamination) of the packed food and pharmaceuticals mostly caused by mass transfer phenomena such as moisture absorption, oxygen invasion, flavour loss, undesirable odour absorption, and the migration from packaging into products [5].

The shelf-life is the time during which the food product will remain safe, retain desired sensory properties, chemical, physical and microbiological characteristics as well as comply with any label declaration of nutritional data, when stored under the recommended condition [6]. The shelf-life is influenced by various factors, i.e. intrinsic (water activity, pH value, redox potential, available oxygen, nutrients, natural microflora, biochemical product and preservative), and extrinsic factors (time-temperature profile, temperature control, relative humidity, exposure to light including spectroscopy in ultraviolet and infrared irradiation, environmental microbial count, composition of



atmosphere in packaging, subsequent heat treatment and consumer handling) during processing, storage and distribution [6]. As a result of the interactions of these factors, the shelf-life limiting processes take place in packed product.

Biodeterioration of packaged products takes place due to microbiological, chemical and physical sources. Microbiological sources can be present in food before packing or on the surface of packaging materials. In that case, the shelf life of the food will depend on the types of microorganisms and their numbers. The chemical source is represented by enzymes produced by microorganisms which decompose food substrates into small compounds that can penetrate the cellular wall of microorganisms. Physical damage may be caused by microorganisms and result in biodeterioration of packed product [8]. Hence, packaging is an effective solution aimed at extending the shelf-life and maintaining the quality and safety of the products.

Generally, recent studies on food packaging tend to the development of new materials with high barrier properties because it can minimize the total amount of materials required and thus it is effective as regards the costs in material handling, distribution and waste reduction. Another approach is safety that is connected with public health and protection from biodeterioration. In that field, new materials and new packaging techniques have been developed. Finally, packaging should be designed environmentally friendly. For instance, it can be performed by a partial amount of synthetic packaging materials substituted by biodegradable or edible materials [9].

### *Plastics in food and pharmaceutical packaging*

Packaging is one major field of application for plastic materials that has been one of the great industrial success stories of the last century [10]. Since plastic is vital for people's lives, it is widely used in all fields such as food industry, electronics, automotive, building, agricultural and medical applications. Plastics

can be defined as organic macromolecular compounds made by condensation polymerization (polycondensation) or addition polymerization (polyaddition) or any similar process concerning molecules with a lower molecular weight or by chemical alteration of natural macromolecular compounds [1, 11].

In accordance to consumption, food packaging is an important sector in the packaging industry. New concept and new materials for food packaging result from developing manufacture and trade and are assisted by economic globalization [12]. The main reasons why plastics are applied for food packaging are that they protect food from spoilage, neither interact with food product nor support microorganisms; are relatively light in weight, are not prone to breakage, do not result in splintering and are available in a wide range of packaging structures, shapes and designs which are effective, convenient and attractive as regards the food products' costs. In fact, many plastics are heat sealable, easy to be printed on and can be integrated into production processes where package is formed, filled, and sealed within the same production line. However, the major disadvantage of plastics in this area is their variable transparency to light, permeability to gases, vapours and low molecular weight molecules [1, 11, 13]. In addition, it must not release harmful substances during the food preservation [14].

In the food packaging area numerous types of plastics are being used, including polyolefin, polyester, polyamide, polyvinyl chloride, polystyrene, polyamide, ethylene vinyl alcohol and cellulose based materials. Although more than 30 types of plastic have been used as packaging materials, polyolefin and polyesters is the most common [15]. Generally, synthetic polymers are a very attractive class of materials which may be obtained by the calculated manipulation of chemical reagents and possesses an advantage over most other materials i.e. their physical, chemical as well as in some cases biological properties can be tailored for the desired end use [16]. Nevertheless, interest has transferred to natural polymers from agricultural feedstock, animal sources,

marine food processing industry wastes or microbial resources because of increasing environmental concerns arising from non-biodegradable plastics and a problem of the restriction of petroleum resources [12]. Moreover, natural polymers have great advantages for biological applications.

### **1.1.2 Introduction to bioactive polymer systems (BPS)**

In the last few decades, there is a rapidly growing interest in the use of synthetic polymers for biological applications; new biomaterials have been studied in order to find important and superior biological activities [17]. The bioactive polymers maybe defined as materials based on synthetic polymers with additional incorporation of bioactive agents that elicits a specific biological response.

In food packaging, the goal is to use bioactive materials to get desirable response, for example the inhibition of microbial growth, adjusting barrier materials, indicating and sensing materials as well as flavour maintenance and enhancing materials [3]. Furthermore, BPS may support consumers' health due to its unique ability of enhancing the food impact [4].

In this area, biopolymers have received increasing attention, however, synthetic polymer based biodegradable systems are more effective than biopolymers from the economical point of view and as regards the properties. In that system, chemical and natural bioactive agents are applied due to their specific biological activity. Bioactive agents can be incorporated through immobilization or release allowing techniques, depending on the mechanism of action of the agent. Bioactive polymer systems may be classified as migratory bioactive polymers and non-migratory bioactive polymers according to the release mechanism of active agents and the biodegradable polymer system.

### **1.1.2 Non-migratory bioactive polymer system (NMBPS)**

The concept of NMBPS has been outlined several times to date and this polymer is only becoming of interest in packaging applications. Non-migratory polymers can be defined as polymers with bioactivity without the active components migrating from the polymer to the substrate [4, 19, 20]. The reason for non-migration of bioactive compound is due to its covalent attachment to the polymer backbone. From Figure 1a, it can be seen that the active agents are not mobile, their activity is limited only to the contact surface and thus, it is more critical in solid and semi-solid substrates [9, 20].

In the food packaging technology, the non-migration system has unique advantages in marketing and regulation. Actually, this system requires a very small amount of attached agent as active agents are not migrating, and it may decrease the cost of packaging system which utilizes very expensive bioactive agents. Another point in favour of that system is the fact that it can be combined with bioactive agents that are not allowed as food ingredients and food additives with substantiation of non-migration, the packaging material may consist of any food contact substances. However, this system has limited selection options for the bioactive agents [9]. In addition, from the application point of view, the non-migratory system is more effective in case of liquid food products compared to solid food which is connected with contact surface of package and food [22].

NMBPS is used as moisture absorber, oxygen scavenging system and ethylene scavenger and it is under investigation in the area of in-package enzymatic processing and non-migratory antimicrobial packaging [21]

Generally, NMBPS can be divided into two main groups:

- inherently bioactive polymers
- polymers with immobilized bioactive compounds.

The former is naturally bioactive, e.g. polymers containing free amines have antibacterial activity. For the latter, the system is based on polymer modified

with bioactive agents that hold specific properties. A number of materials have been investigated to have an inherent bioactivity and most of them have an antibacterial activity [3].

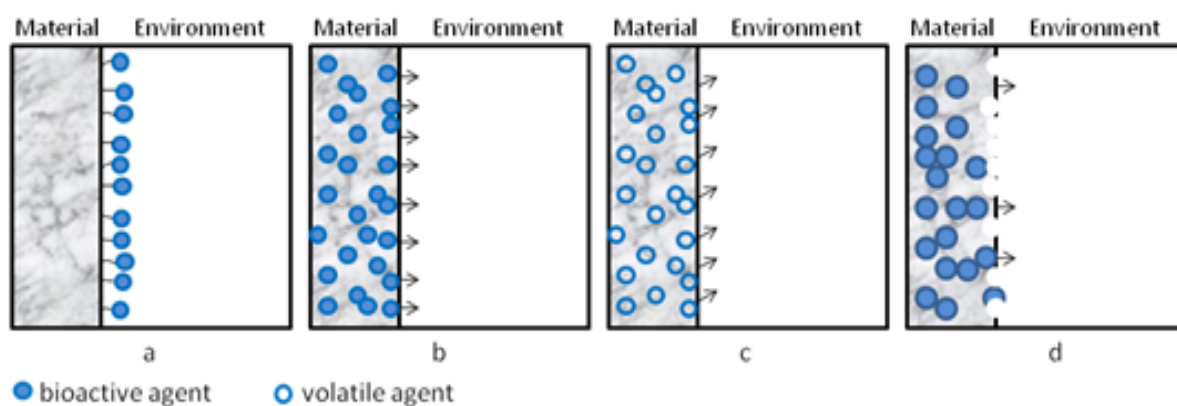


Figure 1: Schematic models of polymer systems with bioactive agents. (a) non-migratory, (b) and (c) migratory, and (d) biodegradable systems

### ***Inherently bioactive polymers***

Polymers that belong to this group are naturally bioactive themselves without any additional compound. At present, various polymers display inherent antimicrobial properties, chitosan and UV-treated polyamide are mentioned as examples here.

#### *Chitosan*

Chitosan is one of the most common polysaccharide based on chitin and is widespread in nature, e.g. in crab shells, lobsters, shrimps, insects and mushrooms. It is a  $\beta$ -1, 4-linked polymer of 2-acetamido-2-deoxy-glucopyranose (GlcNAc) and 2 amino-2-deoxy-glucopyranose (GlcN), and is investigated as a non-toxic, biodegradable and biocompatible material [23-25].

It has received increased attention as a food preservative particularly because of its antibacterial and antifungal activity; it is more effective against spoilage yeast and some Gram-negative bacteria including *Escherichia coli*, *Pseudomonas aeruginosa*, *Shigella dysenteriae* and *Salmonella typhinurium*.

Nowadays, some researchers mention that chitosan disrupts barrier properties of the outer layer of bacteria [3, 26]. A number of studies have investigated the degree of acetylation and molecular weight of chitosan as significant factors which play an important role for the antimicrobial activity of chitosan solution and physical properties [26]. Interestingly, according to the published reports and papers, films prepared using high molecular weight chitosan with low levels of acetylation degree will reveal good water resistance and poor antimicrobial activity [27].

Chitosan is mostly used in antimicrobial films to supply edible protective coating and it can be formed into fibers, films, gels, sponges, beads or nanoparticles [28]. According to the literature review, chitosan based antimicrobial films were prepared with water-resistant gliadin proteins isolated from wheat gluten [27], lysozyme [29], polylactic acid [23] and natural rubber latex [30] and its antimicrobial activity, physical, mechanical and thermal properties were tested.

#### *UV-irradiated nylon*

Surface treatment of nylon with excimer laser at UV wavelengths (193 nm) produces as an inherently antimicrobial polymer. This has been mentioned as a physical modification; actually it is a chemical change of amides on nylon surface, those are converted to amines [3, 31].

The antimicrobial activity of UV irradiated nylon film has been investigated against various bacteria and compared to untreated nylon. In some cases, bacterial reduction was observed for the untreated nylon, supposedly because of bacterial adsorption. As regards the activity against *Escherichia coli* and *Pseudomonas aeruginosa*, there was a slight reduction in treated nylon and untreated nylon films; however, there was no significant difference between them in case of *Enterococcus faecalis* and *Pseudomonas fluorescense* [3].

Therefore, there is no definitive result concerning the UV-irradiated nylon from the antibacterial point of view and more investigation is needed.

### ***Polymers with immobilised bioactive compounds***

In the last decade, the bioactive compounds covalently attached to the polymers have received increasing attention in such fields as biomedical, food packaging, textiles and bioprocessing. In fact, covalent immobilization can play an important role providing the most stable bond between the bioactive compound and the functionalized surface of polymer [34]. Moreover, covalently attached active agents to the polymer backbone can be called one type of the non-migratory bioactive polymer, in which a covalent linkage ensures that bioactive compound will not migrate to the food and thus may offer the regulatory advantage of not requiring approval as food additive [3].

Depending on the polymer nature, in certain cases, polymer functionalization is needed to create reactive functional groups for providing attachment sites. In order to functionalize a polymer, a selection of polymer is required because of its properties such as origin, optical clarity, strength, elasticity and degradability [33]. Polyolefin, poly(ethylene terephthalate), poly( $\alpha$ -hydroxyacids), poly(methyl methacrylate), poly(pyrrole) and methacrylate copolymers have been used as a substrates for biofunctionalization. Polymer functionalization can be performed by surface treatment (wet chemicals, physical surface treatment and plasma surface treatment), grafting, using polymer spacers and coupling chemistry (carbodiimide, glutaraldehyde coupling) [3]. The Figure 2 shows the surface functionalization of polymer that provides the desired type and quantity of reactive functional groups prior to the attachment of a bioactive compound.

During the immobilization of bioactive compound in bulk polymer matrixes, the active agent will not be able to migrate from bulk of the polymer to the surface, where it will be active, so that the application of non-migratory bulk

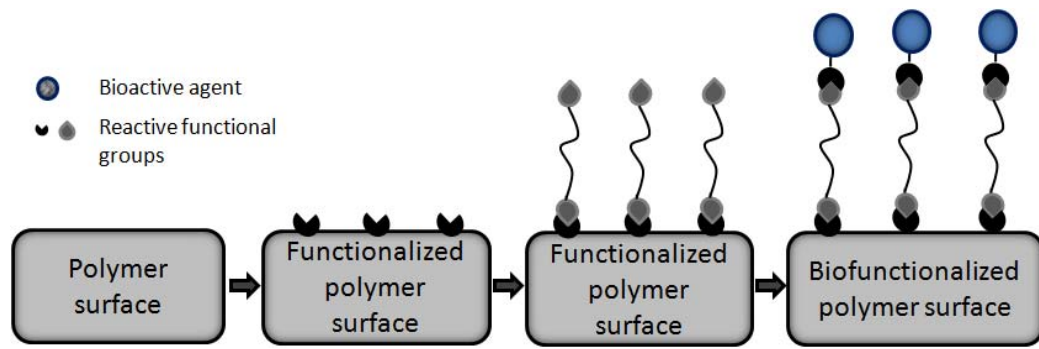


Figure 2: Concept of biological surface modification

immobilization in food packaging is limited and therefore, covalent attachment of bioactive compound to the surface of a polymer film is important in this area [35].

Natural and chemical bioactive compounds such as enzyme, peptide, polysaccharide, antibody and different types of antimicrobials can be used due to their specific response to the biological system. For example, incorporation of lactase into low-density polyethylene films [35], lysozyme with zein film [36], polyvinyl alcohol (PVOH) [37], nylon 6, 6 and cellulose triacetate (CTA) [38], naringinase in PVOH film [39] and CTA [40] as well as invertase attached to the cellulose and polystyrene resin [40] can be used for active packaging purposes.

### 1.1.3 Migratory bioactive polymeric system (MBPS)

In this type of system, bioactive agents can release from the polymeric system due to incorporation methods of active agent into polymer matrix [42]. For example, direct incorporation methods and coating techniques allow migration of bioactive agents. MBPS may be divided into two groups depending on the nature of the bioactive agent:

- volatile
- non-volatile



The active compound used in migratory bioactive systems must be non-toxic to human health and is regulated by a number of regulatory agencies such as Food and Drug Administration (FDA), Environmental Protection Agency and United States Department of Agriculture (USDA) [31, 42].

In practice, well-known examples of migratory bioactive packaging are releasing systems such as carbon dioxide generating system, which is used for fresh meat, sulphur dioxide releaser for grape preventing from mould and ethanol generating system is applied in the food to inhibit microbial spoilage, to decrease the rate of oxidation in the bakery products and cheese. Nowadays, the ethanol generators are more often used in medical and pharmaceutical applications. In addition, research in the area of antimicrobial packaging materials combined with natural or synthetic antimicrobial agents has significantly increased during the recent few years [20].

### ***Non-volatile MBPS***

Non-volatile active agents are incorporated directly into packaging material or placed between the package and the food. In case of compounds attached to the packaging material, they transfer from the polymer system to the food surface through diffusion which is described in Figure 1b. The constant activity of the system is affected by constants of the mass transfer profile such as diffusivity of the agent in the packaging material, solubility of the agent in the food on the surface, and diffusivity of agent in the food [9]. In addition, a regular contact is required between that type of MBPS and product which should be a uniform matrix without significant pores, holes, air gaps or heterogeneous particles. This system is simple compared to other systems and can be suitable for solid, semi-solid foods and liquid products [9].

## ***Volatile MBPS***

Obviously, the intact contact of the active agent with the food surface can produce the maximum effectiveness. However, this is not required when using volatile bioactive agents that can migrate without contact with food and its corresponding mass transfer is more complex [9, 45]. The headspace gas concentration of the package is important for the surface concentration above a certain minimum inhibitory concentration. Initially, volatile bioactive agent combined with packaging evaporates on the packaging surface, crosses the packaging/air interface, crosses the air/food interface and diffuses into the food surface. (See Figure 1c) The migration rate of volatile active agent from the packaging system depends on the volatility, which is caused by chemical interaction between packaging material and volatile agent, while the absorption rate of volatiles into the food surface is related to the food composition that interacted with gaseous agents [9].

There are some advantages produced when using volatile agent in MBPS. This system is convenient for highly porous, irregularly shaped or powdered foods. Also the most part of volatile compounds originates from natural herbs and spice extracts, since they can easily be accepted by consumers and regulatory agencies [20].

## ***Controlled release technology***

A migratory bioactive system can be designed as a controlled release system that plays an important role for the sustained constant concentration of bioactive agent in food and pharmaceutical products without waste of bioactive agent for a long period of time. It could be one of the requirements for MBPS. For instance, in case of an antimicrobial system, if the migration rate of antimicrobial agent is faster than the growth of microorganisms, added antimicrobial agent will be weakened to less than the effective critical concentration before the expected

period. On the contrary, if the release is slow in order to maintain the concentration above the minimum inhibitory concentration, microorganisms can grow quickly, before the antimicrobial agent is released. Therefore, the migration rate of active agent from the packaging must be controlled specifically [9].

In Figure 3, various types of controlled release systems are distinguished according to the release control mechanism [44].

The materials used in a controlled release system can be selected due to their desirable physical properties such as elasticity (polyurethanes), insulating ability (polysiloxanes or silicon), hydrophilicity and strength (polyvinylalcohol), and suspension capabilities (polyvinyl pyrrolidone) etc. Recently, the biopolymers including polylactic acid, polyglycolides and polyorthoesters have been important in controlled release [52].

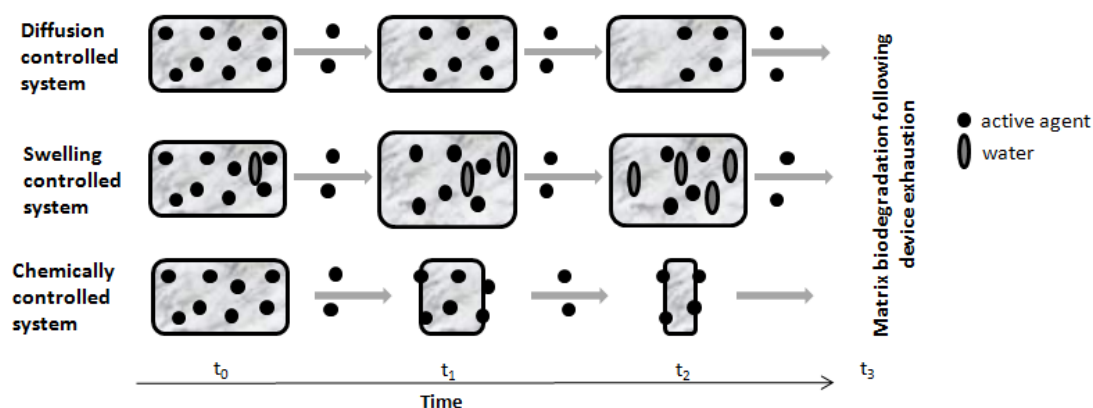


Figure 3: A schematic drawing illustrating the three mechanisms for controlled drug release from a polymer matrix.

The rate control of active agents is affected by many factors. In the packed food and pharmaceutical system, the migration rate of active agents can be controlled by the mass transfer behaviour such as solubility, permeability and diffusivity of the active agent depending on the nature of both active agent and product. For example, if the agent is very soluble in the water, the release of that agent from hydrophilic polymer will be very fast [9].

## Mass transfer

In the migratory bioactive polymer system, mass transfer of volatile and non-volatile agent is described by permeation; absorption and diffusion (see Figure 4). Permeation takes place when a molecule passes through a material or membrane from an area of high concentration to an area of low concentration. Diffusion can be defined as a movement of molecules within the material based on concentration difference. Absorption is the surface sorption of the molecules from the surroundings to the material [43].

Mass transfer through diffusion obeys Fick's law and Fick's first law can be expressed as:

$$J_d = -D \frac{\partial C}{\partial x} \quad (1)$$

where,  $J_d$ ,  $D$ ,  $C$  and  $x$  are the flux per unit cross-section [ $\text{mol m}^{-2}\text{s}^{-1}$  or  $\text{kg m}^{-2}\text{s}^{-1}$ ], diffusivity [ $\text{m}^2\text{s}^{-1}$ ], the concentration of diffusant, and the distance across which the diffusant has to transfer, respectively. Fick's second law can be applied to analyze unsteady state diffusion with time  $t$ :

$$\frac{\partial C}{\partial t} = -D \frac{\partial^2 C}{\partial x^2} \quad (2)$$

Fick's law is used in the diffusion of solid, liquid and gases.

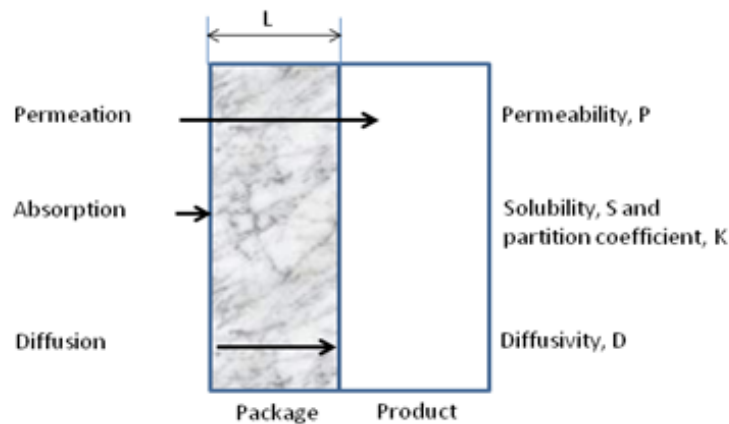


Figure 4: Mass transfer phenomena and their characteristic coefficients

In case of volatile compounds, it must dissolve into the packaging material, and then it can diffuse through the packaging. In general, the sorption of a gas into a packaging material has a linear relationship to the partial pressure of the gas as shown in Henry's law [41].

$$p = \sigma X_s \quad (3)$$

where,  $p$ ,  $X_s$  and  $\sigma$  are the partial pressure of the gas in the atmosphere, the molar fraction of the gas in the packaging material and Henry's law constant, respectively. However, Henry's law is not relevant for the solute permeates.

Generally, in packaged food systems, mass transport evolves from the package into the food or in opposite direction depending on the concentration differences of permeates in both sides. Theoretically, solute permeation is significant for the release of active agent in drug delivery as well as active packaging system. For the BPS, the mass transfer of non-volatile agents into food is dominated by Fick's laws (see above). The parameters of the equations 1 and 2 are used as the predominant characteristics describing the transfer of both an antibacterial agent and other polymer additives within the system package-food or pharmaceutical product.

#### **1.1.4 Biodegradable polymer systems**

##### *Definition and classification*

In the ISO 472 standard, biodegradable polymer is defined as a material designed to undergo a significant change in its chemical structure under specific environmental conditions resulting in a loss of some properties that may vary when measured by standard test methods appropriate to the plastic and the application in a period of time that determines its classification. The change in the chemical structure results from the action of naturally occurring microorganisms [23].

According to their origin, biodegradable polymers can be divided into two main classes called natural and synthetic polymers. This classification is more detailed in Figure 5.

Natural biodegradable polymers are produced renewably in the nature. Polysaccharides (e.g. starch, alginate, chitosan and cellulose), proteins (e.g. collagen, gelatin, whey protein), and lipids have been successfully used in edible coating as well as in medical fields. Polyhydroxyalkanoates (PHA), polyhydroxybutyrate (PHB) and poly ( $\beta$ -malate) are the most representative polyesters synthesized by microorganisms. These polyesters are of interest for medical applications because of their biocompatibility and bioresorbability. Polylactic acid may belong to natural polymer due to its bio-derived monomer. It is also subordinated to the synthetic aliphatic polyester because it can be produced from oil [24].

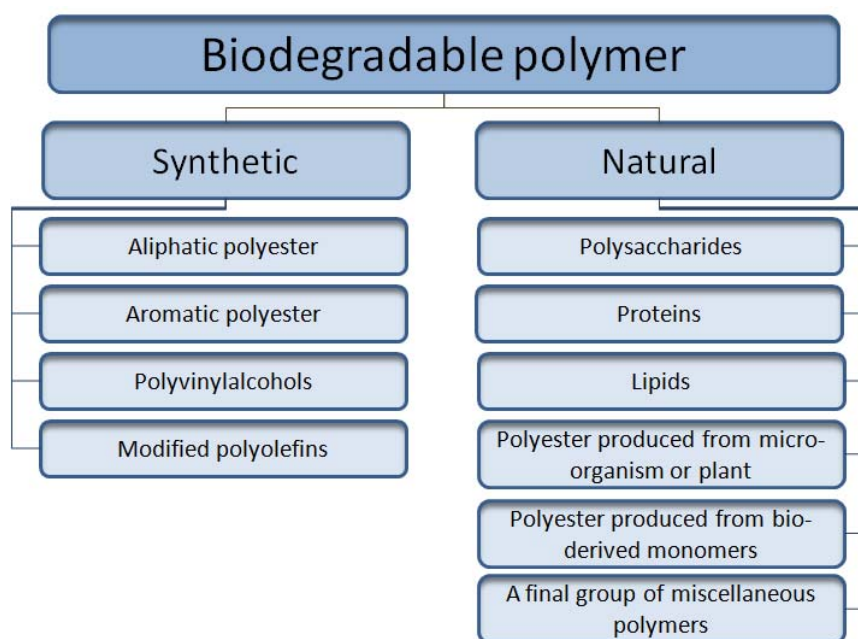


Figure 5: Classification of biodegradable polymers

Obviously, at present, synthetic biodegradable polymers have been increasingly used in many fields, because they have better properties compared to natural polymers. From all of these polymers, polylactic acid is one of the

most promising biopolymers obtained from lactic acid. As regards the application, it is used in food and crop fields (films, food packaging) because it possesses resistance properties to fat, food oil, humidity, solvent and smells [47]. Also, it has been widely used in medical applications (drug delivery, suture threads and clips, orthopedic fixations, and resorbable implants) because of its bioresorbable and biocompatible properties in the human body [24]. In practice, several types of commercially available PLA based blends are used that consist of base component, PLA and other biodegradable components such as starch, dextrose, minerals, and polyesters as well as special additives, which have been used in many applications because of their specific advantages. There are several companies dealing with PLA production such as Nature Works (USA), Fkur (Germany), BASF (Germany), Shimadzu Corporation (Japan), Kanebo Gosheu (Japan) [24].

### ***Mechanism of biodegradation***

Biodegradation process in polymers takes place through following mechanisms: solubilization, charge formation followed by dissolution, hydrolysis, microbial and enzyme-catalyzed degradation [49].

#### ***Solubilization***

The hydration of polymers leads to the disruption of secondary and tertiary structure stabilized by van der Waals forces and hydrogen bonds. As a result of hydration, the polymer chains may become water soluble and/or the polymer backbone may be broken down by chemical or enzyme-catalyzed hydrolysis to result the loss of polymer strength [49].

### *Ionization*

In this case, initially water insoluble polymers can be solubilized by ionization or protonation of a pendent group at certain conditions. For example, polyacids are soluble at high pH and become hydrophilic [49].

### *Hydrolysis*

Hydrolytically degradable polymers are polymers with hydrolytically unstable chemical bonds such as esters, anhydrides, carbonates, amides, urethanes and ureas in the backbone of polymer, which degrade by hydrolysis to low molecular weight oligomers at the primary degradation with subsequent microbial assimilation in the biodegradation process [48]. The hydrolytic degradation is classified below in Figure 6.

### *Enzymatic degradation*

Generally, naturally occurring polymers such as proteins, poly(amino acids) and polysaccharides are degraded by enzymatically. During the enzyme-catalyzed hydrolysis of polymer, the enzyme initially binds to the substrate then subsequently catalyzes a hydrolytic cleavage.

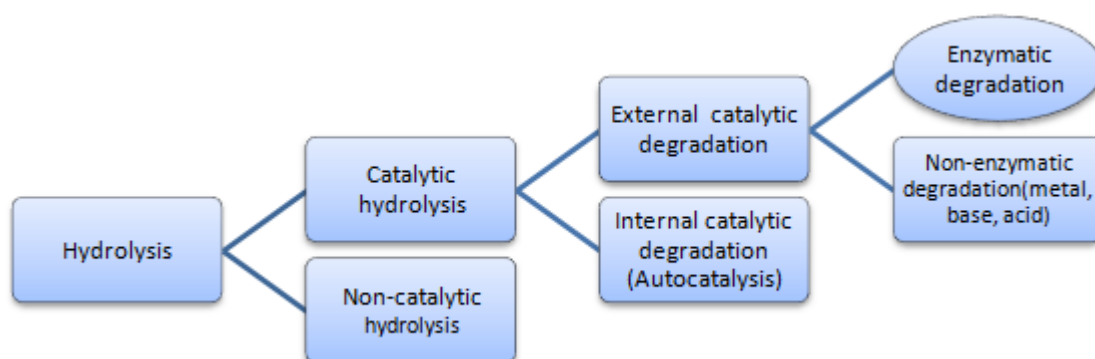


Figure 6: Classification of hydrolytic degradation of hydrolysable polymers



### *Microbial degradation*

Microbial degradation occurs due to the action of naturally occurring microorganisms such as bacteria, fungi algae, etc. The most commonly used bacterial strains for the polymer degradation are *Pseudomonas aeruginosa*, *Pseudomonas fluorescens* and fungi *Penicillium simplicissimum* [49].

### *Drug release mechanisms based on biodegradable polymers*

According to the literature review, three basic mechanisms of drug release system based on biodegradable polymers were mentioned. (See Figure 1d)

- Erosion of polymer surface occurring together with the release of physically entrapped BA
- Cleavage of covalent bonds between polymer and BA, occurring in the polymer bulk or on the surface, followed by drug diffusion
- Diffusion controlled release of physically entrapped BA, with bioabsorption of the polymer delayed until after drug depletion [51].

### *Applications of biodegradable polymer*

Biodegradable polymers have been used in a wide range of biomedical technologies including tissue engineering, regenerative medicine, controlled drug delivery and gene therapy [50]. Among all, the application in drug release has been in the focus of interest for recent decades. There are two types of drug release systems using biodegradable polymers. The first one is an independent cover or coating made by biodegradable and bioresorbable polymer for the drug and it can be used either orally or implanted. In the second type of the system, the drug is uniformly distributed in the bioresorbable polymer and is absorbed by the organism as the polymer degradation. Biodegradable polymers have already found acceptance in application areas such as food packaging, bags and

sacks, loose-fill packaging agricultural film and many niche market applications [52].

### **1.1.5 Bioactive agents (BA)**

Bioactive agents used in bioactive polymer systems can be defined as substances which give the desirable biological effect to surrounding environment. Apart from its specific biological activity in the system, the physicochemical properties of the bioactive agent such as solubility, reactivity and compatibility are important factors for the activity. Moreover, incorporated bioactive agents influence the physical and mechanical properties of polymer systems. For example, an excess amount of bioactive agent blended with polymers will lead to a decrease in physical and mechanical properties [9].

Generally, they can be classified into two groups; natural and chemical. The selection of the bioactive compound is limited by the incompatibility of the component with the material or by the heat lability during thermal processing [53]. For heat-sensitive bioactive agents such as enzyme, protein and volatile agents, solvent compounding may be the appropriate incorporation method.

#### *Bioactive agents for food packaging*

BA is applied for food packaging, e.g. as antimicrobials, biocatalysts, absorbers or scavengers. The most of them are used in practice as antimicrobial agents. In order to use BA for food, they must be non-toxic or regulated.

#### *Chemical bioactive agents*

Chemical bioactive agents include organic acids, fungicides, alcohols and antibiotics and all of them should be food-grade. In the packed food system, they can be added directly to food ingredients, incorporated into packaging

material as well as placed in the atmosphere of head-space. There is only one possibility for the non-food grade chemical bioactive agents, i.e. combination with packaging system through chemical binding especially by immobilization related to the migration of residues of chemical agents [42].

- Organic acids such as sorbic acid, lactic acid, acetic acid, citric acid and propionic acids, their salts as well as anhydrides are very common antimicrobial agents with high efficacy and cost effectiveness, and approved as additives for certain foods. They are effective against various types of microorganisms and correct selection is required for efficient antimicrobial activity. In some cases, either mixture of organic acids or combination of organic acid with other bioactive compound has stronger antimicrobial activity than a single organic acid [9].
- Ethanol has strong activity against bacteria and fungus; however, it is not effective for the growth of yeast.
- Desiccating agents such as silica gel, natural clays and calcium dioxide are used for high moisture foods and pharmaceuticals. They can be incorporated in packaging materials, also in the form of porous sachets [54].
- Potassium permanganate is used in packaging systems as an ethylene removing agent, which oxidizes ethylene to acetate and ethanol. It is mostly applied in form of sachets, may also be incorporated into packaging materials [54].
- For many decades, different types of metals such as copper, zinc, titanium, magnesium, gold and silver have been identified as antimicrobial agents used in many fields including biomedical, food packaging, etc. Nowadays, their related nanoparticles have received increasing attention particularly; silver nanoparticles have been demonstrated as the most effective antimicrobial agent against various

microorganisms [55]. Of all metallic antimicrobial compounds, silver-substituted zeolites are the most widely used polymer additive for food packaging, especially in Japan. Some silver-substituted zeolites are commercialized. [31, 38].

- Gaseous antimicrobials are known as beneficial due to their vaporization and penetration compared to solid and solute types of chemical antimicrobials. According to literature review, the uses of chlorine dioxide and ozone have been approved by FDA and can be incorporated into packaging materials [42, 56].
- Antibiotics are not permitted as package additives for the purpose of antimicrobial activity; however, they may be applied for short-term use of medical devices and other non-food products [42].
- The use of antioxidants is desirable for the food packaging due to its efficient antifungal activity. Natural antioxidants such as  $\alpha$ -tocopherol and ascorbic acid are important in food applications concerning the use of food chemicals [57].

### *Natural bioactive agents*

- Some bacteriocins including nisin, lacticins, pediocins and diolococin produced by microorganisms are capable of developing activity in order to inhibit the growth of pathogenic microorganisms [42]. Particularly, nisin is an effective bactericidal against Gram-negative and Gram-positive bacteria and it has been accepted as a food additive by the FDA and WHO [58]. In addition, nisin has surface-active molecules that may be suitable for adsorption to solid surface used for antibacterial packaging [59]. The activity and release of nisin from the film strongly depends on pH and temperature; precisely a lower pH and

a higher temperature were most effective for the migration from the film [59].

- Likewise, some other natural bioactive agents, enzymes can be added directly to food product or can be incorporated into packaging material, in which the enzymes must be immobilized [60]. In the food packaging area, some enzymes such as immobilized naringinase in plastic packaging are intended for reduction of grapefruit bitterness, and lactase [33] is suitable for low-lactose or free-lactose milk, and cholesterol reductase is intended for the hydrolysis of cholesterol in packaged food. Moreover, enzymes with antimicrobial properties control the amount of oxygen against aerobic bacteria or direct antimicrobial activity into on microorganisms present in packaged food.
- Natural plant extracts such as grapefruit seed, cinnamon, horseradish and clove have received increasing attention as regards their antimicrobial activity against spoilage and pathogenic bacteria, therefore, a great deal of natural extracts is expected due to this advantage when compared to chemical active agents. Grapefruit seed extract has a broad range of antimicrobial activity which was stable at high temperatures of up to 120°C [57]. The horseradish contains volatile allyl isothiocyanate which shows antimicrobial activity against several fungi and bacteria.

### **1.1.6 Applications of bioactive polymer systems**

BPS can be used effectively in the innovative food and pharmaceutical packaging technologies. The modern food packaging techniques such as active, intelligent or smart, green and bioactive packaging can modify and monitor the internal and external food environment and are developed to prolong the shelf-life, enhance the quality and safety of food [61]. BPS can be designed to guarantee the main functions of these techniques.

#### ***Active packaging***

Active packaging changes the condition of the packed foods to extend shelf-life or improve safety or sensory properties using the incorporation of active agents into the packaging film [13, 62]. That technique is divided into three categories:

- Absorbers (removes undesired compounds such as carbon dioxide, ethylene, oxygen, water and volatile of odours)
- Release systems (adds or emits compounds to packed food or packaging material such as carbon dioxide, antioxidants, antimicrobials and preservatives)
- Miscellaneous (self-heating, self-cooling, surface-treated packaging materials, modifiers for microwave heaters) [13, 61]

#### ***Intelligent packaging***

Intelligent or smart packaging was developed in order to monitor the condition of packaged foods and to give information about the quality of the packaged food [62, 13, and 63]. Some examples of intelligent packaging system include time-temperature indicators, biosensors, gas sensors, freshness or spoilage indicators and pathogen indicators. These systems are based on

enzymatic, chemical, electrochemical or microbiological interaction [61]. The sensing devices may be incorporated in package materials or placed in-side or outside the package, as well as in the lid [63].

### ***Bioactive packaging***

Recently, a concept of bioactive packaging has been developed, in connection with a novel approach regarding the development of functional foods. So, this is the promising new packaging technology, in which a food package or coating is given the unique role of enhancing food impact on the health of the consumer by generating healthier packaged foods [4]. That system can be designed in three different ways:

- Integration and controlled release of bioactive agents or nanocomponents from biodegradable and or/sustainable packaging systems (release systems using phytochemicals, vitamins, dietary fibers and prebiotics, etc.)
- Micro- and nano- encapsulation of active agents either in the package or within the foods (micro- and nano- capsules using probiotics and marine oil, etc.)
- Packaging providing enzymatic activity exerting health-promoting benefits through transformation of specific food-borne components (lactose free milk and cholesterol free foods, etc.)

In these technologies, the packaging and coating materials are aimed at producing unique properties of synthetic and biomass derived biopolymers [4].

## *Green packaging*

In the green packaging technology, the materials can be biodegradable, compostable, sustainable, degradable and recyclable. Packaging made using these materials can reduce the environmental impact. Bioplastics from renewable resources such as starch-based products, thermoplastic starches, polylactic acid, polycaprolactone and copolyesters have received attention in that technology [63].

The one main constituent of the BPS is polymer matrix that mentioned above. There can be a number of choices to select appropriate one for the end product (BPS) depending on the many factors such as properties, cost, toxicity, source, production e.g. Therefore, polymer blend can be more suitable selection because its unique properties compared to single polymers and cost effectiveness.



## 1.2 POLYMER BLEND

### 1.2.1 Introduction to polymer blend

Polymer blending is an effective solution to produce new materials with superior properties to those of the single components. It has been considered one of the most rapidly growing fields in polymer science. Statistically, polymer blends provide nearly 40% of the total consumption of the polymer, and there is an increasing trend on it [64-65]. In connection with this there are number of advantages can be mentioned from the economical and material point of view. For example, blends are prepared with desirable properties at lowest price, improvement for target specific properties such as antimicrobial, barrier, drug release and compatibility e.g., and its creation is less-time consuming, easier and cheaper than to develop new polymer or monomer with similar properties [64-66]. In addition, the properties of the blends can be adjusted by the selected polymer and changing the blend composition [66].

#### *Thermodynamic relationship*

The most important characteristic of a polymer blend is the phase behaviour. Polymer blends can exhibit miscibility or phase separation and various levels of mixing in between the extremes (e.g., partial miscibility). Another crucial factor leading to miscibility in low molecular weight material is the combinatorial entropy contribution which is very large compared to high molecular weight polymers. The combinatorial entropy is the part that originates from the number of possible placement of molecules in the lattice of an athermal solution [67].

The most important relationship governing mixtures of two polymers with different properties is shown in Equation 4:

$$\Delta G_m = \Delta H_m - T\Delta S_m \quad (4)$$

Where,  $\Delta G_m$  is the free energy of mixing,  $\Delta H_m$  is the enthalpy of mixing (heat of mixing) and  $\Delta S_m$  is the entropy of mixing. For miscibility to occur  $\Delta G_m$  must be negative. While this is necessary requirement, it is not a sufficient requirement as the following expression must also be satisfied:

$$\left(\frac{\partial^2 \Delta G_m}{\partial \phi_i^2}\right) > 0 \quad (5)$$

where,  $\phi$  is the volume fraction of component i. Equation 4 and Equation 5 are the important and sufficient condition for miscibility [68-70]. On the other hand, the most important characteristic of a real miscibility is its thermal stability or equilibrium state [69, 71].

A system is thermodynamically stable if its formation is accompanied by a decrease in the Gibbs free energy. The Gibbs free energy decreases to definite equilibrium value which does not change subsequently with time [69].

Negative values of Equation 5 (even though  $\Delta G_m < 0$ ) can yield an area of the phase diagram where the mixture will separate into a phase rich in component 1 and a phase rich in component 2. For low molecular weight materials, increasing temperature generally leads to increasing miscibility as the  $T\Delta S_m$  term increases, thus deriving  $\Delta G_m$  to more negative values. For higher molecular weight components, the  $T\Delta S_m$  term is small and other factors (such as non-combinatorial entropy contributions and temperature dependant  $\Delta H_m$  values) can dominate and lead to the reverse behaviour, namely, decreasing miscibility with increasing temperature.

### ***Flory-Huggins theory***

Flory and Huggins established a theory which is the most relevant for designing the free energy of binary polymer mixtures. There are several equivalent forms expressed in Equations 6-8 [64, 68].

$$\Delta G_m = RTV \left[ \frac{\phi_1}{v_1} \ln \phi_1 + \frac{\phi_2}{v_2} \ln \phi_2 \right] + \phi_1 \phi_2 \chi_{12} RTV / v_r \quad (6)$$

$$\Delta G_m = RTV \left[ \frac{\phi_1}{v_1} \ln \phi_1 + \frac{\phi_2}{v_2} \ln \phi_2 \right] + \phi_1 \phi_2 B \quad (7)$$

$$\chi'_{12} = \chi_{12} / v_1; \quad B = \chi'_{12} RT \quad (8)$$

where,  $V$  –total volume,  $R$ -gas constant,  $\phi_i$  -volume fraction of component  $i$ ,  $v_i$ -molecular or molar volume of specific segment,  $\chi_{12}$  -Flory-Huggins interaction parameter,  $v_r$  is often calculated as the square root components ( $v_r = \sqrt{v_1 v_2}$ ).  $\chi'_{12}$ - binary interaction parameter,  $B$ - binary interaction density parameter [64].

According to the literature, the first two logarithmic cases offer combinatorial entropy of mixing, while third one is the enthalpy. In case of polymer blends, large molar volume,  $v_i$  results small combinatorial entropy, indicates that the miscibility and phase separation of the system is basically affected by the value of  $\chi_{12} \phi_1 \phi_2$  [4].

### ***Miscibility***

Polymer blends are classified as miscible (poly(methacrylate)-poly(vinylidene fluoride), partially miscible (polystyrene-poly(vinyl methyl ether) and immiscible (polyamide 6-polyethylene) blends according to their phase behaviour. Related terms are defined by Utracki [64] from the thermodynamical point of view, listed on Table.1. Also, these blends are defined from morphological side by Kulshreshtha [69] and others that immiscible polymer blends are subclass of polymer blends referring to those blends exhibit two or more phases on entire composition and temperature range, while partially miscible polymer blends exhibit a ‘window’ of miscibility, i.e., they are miscible only at certain concentrations and temperature. In case of miscibility, Robinson [68] define that miscibility is the level of mixing of

polymeric constituents of a blend yielding a material which exhibits the properties expected of a single phase material. In general, most of polymer blends form immiscible or partially immiscible blends and some of those combinations result good mechanical, thermal and other properties are named as compatible [66].

Table 1: Definitions of the various polymer blends [64]

<b>Term</b>	<b>Definitions</b>
<b>Polymer blend</b>	Mixture of at least two macromolecular substances, polymers or copolymers, in which the ingredient content above 2 wt.%
<b>Miscible blend</b>	Polymer blend, homogenous down to the molecular level, associated with the negative value of the free energy of mixing: $\Delta G_m \approx \Delta H_m \leq 0$ , and a positive value of the second derivative: $\partial^2 \Delta G_m / \partial \phi^2 > 0$ . Operationally, it is a blend whose domain size is comparable to the dimension of the macromolecular statistical segment.
<b>Immiscible blend</b>	Polymer blend whose free energy of mixing: $\Delta G_m = \Delta H_m > 0$

The main requirement for miscibility is negative free energy of mixing which is given by Equation 4 above. The miscibility formation depends on a number of factors, including the nature of the polymer constituents, their molecular weights, composition, and strength of the interactions, steric factors, and structure. In Table 2 some approaches to obtain miscible blends are shown.

Also, the miscibility is expected in connection with the heterogeneity diameter,  $d_d$  which is usually explained by the density fluctuation [64]. Many authors noticed differently that the heterogeneity diameter in miscibility is observed in the range of 1-2 nm [68] 2-3 nm [72], 2 to 7 nm. Thus,

heterogeneity diameter  $d_d < 10$  seems to be responsible for the true miscibility [64].

Moreover, authors mention about specific interactions to generate miscible blends from high molecular weight polymers, i.e. purely dispersive interactions and intramolecular repulsion are responsible for the negative heat of mixing [64, 68, 70]. In case of low molecular weight liquids, hydrogen bonding, acid-base, charge transfer, dipole-dipole, ion-dipole, induced dipole-dipole,  $\pi$ -hydrogen bonding, and  $\pi - \pi$  complex formation [68, 70]. Particularly, hydrogen bonding is studied most predominantly in polymer blends. Actually, except from its effectiveness on miscibility, now it is considered a well-known strategy to improve compatibility of the immiscible blends [66]. Hydrogen bond forms between hydrogen (proton donor) and another group (proton acceptor or electron donor) such as usually oxygen, nitrogen, or fluorine, which has partial negative charge. The inter-associated hydrogen bonds are detected in almost all blends identified as either miscible or partially miscible blends [66]. One of the analysis to determine hydrogen bonding in polymer blends is infrared spectroscopy, by which specific groups are detected including the hydroxyl group of secondary alcohols ( $3630 \text{ cm}^{-1}$ ), and carboxylic group ( $3530 \text{ cm}^{-1}$ ), the carbonyl group ( $1730 \text{ cm}^{-1}$ ) and the N-H group at  $3400 \text{ cm}^{-1}$ . A shift to lower frequency in the stretching band related to these peaks is the main indication of hydrogen bonding exists in polymer blend [66].

In majority of cases, the glass transition temperature,  $T_g$  is the main detector for the miscibility. It is noted that miscible blends show single  $T_g$  appeared between the glass transition of pure constituents. However, there are some requirements for the prediction of miscibility by measuring  $T_g$  [73]. The  $T_g$  should be measured when the amount of the second component is higher than 10 wt%, because  $T_g$  is unsusceptible with the presence of less than that amount of minor polymer. In addition, the method should not be used for blends containing polymers whose  $T_g$  is do not differ at last by  $10^\circ\text{C}$  from each other [64].

However, in some cases, a single  $T_g$  may be appeared in miscible blends with finally dispersed phases. Finally, Utracki mentioned that more than one  $T_g$  can be appeared depending on the chemical nature of the components, weight ratio and processing condition. Also, for detection of miscibility, limited information is given by light scattering that is observed only when size of heterogeneity is larger than 100 nm [64].

The properties of polymer blends depend mainly on miscibility of the polymers and their structure. In the miscible blends, its chemical, physical and mechanical properties can be predicted from the composition weighted average of the properties of the individual components, while immiscible blends are phase separated, exhibiting the glass transition temperatures and/or melting temperatures of each blend component [74].

Table 2: Approaches for achieving miscible blends or compatible phase separated blends [68]

<b>Miscibility</b>	<b>Compatibility in phase separated blends</b>
Hydrogen bonding	Ternary component addition
Dipole-dipole interaction	Block and graft copolymer addition
Matched solubility parameter	Reactive compatibilization
Ion-dipole interaction	Cocrosslinking
Mean field approach	Interpenetrating networks
Association model	In-situ polymerization
	Nanoparticle addition

In fact, immiscible polymer blends are much more interesting for commercial development. This is because immiscibility allows one to preserve the good features of each of the phase polymer components of the blend. Some properties only achieved by through immiscible blends. For example, the impact strength of a polymer cannot be improved significantly by adding an elastomer miscible to it. It is thus fortunate, that most polymer pairs are immiscible.

The challenge is to develop processes or techniques that allow control of both the morphology and interfaces of phase separated blends. Such processes or techniques are called compatibilization [74].

### 1.2.2 Compatibilization

The most of polymer blends are not only immiscible but also are mechanically incompatible. In such blends, compatibilization process is required to provide improved properties and less immiscibility. There are three functions of compatibilization are noticed that:

- To reduce the interfacial tension for obtaining more uniform blend with smaller particle size (See Figure 7)
- To make certain that the morphology generated during the alloying is resistant to higher stress and strain forming
- To enhance adhesion between the phases in the solid state, facilitating the stress transfer, hence improving the mechanical properties [ 68, 74-75]

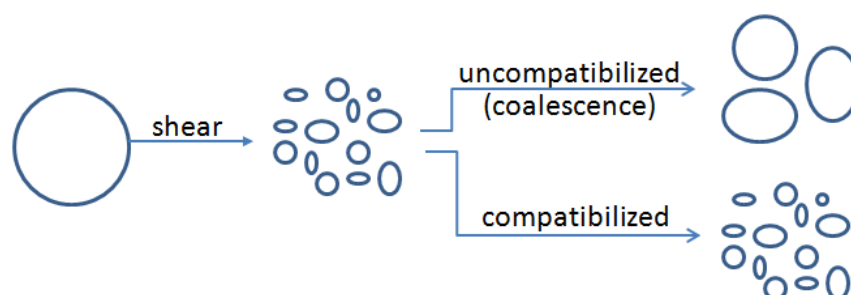


Figure 7: Generalized illustration of effect of compatibilizer methods on the particle size [68]

The approaches to provide the compatibility are listed in Table 2 and they are related into three major methods:

- Non-reactive compatibilization: adding non-reactive block or graft copolymers

- Specific compatibilization: attaching to polymer groups having non-bonding specific interactions
- Reactive compatibilization: introducing reactive molecules leads to form the desired copolymers in-situ, directly during blending [75-76].

### ***Non-reactive compatibilization***

Non-reactive compatibilization is efficient for the improved dispersion and properties by using a ternary polymeric component including random copolymers block or graft copolymers. During mixing process, copolymer locates preferentially at the interfaces of two different segments, and then each segment penetrates to the phase with which it has specific affinity [74]. Actually, in case of the use of block or graft copolymers, either morphology or interface of the polymer blend is controlled. However, only specific random and graft or block copolymer required for each immiscible polymer blends. For example, EVA is used to improve dispersion and toughness of PA6/LDPE blend, PHE with addition of phenoxy improves strength, elongation and toughness of PAR/PA66 blend and chlorinated PE is responsible for the stabilization of phase morphology of LDPE/PVC blends [68]. Another limitation is that the excess amount of these copolymers saturates the interface. In other word, the amount of the copolymer not present in the interfaces is unfavourable for compatibilization [74].

### ***Reactive compatibilization***

Reactive compatibilization allows developing desired compatibilizer *in situ* via covalent or ionic bond during melt blending using reactive functionalized polymers [68, 74].



In Figure 8, three cases for reactive compatibilization of two immiscible pairs are illustrated:

- The both polymer components are mutually reactive. In that case, reactive compatibilization is uncomplicated. The reaction between them at the interface leads to the formation of a copolymer.
- One phase has reactive groups, while another phase is chemically inert. In that case, polymer without reactive groups is functionalized with functional groups that can react with reactive phase.

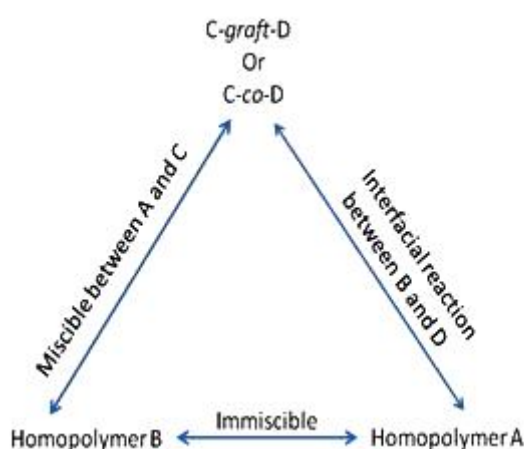


Figure 8: Schematic showing the roles of reactive compatibilizing agent when melt blended with two immiscible homopolymers [77].

- Both two polymer phases are non-reactive. Most of hydrocarbon polymers related in such groups. In this case, some other compatibilization method is used. For example, addition of two reactive polymers (C and D) which are mutually reactive and are miscible with A and B, respectively, and they form C-graft-D or C-co-D copolymer [68, 74, 77].

It is mentioned that, there are only limited number of chemical structures hat can fulfil the requirements for being a reactive compatibilizing agent [77].

### 1.2.3 Controlled morphology

The process of polymer blending is an attractive technique able to combine properties of different individual blend components and thus generate new high performance polymeric materials. However, most polymer blends are immiscible, which leads to a multiphase structure with various morphologies which is due to the natural properties of polymers (viscosity, viscosity ratio, interfacial tension and reactivity of functional groups), volume ratio as well as processing condition (i.e., temperature, time, and intensity of mixing, and nature of the flow) [78-79].

Most of the properties such as mechanical, optical, rheological, dielectric and barrier properties of the multiphase system depend not only on blend components but also on blend morphology. According to the literature review, there are two main types of morphologies in immiscible polymer blends: the matrix-dispersed structure and co-continuous structure. In Figure 9, various types of blend morphologies are shown [80].

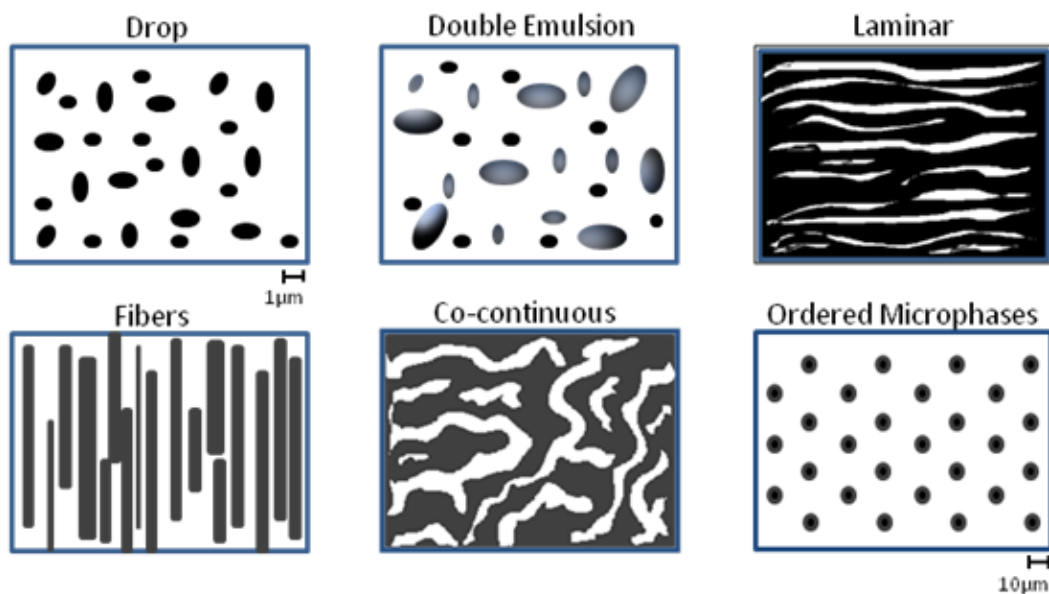


Figure 9. Types of blend morphologies

### ***Co-continuous phase morphology***

During the last few decades, increasing attention was being paid to co-continuous blends which offer well-behaved combined properties than the dispersed structure. Co-continuous structure is a special case of blend morphology in which each phase is fully interconnected through a continuous pathway [81]. It was noticed that co-continuous structures are obtained over a wide range of volume fractions that can be called the co-continuity interval. Most of studies in this field revealed that co-continuous structure occurs near to the phase inversion composition. However, some recent studies remarked that this structure can be obtained in a domain of compositions rather than at a single point and, the formation of co-continuous morphologies, especially at low concentrations, is due to the existence of elongated and interconnected network structures [82]. The formation of these structures is strongly affected by the processing conditions, e.g. the stress levels, volume fraction, viscosity, elasticity and interfacial tension, thus, it can be created and remain only under appropriate conditions. The phase inversion is a process in which two phases reverse: the matrix phase turns into the disperse phase and the disperse phase becomes the matrix one.

### ***Co-continuity and phase inversion predictions***

Several predictions on the phase inversion concentration of two phase system using a number of semi-empirical equations are mentioned. As authors mentioned, the first suggested main parameter for the estimation of phase inversion was the torque ratio of the blend. After this, Paul and Barlow [83] proposed the viscosity ratio of individual polymers as a replacement of mixing torque that is shown by Equation 9-10. However, in case of a big viscosity difference between two polymers, dynamic viscosity can be used.

$$\frac{\phi_1 - \eta_1}{\phi_2 - \eta_2} = \lambda \quad (9)$$

$$\phi_2 = \frac{1}{1 + \lambda} \quad (10)$$

where,  $\phi_{1,2}$ ,  $\eta_{1,2}$  and  $\lambda$  are volume fractions of the blend component, their viscosity and viscosity ratio, respectively. In addition, these equations can be changed by using a prefactor or an exponent for a good adjustment to experimental results.

Krieger and Dougherty [85] derived the equation (Equation 11) with intrinsic viscosity and maximum packing volume fractions.

$$\frac{\eta_1}{\eta_2} = \left[ \frac{\phi_m - \phi_2}{\phi_2 - \phi_1} \right]^{[\eta] \phi_m} \quad (11)$$

where:  $\phi_m$  and  $[\eta]$  are the maximum packing volume and intrinsic viscosity, respectively.  $\phi_m = 0.84$  is accepted to be in case of blends with spherical domains under shear. Furthermore, it is modified by Utracki (Equation 12), but it is responsible for blends with a viscosity ratio range of  $0.1 < \eta_1/\eta_2 < 10$  [84].

$$\phi_{2I} = \frac{1 - \log(\lambda/[\eta])}{2} \quad (12)$$

Another finding was mentioned by Steinmann et al [69], that is illustrated in Equation 13 in which there was a strong correlation between viscosity and elasticity ratio, and the corresponding equation was given based on the viscosity ratio at a certain constant elasticity.

$$\phi_2 = -0.12 \log\left(\frac{\eta_1}{\eta_2}\right) + 0.48 \quad (13)$$

Moreover, the use of the elasticity of blend components for the phase inversion composition was developed by Bourry and Favis [87] in Equation 14-15.

$$\frac{\phi_1}{\phi_2} = \frac{G_2'}{G_1'} \quad (14)$$

$$\frac{\phi_1}{\phi_2} = \frac{\tan\delta_1}{\tan\delta_2} \quad (15)$$

where,  $G_{1,2}'$  and  $\tan\delta_{1,2}$  are the elasticity (storage modulus) and loss angle of the blend phases.

Mechanical properties of the polymer blends, especially the tensile modulus can be used in the determination of co-continuous and phase inversion compositions. Davies suggested the following model, which is accepted as an efficient and simple model by several authors [81, 88].

$$E_B^{1/5} = \phi_1 E_1^{1/5} + \phi_2 E_2^{1/5} \quad (16)$$

where,  $E_B$  and  $E_{1,2}$  are the module of the polymer blend and polymer components, respectively.

Another approach was proposed for the moduli of two-phase material by Budiansky [91]:

$$\frac{\phi_1}{1+\varepsilon\left(\frac{E_1}{E_B}-1\right)} + \frac{\phi_2}{1+\varepsilon\left(\frac{E_2}{E_B}+1\right)}=1 \quad (17)$$

where,  $\varepsilon$  is strain which is expressed below:

$$\varepsilon = \frac{2-(4-5\nu_p)}{15(1-\nu_p)} \quad (18)$$

where,  $\nu_p$  is the Poisson's ratio for the two-phase system.

### ***Applications of the blends with co-continuous morphology***

In recent years, polymer blends with a co-continuous morphology have received much attention because of many desirable properties for a number of promising applications [87]. The structure of this blend can offer improved

mechanical properties such as impact strength and tensile strength. Also, this type of blend has been used to create conductive blends for controlled dissipation of static charge, in which one polymer is liable for the conductive phase whereas the other one is responsible for the mechanical strength [89]. In practice, the package containing moisture permeable phase with a desiccating agent has been used. The co-continuous morphology seems to be very promising for many applications in the packaging and medical fields.

## **AIMS OF WORK**

The aims of this work are development and detailed characterization of the multicomponent polymer blend, which can be utilized for specific applications as a bioactive system for food and pharmaceutical packaging as well as material for medical device preparation.

The key property of the developed bioactive polymeric system is ability to ensure controlled and long lasting release of a bioactive compound (oxygen scavenger, various temperature or pH sensitive indicators etc.), incorporated into the polymer blend. The desired features of the systems mentioned above can be reached by polymer blend morphology controlling through creation so called co-continuous structure, where first polymer matrix serves as a constructional material while second matrix provides the bioactive response to the surrounding environment under given conditions.

The presented work summarize the current state of the art in the field of polymer blending and the already reported knowledge are applied on the developed system based on polyamide 6 and biodegradable co-polyester of polylactide. The main attention is paid to the detailed description of co-continuity formation phenomenon and its occurrence prediction. Moreover, the correlations between morphological arrangement and material properties such as mechanical, rheological, thermal properties are the subsequent goals of this PhD work. Finally, the time dependent release of model component from the blends having various morphologies is the object the detailed investigation to complete the assignment of this thesis.

## RESULTS

The results obtained during the systematic research work on the already introduced topic will be further presented in three separated chapters.

The structure of the chapters consists of an introduction into given field; detailed description of methodology; results and discussion section and conclusions. All presented results are going to be submitted for publication in the impacted journals in a near future. The titles of the chapters are following:

- 3.1 Correlation of morphology and viscoelastic properties of the PA6/BioFlex polymeric blends in molten state
- 3.2 The effect of morphological organization on mechanical and thermal properties of the PA6/BioFlex polymeric blends
- 3.3 Time dependent release of model bioactive component from the PA6/BioFlex polymeric blends with various morphology



## 2. EXPERIMENTAL PART:

### 2.1 MATERIALS AND SAMPLE PREPARATION

#### *Poly(lactic acid) (PLA)*

Poly(lactic acid) (PLA) or polylactide has been receiving more attention because it can be obtained from renewable resources, is biodegradable, can be composted, and can be melted. It can be produced from lactic acid by carbohydrate fermentation or chemical synthesis. For example, Figure 10 shows the production of PLA from lactic acid [90].

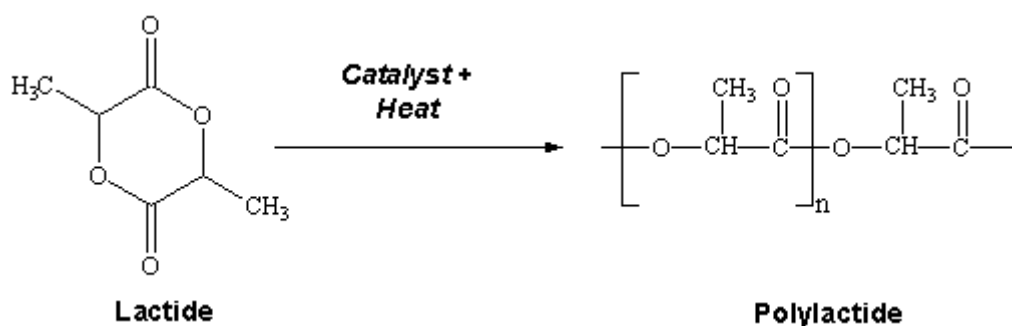


Figure 10: Ring-opening polymerization of the lactide to polylactide [90]

PLA can be a suitable polymer for food packaging, nowadays, it is mostly used as a food packaging polymer for short shelf life products such as drinking cups, salad cups, containers, and overwrap and lamination films [92, 95]. In medical field, PLA is applied for tissue repair and regeneration, surgical sutures and drug delivery system because of its bioresorbability and biocompatible properties in the human body [91, 95]. Apart from its bioability, PLA exhibits many properties that are equivalent to or better than many petroleum-based plastics, which makes it suitable for a variety of applications.

Practically, several types of PLA based blends that consist of base component, PLA and other biodegradable components such as starch, dextrose, minerals, and polyesters as well as special additives have been commercialized and used in numerous applications because of their improved specific properties

and low cost [93]. BioFlex 476F is the one of new PLA based blend available in market, which contains more than 30 % PLA plus biodegradable co-polyester and special additives [93]. In addition, it is a high strength, compostable material [96] and an approval food contact [94].

### ***Polyamide 6 (PA6)***

Polyamide 6 is a thermoplastic that is produced from  $\epsilon$ -caprolactam by the ring-opening polymerization [90]. In Figure 11, the chemical structure of PA 6 is displayed. It offers excellent chemical resistance, higher strength and toughness along with good wear and abrasion resistance properties and gas barrier properties. Moisture in the nylon structure interferes with interchain bonding and adversely affects their properties, including gas barrier. It is sensitive to moisture and drying must be included in processing [114]

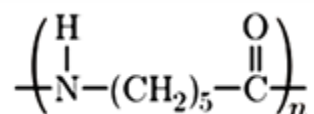


Figure 11: Chemical structure of polyamide 6

PA film has been used increasingly for packaging applications for foodstuffs and pharmaceutical products. In the food packaging, PA 6 films provide excellent barrier properties that keep oxygen out and seal aroma in. In the medical field, PA 6 is fabricated into tough, puncture-resistant packages for medical blister packs. Polyamide will certainly be used even more extensively in all areas, including medical applications. Presently, already it is used in blood transfusion, dialysis, and heart surgery [95]

### ***Crystal violet (CV)***

Crystal violet (CV) known also as gentian violet used as bactericide and an antifungal agent. Its chemical structure is shown in Figure12. CV is stable and incompatible with strong oxidizing agents, and soluble in water and ethanol.

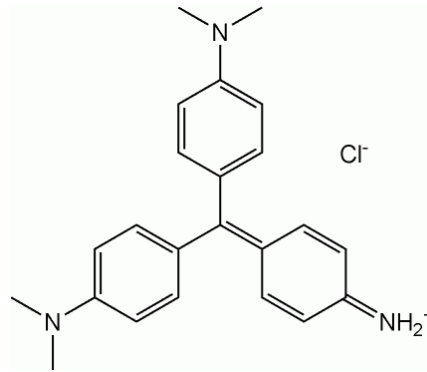


Figure 12: Chemical structure of crystal violet

In medical field, it is effectively used for the treatment of serious heat burns, radiation-induced wound and other injuries to the skin and gums because of its antifungal and antiseptic effects [145].

### ***Polymer mixing***

Polymer mixing is one of the main processing operation to improve the spatial homogeneity of the mixtures that results high-quality products. The basic process involved in mixing is to induce relative motion between the ingredients of the mixture. Bulk or convective motion is the dominant mechanism and it is based typically in pressure difference, creating pressure flow, or a moving boundary, creating drag flow, or a combination of both. In most cases, polymer pairs form immiscible blends because of their limited solubility and nonzero interfacial tension. The mixing of immiscible blends aimed to obtain a dispersed phase with a domain size below a critical level around 1 $\mu$ m [109].

The mixing of two polymers in molten state is considered as liquid-liquid mixture. In the mixing of liquid-liquid system, the properties of the components are affected by the viscosity and the elasticity with their dependence on temperature and strain rate. In addition to these properties, the system properties that describe the interaction between the components are the interfacial tension, interdiffusion rate and the mutual solubility. Immiscible blends show considerable interfacial tension and low mutual solubility [109].

### **Internal mixers**

The simplest type of mixing machine is the internal batch mixer, in which all materials are introduced to a closed chamber where rotor produces a homogeneous mixture [98]. The main process variables in the internal mixing process are:

- batch weight
- material feed temperature
- mixing temperature
- rotor speed
- ram pressure
- sequence and timing of the feeding of the ingredients [98, 109].

## 2.2 CHARACTERIZATION METHODS

This chapter introduces the basic principles of the methods and techniques used in this work.

### **Microscopic analysis**

Microscopic analysis is applied to realize the structure-property relationship of the polymer blend through its morphology. In particular, morphology characterization gives the information on phase structure and distribution of the components, effect of interfacial addition on the particle size, dispersion and agglomeration of particles, and effect of compatibilizer on morphology [68]. Moreover, it is clear that the polymer structures reflect the process variables, and they affect significantly the physical and mechanical properties. Morphologies of the polymer blends are displayed using a number of microscopic methods in several orders of magnitude of length scale [64, 75]. For example, the fracture of a multiphase polymer may require a light-optical technique for the "big picture" but a study at higher resolution using electron microscopy and scanning probe microscopy to see fine details on the fracture surface [99].

#### *Scanning electron microscopy (SEM)*

The scanning electron microscope forms an image by scanning a probe across the specimen using electron beam [100]. SEM has higher resolution and a much larger depth of field. Magnification is from 20-100000 [101] and the resolution of the order 2 nm is achievable [68].

SEM plays important role for a broad range of polymer studies and applications, including surface roughness, adhesive failures, fractured surfaces, networks, and phase boundaries in blends. For the sample preparation in SEM measurement, coating with thin layer (~10 nm) of conductive metal such as gold or platinum is required for surface conductivity to prevent them from charging

up in the electron beam [68, 101]. In addition, for the emphasizing the surface features chemical including solvent or acid exposure and plasma etching is applied. For example, formic acid is used for etching the nylon 6 phase in PP/nylon 6 blends, and hexafluoroisopropanol is employed for etching of the ethylene-vinyl alcohol (EVOH) in PP/EVOH blends [68].

### **Mechanical properties testing**

The mechanical properties of polymeric blends depend on the type of polymer, molecular structure, molecular weight, cross-linking or branching, crystallinity, plasticization, fillers and blending. Also, the environmental or external variables (temperature, time, frequency, moisture content e.g.), testing methods, test procedures are important to evaluate mechanical properties [102-103].

#### *Tensile test*

One of the widely used methods to characterize the mechanical properties of polymer blends is tensile test which examines the stress-strain curve in tension. This curve is generated by the stress that develops elongation at constant rate of extension [68, 103]. The tensile stress is defined as a force per unit of cross-sectional area at any given point.

$$\sigma = F/A \quad (19)$$

where,  $\sigma$ ,  $F$  and  $A$  are the tensile stress, force and area, respectively.

The strain is the elongation to the original length of the test specimen, and given as follows:

$$\varepsilon = \Delta l/l_0 \quad (20)$$

where,  $\varepsilon$ ,  $\Delta l$  and  $l_0$  are the strain, amount of elongation and original length of specimens, respectively.

In Figure 13, the stress-strain curve of a thermoplastic resin displays a number of terms.

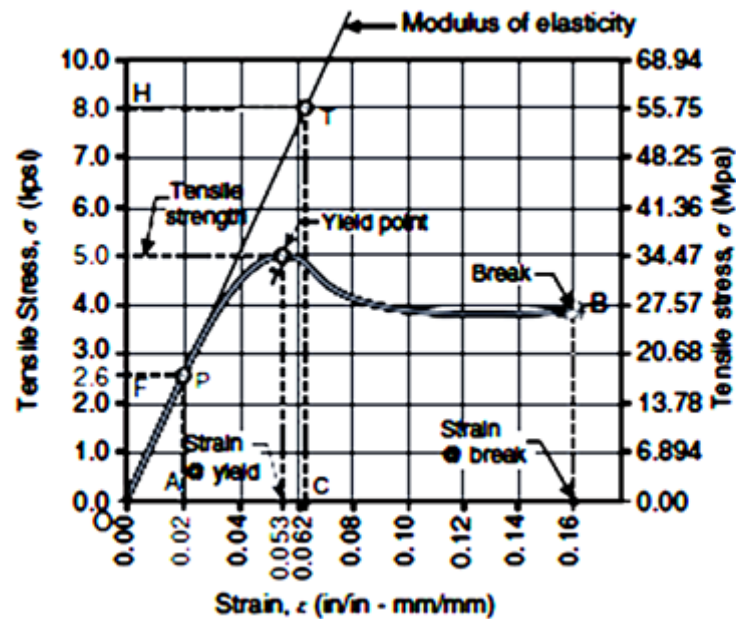


Figure 13: Tensile stress-strain curve of thermoplastic resin [94].

From the Figure 13, it can be seen that the tensile strength is related to the original unstretched dimension and observed at the highest peak on stress-strain curve. The linear part of curve is produced by elastic deformation where stress and strain are proportional. In that case, the slope of such plot gives the tensile modulus (Young's modulus) [101]. Above mentioned two terms are main indicator of the strength and stiffness of the polymer blends.

Yield point appears on the stress-strain curve at which an increase in strain occurs without an increase in stress.

At the higher strain rate, the tensile modulus of the polymer increases, while the elongation rate is decreased [103].

## Impact testing

Impact testing techniques can be used to understand and evaluate the fracture characteristic of polymer. The test measures the impact energy, or the energy absorbed before and after fracture. There are two standard impact tests, Charpy and Izod. Impact tests can be used to determine whether a polymer shows a brittle-to-ductile transition with decreasing temperature [92].

## Thermal analysis

The thermal analysis is used to measure a physical property of a material as a function of temperature [104].

### *Differential scanning calorimeter (DSC)*

DSC measures the difference in heat absorbed or released by a sample, as compared to a reference as a function of time or temperature. This instrument determines specific heat, glass transition temperature, melting and crystallization points, heats of fusion or crystallization, onset of thermal degradation and heat of reaction [68].

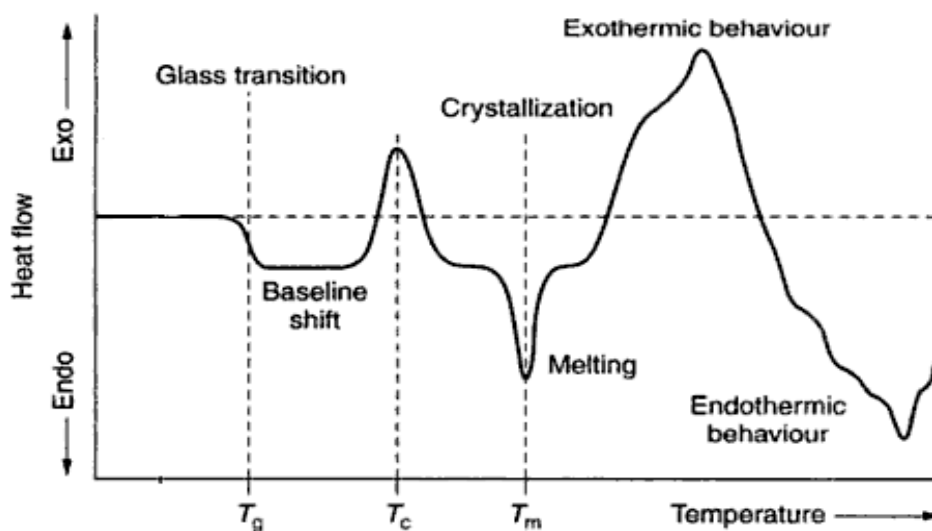


Figure 14: Typical DSC curve obtained for semicrystalline polymer sample [92]



In that method, certain amount of sample (5-20 mg, however to increase sensitivity sample >10 mg) is placed into specific metal (Ag and Cu) pan and examined under heating or cooling rate and the sample temperature can be rapidly changed to allow for sample quenching or heating to determine isothermal crystallization data [68, 105].

Figure 14 shows a typical curve obtained for semicrystalline polymer sample. In this figure, a shift in the baseline results from the change in heat capacity of the sample. The basic equation used in DSC is:

$$\Delta T = qC_p/K \quad (21)$$

where,  $\Delta T$ ,  $q$ ,  $C_p$  and  $K$  are the differences in temperature between the sample and reference, heating rate, heat capacity (at constant pressure), and calibration factor for the particular instrument being used [101].

DSC can be applied for measuring the enthalpy involved in polymer transitions. The peak area between the curve and the baseline is proportional to the enthalpy change in the sample. Change in the enthalpy is described from the area of curve peak:

$$\Delta Hm = KA \quad (22)$$

where,  $\Delta H$ ,  $m$ ,  $K$  and  $A$  are the enthalpy change, weight of the sample, calibration factor and area of the curve peak, respectively [101].

#### *Dynamic mechanical analysis (DMA)*

DMA is the common method to characterize the elastic modulus of a material and its mechanical damping or energy dissipation characteristics as a function of frequency and temperature. Also, DMA determines transitions of polymeric systems. The  $T_g$  is often measured by DSC, but the DMA technique is more sensitive and yields more easily interpreted data [68].

DMA works by vibrating the sample and varying the applied frequency. The changes can be related to the relaxation processes in a polymer. Generally, the stress is varied sinusoidally with time. As a result of time dependent relaxation processes, the strain lags behind the stress. [101].

## **Spectroscopic analysis**

Electromagnetic radiation and the interaction with specific groups of a polymer blend as a function of wavelength is an important method to determine specific interactions between blend constituents.

### *Fourier transform infrared spectroscopy (FTIR)*

FTIR is a technique that is extremely useful for the characterization of polymer blends. This technique is based on the vibrations of the atoms of a molecule. The spectra obtained by passing infrared radiation through a sample and determining which fraction of the incident radiation is absorbed at a particular energy. The energy at which any peak in an absorption spectrum appears corresponds to the frequency of a part of the sample molecule (Stuart, 2005). Infrared radiation ranges from 50-0.8  $\mu\text{m}$  [68].

### *UV-Visible spectroscopy*

UV-vis spectroscopy is used to analyze compounds in the ultraviolet (UV) and visible (Vis) regions of the electromagnetic spectrum. In the UV-vis spectroscopy, light is absorbed by bonding and non-bonding electrons that are maintained from their ground states to higher energy states (excited).

The absorbance is directly proportional to the path length, and the concentration of the absorbing species. Beer's law states that:

$$A = \epsilon lc \quad (23)$$

where,  $e$  is a absorption coefficient [in  $\text{dm}^3 \text{mol}^{-1}$  units],  $l$  and  $c$  are the path length [in cm units] and concentration of absorbent [in  $\text{dm}^3$  units], respectively. Light absorption can occur in 190 nm-900 nm of wavelength range [101].

### **Rheological properties testing**

Rheology is the field of science that studies fluid behaviour during flow-induced deformation. Viscosity is the most widely used material parameter when determining the behaviour of polymers during processing. The rheological properties of the polymers are measured by rheometry [106].

#### *Rotational rheometry*

A rotational rheometer is a type of rheometer in which the shear is produced by a drag flow between a moving part and a fixed one, including plate-plate, cone-plate, and concentric cylinders. This type of rheometer measures the properties under transient and steady state conditions at lowest rates ( $10^{-6}$ - $2.5 \times 10^2 \text{ s}^{-1}$ ) compared to other rheometers. It is used to determine shear viscosity, creep or stress relaxation and elasticity of the material. During the testing, the deformation is obtained by rotating rather than oscillating one plate relative to other [106].

### **Release testing**

In vitro release testing is aimed to measure the availability of bioactive agent quantitatively and qualitatively. The release profile gives the information on structure, interactions between bioactive agent and polymer and their influence on the rate and mechanism of drug release. In fact, releasing amount of bioactive agent is affected by the sample uniformity and testing procedure, i.e. agitation rate, release media and temperature [107]. In order to detect released amount of bioactive agent, spectroscopic analysis is carried out.

## **Water uptake testing**

Water uptake measurement is used to determine the amount of water absorbed under specified conditions. It can be important for the detection of properties of materials because slight amount of water can significantly affect the mechanical, optical, permeability and other properties. Plastic materials have tendency to absorb moisture depending on their type and composition. Also, processing condition affects. In most cases, ASTM D 570 standard is applied for the water uptake measurement of materials [108].

### **3. RESULTS AND DISCUSSION**

#### **3.1 Correlation of morphology and viscoelastic properties of the PA6/BioFlex polymeric blends in molten state**

##### **INTRODUCTION**

Thermoplastic blending of different polymers have been studied widely for many years because this process allows obtaining a new material with specific properties, which are, in some cases, even better than those of the individual homopolymers [87, 110-112].

There are many reasons for blending of polymers together, for instance, achievement of better mechanical or barrier properties. It is known that most of the polymers are immiscible and resulting blends show incompatibility, which is often connected with poor mechanical properties, therefore, blending process usually leads to heterogeneous morphologies. So, methods to improve the adhesion between two immiscible polymers have been subject of considerable research as well [114]. On the other hand, some of the applications can avail the phase separation process, such as preparation of porous materials for medical applications [115].

The main idea presented in this work is the possibility of partially biodegradable polymer blend preparation with co-continuous morphology, where biodegradable polymer can serve as a carrier of an active agent (e.g. drug or other specific substances). The surrounding bioinert polymer can provide optimal mechanical properties and conditions for controlled release of an incorporated bioactive substance. The potential applicability could be found in medicine, agriculture and packaging industry.

In this direction polylactide, PLA, and its co-polyesters seem to be promising materials because of their biodegradability and biocompatibility. PLA based polymers have been reported as suitable materials for medical purposes

including drug delivery systems. In addition, PLA represents one of the possibilities of petroleum based polymers substitution for some of the packaging application due to its availability from some of the natural renewable sources [95-96, 116].

Another attractive polymer is polyamide 6 (PA6). It is suitable for various engineering applications because of its excellent mechanical properties, relatively good process ability as well as chemical resistance against oils and petrol. The key property of PA is its barrier properties against oxygen which makes PA attractive for use in packaging of food and various medicaments [117].

The previous research in the field of polymer blending of both PLA and PA has concentrated on the improvement of their drawbacks in their properties. For instance, PLA and its copolymers have been blended with poly(epsilon caprolactone), starch or polyethylene [118-120]. PA has been blended with e.g. poly(ethylene terephthalate), polystyrene, poly or poly(vinyl chloride) [121-123]. Interestingly, there is a few works dedicated to the blends of PA and biodegradable polyesters based on PLA. One of a few current works dealing with PLA and PA blends (polyamide elastomer in this case) have been reported by *Zhang et al.* This blend was developed for medical purposes as well it is in our case [124]. This encourages us to blend PA6 and PLA based commercially available biodegradable polymer BioFlex to obtain partially biodegradable polymer blend with improved mechanical properties as well as bioactivity towards to the potential applicability of the blend in medical field.

The main objective of the present chapter is the description of the PA6/Bioflex blends preparation and characterization of their viscoelastic properties in molten state in correlation with morphology of the prepared systems. The finding of the blend composition, which provides desired co-continuous morphology, is subsequent aim of this work.

## **EXPERIMENTAL PART**

### ***Materials***

Polyamide 6, Ultramid® B40LN (melting point 220°C, density 1.12-1.15 g.cm<sup>-3</sup>) is product of BASF, Germany. Biodegradable PLA/co-polyester blend, BioFlex® 467F (melting point 155°C, density 1.26 g.cm<sup>-3</sup>) was purchased from FKUR, Germany.

### ***Sample Preparation***

The PA6/Bioflex blends were prepared by using Brabender Plasti-coder kneader. The volume of chamber was 50 cm<sup>3</sup>. The blending was carried out at 230 °C and 25 rpm for 8 min. The resulting products of mixing were pulverized and molded into the thin plate (thickness 1mm) in a manual press at 235°C for 10 min and subsequently cooled under pressure of 10 MPa. The blends of PA6/Bioflex were prepared in ratios of 100/0, 90/10, 75/25, 60/40, 50/50, 40/60, 25/75, 10/90 and 0/100 in wt. %.

### ***Morphological studies***

Scanning electron microscopy (TESCAN VEGA II LMU, Czech Republic, equipped with thermo-emission cathode) was applied to characterize the structural arrangement of PA6 and BioFlex in the prepared blend. The investigation was realized on the impact fracture surface of the specimens PA6/BioFlex 100/0, 90/10, 75/25, 60/40, 50/50 and 25/75. The BioFlex rich specimens (10/90 and 0/100) were too flexible to be fractured. To highlight the morphology of the blend, some of the specimens were treated by chloroform subsequently, which was employed as co-polyester solvent. All specimens were coated with a thin layer of Au/Pd finally. The microscope was operated in high vacuum mode at acceleration voltage 5kV. The investigation of domains size distribution was done by software VEGA Particle Analyzer, version 3.5.12.0.

The measured particle size of the dispersed phase was characterized by evaluating number average diameter  $d_n$  and weight average diameter  $d_w$  from more than 150 articles counterparts. The interparticle distance,  $\tau_p$ , was determined on the basis of Wu's model assuming simple cubic lattice structure (Equation 24) [125]:

$$\tau_p = d_w \times \left( \sqrt[3]{\frac{\pi}{6 \times \phi_{BioFlex}} - 1} \right) \quad (24)$$

where,  $\phi_{BioFlex}$  is volume fraction of BioFlex matrix.

### ***Co-continuity index determination***

The solvent extraction method was used to determine the co-continuous morphology expressed of BioFlex co-continuity index,  $CI_{BioFlex}$ . A piece of polymer sample of circular shape and known composition (diameter 8 mm, thickness 1 mm) was soaked in chlorophorm for 1 week at 35 °C under occasional shaking. After those specimens were taken out, washed by chlorophorm and dried up to the constant weight at 70 °C. The co-continuity index was calculated according the following equation [126]:

$$CI_{BioFlex}(\%) = \frac{m_0 - (m_0 - (m_B - m_A))}{m_0} \times 100 \quad (25)$$

where,  $m_0$  is weight of BioFlex initially presented in the blend,  $m_A$  and  $m_B$  represent weight of the specimens after and before extraction experiment, respectively.

### ***Characterization of viscoelastic properties***

The viscoelastic properties of the prepared PA6/BioFlex blends were investigated in molten state by using rotary viscometer (ARES 2000,



Rheometrics). A parallel-plate measuring geometry (diameter 25 mm) with gap about 1 mm was used, employing a small strain (1 %) to maintain the measurements within the linear viscoelastic region. Dynamic frequency sweep tests were carried out at 235°C, 240°C and 250°C to follow, storage ( $G'$ ) and loss ( $G''$ ) modulus as a function of frequency,  $\omega$ , from 0.1 to 100 rad.s<sup>-1</sup>. Another parameter describing viscoelastic behavior, complex viscosity ( $\eta^*$ ), was calculated by following equation:

$$\eta^* = \sqrt{\left(\frac{G'}{\omega}\right)^2 + \left(\frac{G''}{\omega}\right)^2} \quad (26)$$

## RESULTS AND DISCUSSION

### *Morphological studies*

The SEM pictures of non-treated binary PA6/BioFlex blends are shown in Figure 15. It can be noticed, the PA6 rich samples (PA6/Bioflex 90/10 (Figure 15a), 75/25 (Figure 15b) and 60/40 (Figure 15c)) show typical distribution of two incompatible polymeric matrixes. The size of dispersed BioFlex domains is increasing with its raising content in the blend up to 50 wt. % (Figure 15d). At this composition, there is no clear border between dispersed and continuous phase. The similar situation can be observed for 60 wt. % of BioFlex (Figure 15e). On the other hand, further increase of biodegradable component leads to the system with inverse configuration, where BioFlex creates continuous phase and PA6 is dispersed within it (Figure 15f). Furthermore, SEM observations reveal weak adhesion between both polymers.

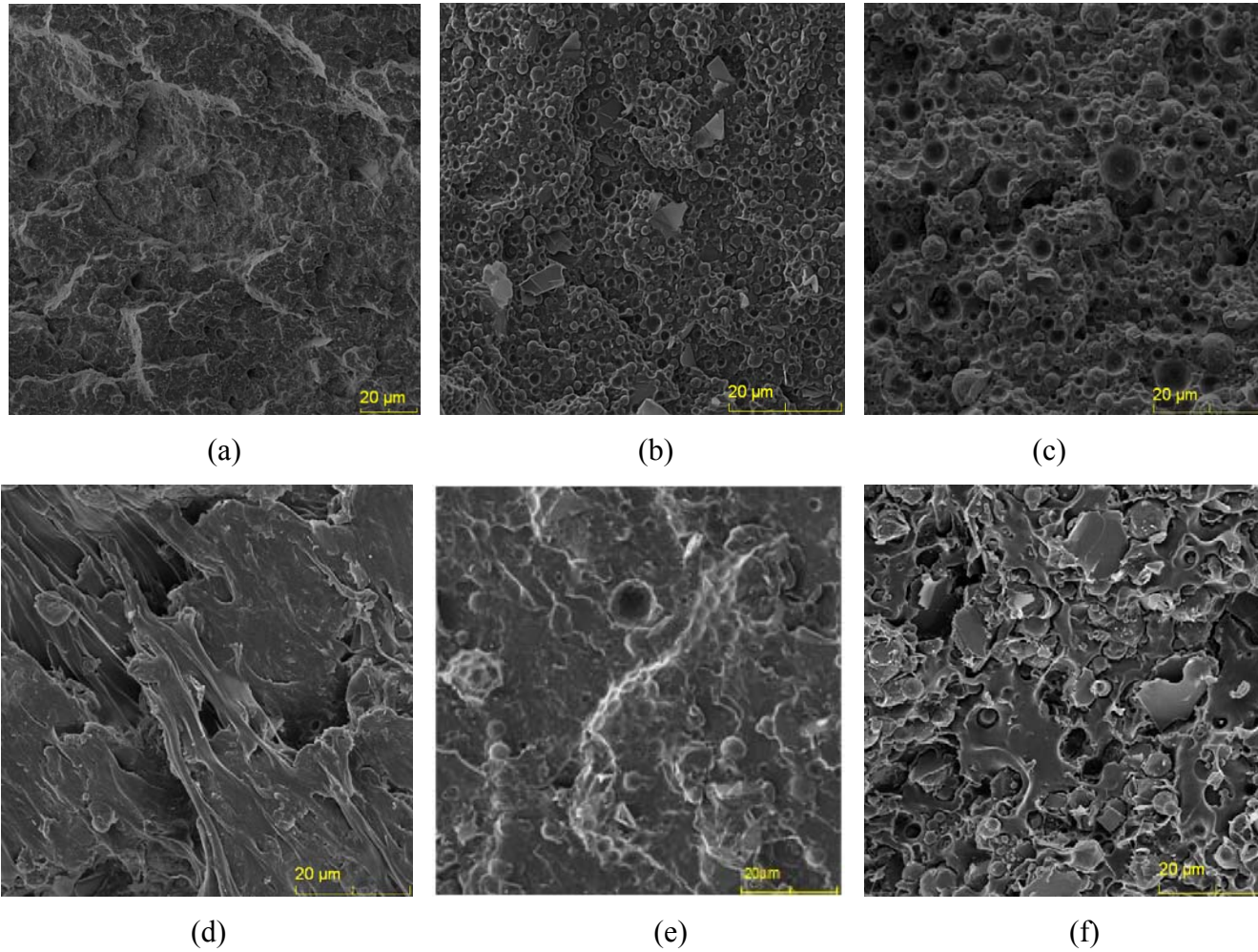


Figure 15: SEM picture of the cold fractured specimens of PA6/BioFlex blends (a) 90/10, (b) 75/25, (c) 60/40, (d) 50/50, (e) 40/60 and (f) 25/75 (wt. /wt.) before chloroform treatment

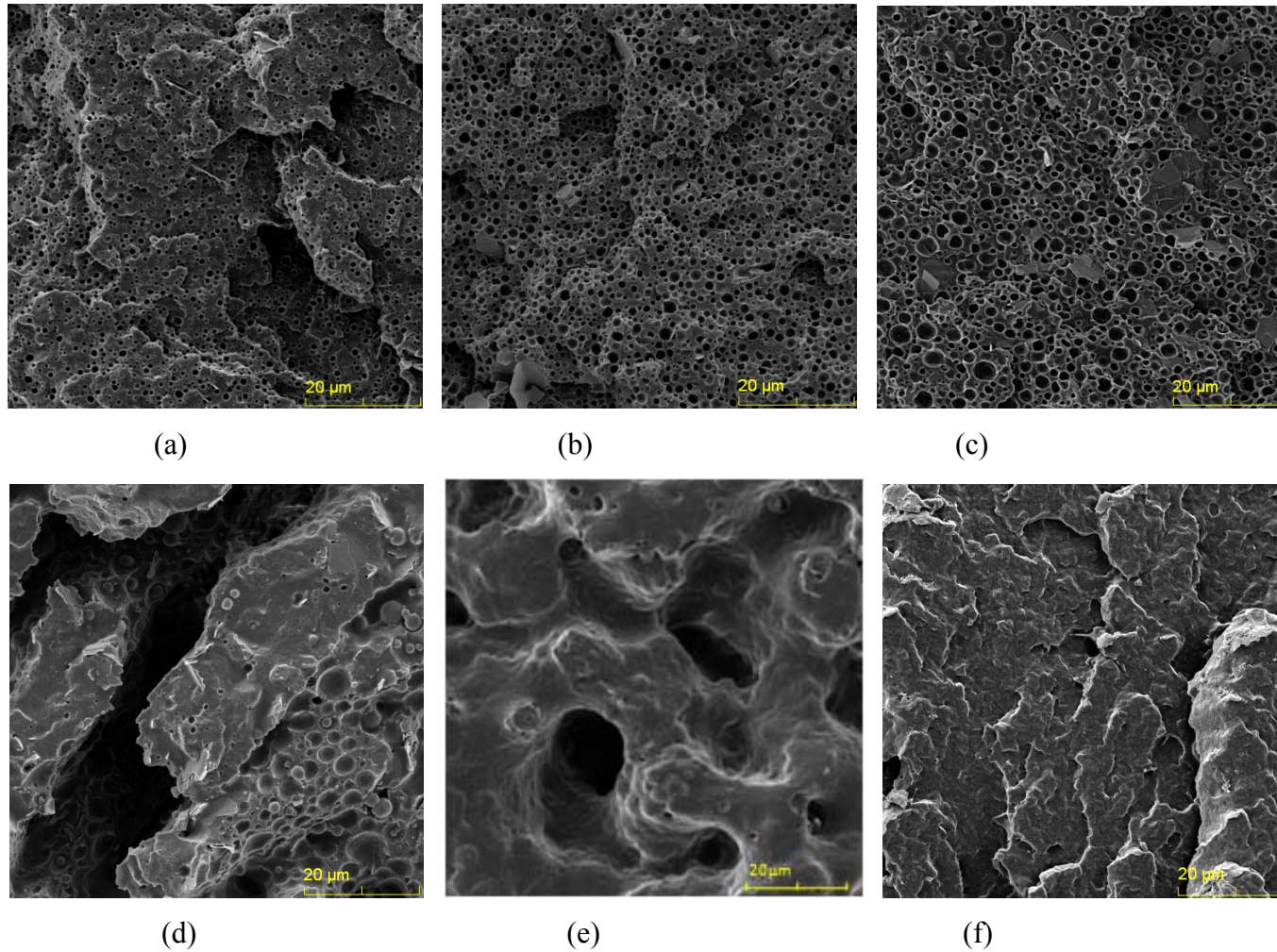


Figure 16: SEM picture of the cold fractured specimens of PA6/BioFlex blends (a) 90/10, (b) 75/25, (c) 60/40, (d) 50/50, (e) 40/60 and (f) 25/75 (wt./wt.) after chloroform treatment

Better visualization of the blends morphology can be obtained by dissolution of BioFlex phase by chloroform treatment of the investigated specimens. SEM pictures of treated fractures can be seen in Figure 16. It has been mentioned above that PA6 rich blends are characteristic of occurrence of BioFlex domains. They are the consequence of PA6 and BioFlex mutual immiscibility and their dimensions increase with BioFlex content. The chloroform treatment allows the statistical analysis of the domains size distribution, which is shown in Figure 17. It can be noticed that the blend with low content of BioFlex (10 wt. %, Figure 16a) has narrow distribution of its domains dimensions. The blend with the composition PA6/BioFlex 75/25 (Figure 16b) has much broader distribution and the diameters of the domains are shifted towards higher values and the same trend can be observed for the sample containing 40 wt. % of BioFlex (Figure 16c). The growing of the dimensions is expected until phase inversion point.

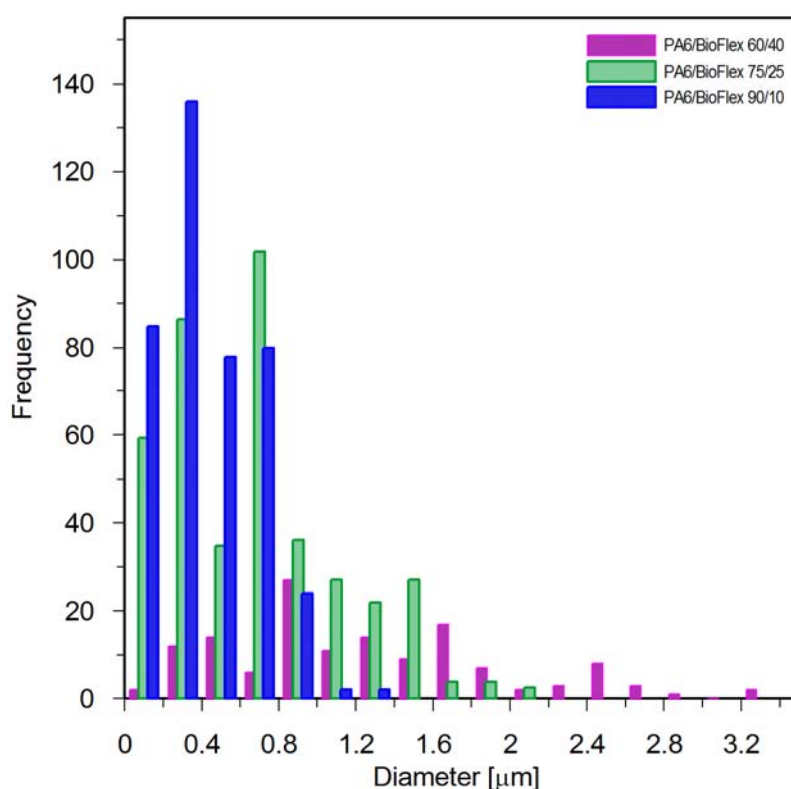


Figure 17: Particle size (diameters) distribution of the BioFlex domains within PA6/BioFlex blends

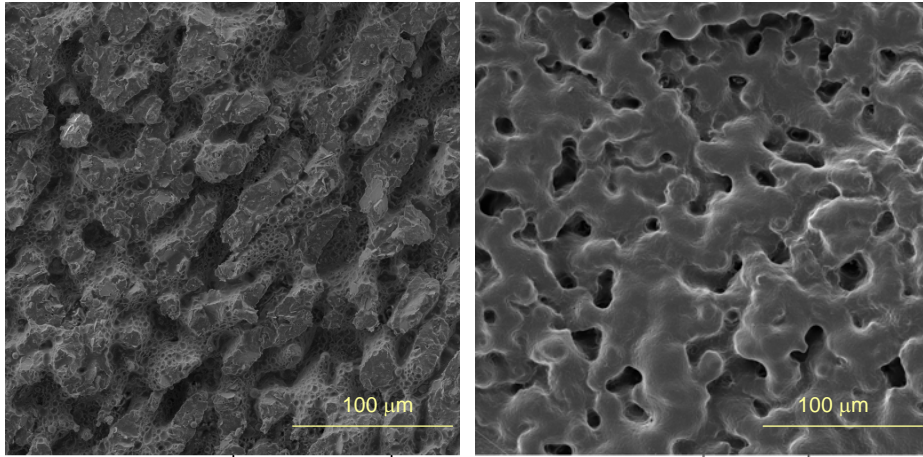
The measured particles size was characterized by evaluating number average diameter  $d_n$  and weight average diameter  $d_w$  and interparticle distance  $\tau_p$ . The obtained data are shown in Table 3. It can be noticed that the increased content of BioFlex is followed by raised  $d_w$ . Polydispersity ( $d_w/d_n$ ) is increased significantly at 40 wt. % of BioFlex presence which indicates the formation of co-continuity structure. The interparticle distance,  $\tau_p$  decreases when the concentration of BioFlex is raised to 25 wt. %. However, co-continuity formation leads to aggregation of the co-polyester and formation of the larger domains, which are transformed into continuous phase with further BioFlex addition.

Table 3: Characteristics of the BioFlex domains dispersed within PA6 matrix

<b>PA6/BioFlex</b>	<b><math>d_n</math> [<math>\mu\text{m}</math>]</b>	<b><math>d_w</math> [<math>\mu\text{m}</math>]</b>	<b><math>d_w/d_n</math></b>	<b><math>\tau_p</math> [<math>\mu\text{m}</math>]</b>	<b><math>d_z</math> [<math>\mu\text{m}</math>]</b>
90/10	0.42	0.57	1.35	0.45	0.67
75/25	0.67	0.97	1.45	0.31	1.18
60/40	0.42	4.96	11.8	0.58	1.96

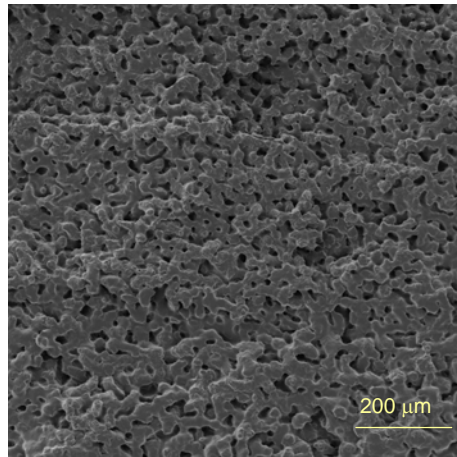
Rather different morphology can be seen in case of PA6/BioFlex 50/50 (Figure 16d) and 40/60 (Figure 16e), where large channels of BioFlex phase are created within PA6 matrix. It reveals the occurrence of a phase inversion process and formation of co-continuous structure, which is characteristic by appearance of two parallel continuous phases. The chloroform treatment of BioFlex rich blend is not suitable and the SEM observations of such specimens do not provide relevant information about morphology of these samples due to dissolution of BioFlex matrix as happened in case of PA6/BioFlex 25/75 (Figure 16f). This can be clearly seen in Figure 18 where SEM photographs of PA6/BioFlex 50/50 (Figure 18a) and 40/60 (Figures 18b and 18c) blends after chloroform treatment shown in lower magnification is presented.





(a)

(b)



(c)

Figure 18: SEM picture of the cold fractured specimens of PA6/BioFlex blends (a) 50/50, (b) 40/60, (c) 40/60 (lower magnification) after chloroform treatment

### ***Co-continuity index determination***

The co-continuity index,  $CI_{\text{BioFlex}}$ , determined by Equation 25 is plotted against BioFlex concentration in Figure 19. As it can be seen, the value of  $CI_{\text{BioFlex}}$  is equal zero for PA6 rich blends (pure PA6, PA6/BioFlex 90/10 and 75/25), which is the consequence of not availability of the polyester based dispersed phase entrapped in PA6 continuous phase. However, the blends above 40 wt. % of BioFlex show certain degree of co-continuity. It is rising with increasing biodegradable component presence and it approaches 100 % at 60 wt. % of BioFlex. The BioFlex rich blends were disintegrated during extraction process, thus their  $CI_{\text{BioFlex}}$  is considered as zero. These observations fully correspond to SEM study presented above (see Figures 15, 16 and 18).

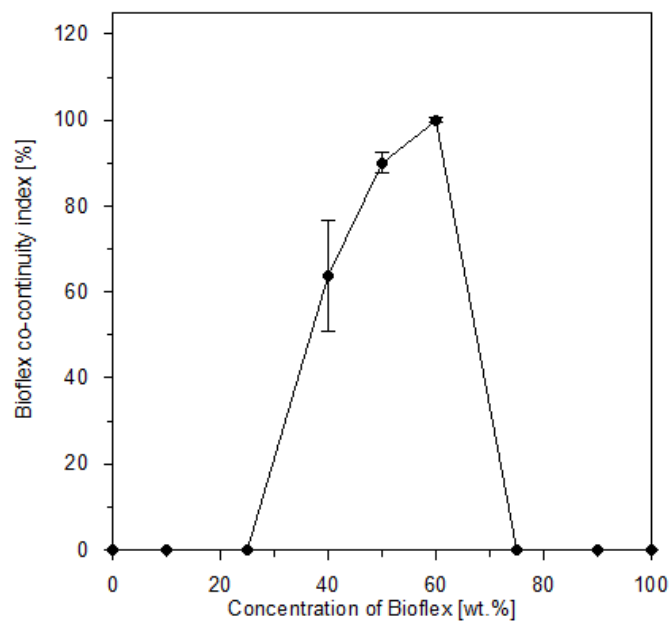


Figure 19: Co-continuity index versus BioFlex concentration

## *Characterization of viscoelastic properties*

### **Angular frequency dependence**

The elastic properties of the blends in form of storage modulus ( $G'$ ) angular frequency dependencies at 240 °C are depicted in Figure 20. As it can be noticed both polymer matrixes (PA6 and BioFlex) have considerably different elastic properties. While pure PA6 shows significant linear increase of  $G'$  with rising  $\omega$ , BioFlex shows non-linear elasticity. The addition of low amount of the biodegradable polymer causes noticeable increase of  $G'$  values (more than 1100 %, taken at 240°C and 1 rad.s<sup>-1</sup> for the sample 75/25). The slope of PA6 rich blends (up to 25 wt. % of BioFlex) is significantly higher than other blends. On the other hand, its slight decrease can be observed with increasing BioFlex concentration and it becomes the same at the highest studied frequencies (20-100 rad.s<sup>-1</sup>). The blends with co-polyester content above 40 wt. % have similar  $G'$  frequency dependence to the pure BioFlex, which is characteristic by convex shape of the curve, unlike the former discussed PA6 rich blends. In addition, minimal difference in  $G'$  at  $\omega > 10$  rad.s<sup>-1</sup> can be seen in case of the dependence  $G'$  vs.  $\omega$ . It is similar to the pure PA6 up to  $\omega = 1$  rad.s<sup>-1</sup>. The data obtained at low  $\omega$  reveal that the blend 50/50 has the lowest  $G'$  from this group of studied blends.

The angular frequency dependences of loss modulus,  $G''$ , describing viscous properties at 240 °C are shown in Figure 21. The trends have certain analogy with  $G'$  observed in Figure 16. Pure PA6 and the blends containing up to 25 wt. % of BioFlex have significantly higher  $G''$  than the rest of the samples over whole range of frequencies. As well as in previous case, presence of small amount of the biodegradable component increases  $G''$  values in comparison to the pure PA6 at  $\omega < 1$  rad.s<sup>-1</sup>.

The logarithmic dependences of complex viscosity,  $\eta^*$ , on the angular frequency of the samples at 240 °C are shown in Figure 22.



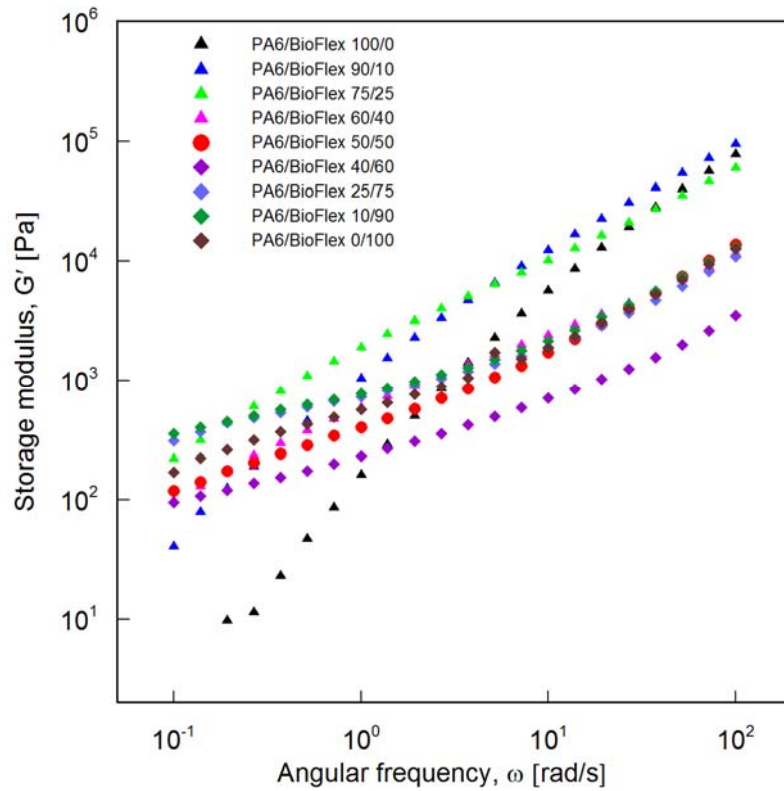


Figure 20: Storage modulus as a function of angular frequency (at 240°C)

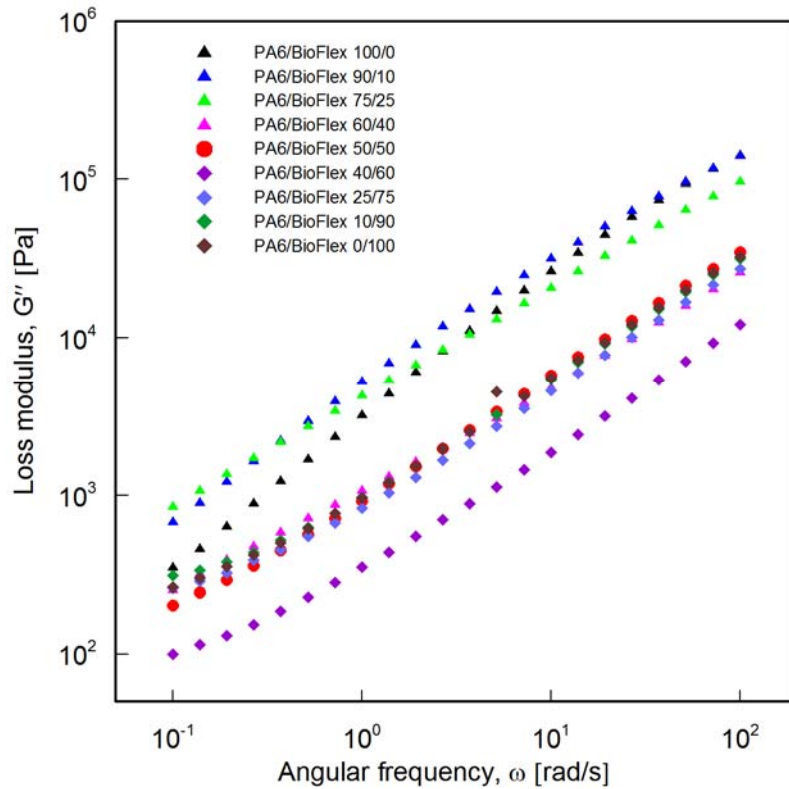


Figure 21: Loss modulus as a function of angular frequency (at 240 °C)

The pure PA6 proves Newtonian like behavior at low and middle  $\omega$  (up to  $1 \text{ rad.s}^{-1}$ ). Its complex viscosity is  $\eta^* = 3.2 \times 10^3 \text{ Pa.s}$  and then slightly decrease with increasing  $\omega$ . Similar trend was observed for the blend 90/10. However,  $\eta^*$  raised approx. to  $6.5 \times 10^3 \text{ Pa.s}$  (at  $\omega = 5.4 \times 10^3 \text{ rad.s}^{-1}$ ) and the decrease at higher  $\omega$  was more noticeable. The composition 75/25 seems to be border between two different kinds of complex viscosities behavior. The almost linear decrease of  $\eta^*$  in double logarithmic coordinate plot was found over the investigated frequency range for the blends up to 25 wt. % of the copolyester content. The blend 50/50 and others, with higher additions of BioFlex (25/75, 10/90 and 0/100), generally, have similar trends, which can be divided into two parts. At first, relatively sharp decrease of  $\eta^*$  were observed from 0.1 to  $1 \text{ rad.s}^{-1}$ . The lowest  $\eta^*$  values were found for 50/50. Second phase represents decreasing  $\eta^*$  at  $\omega > 1 \text{ rad.s}^{-1}$  as well, however the slope is not so steep.

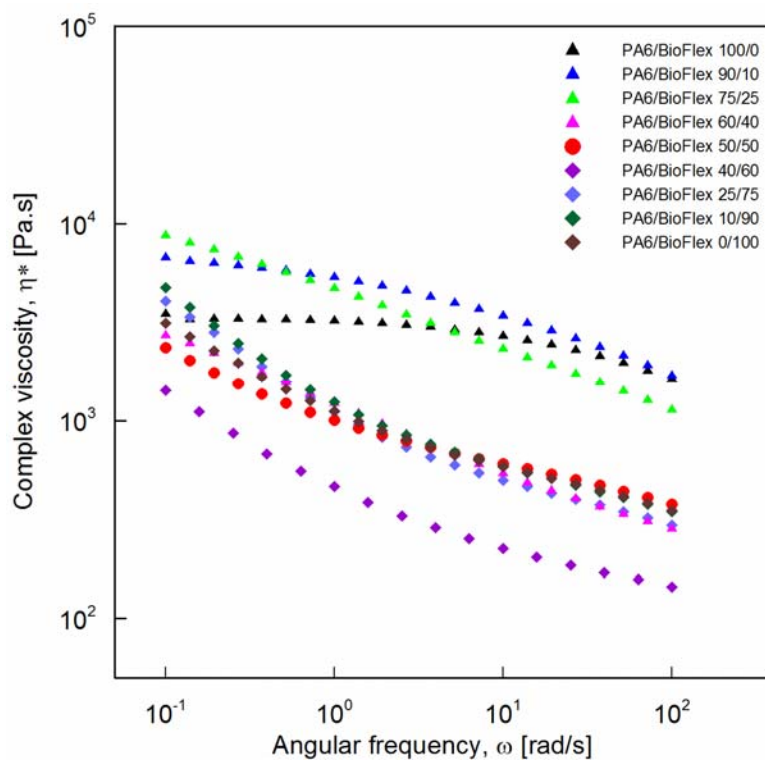


Figure 22: Complex viscosity as a function of angular frequency (at  $240 \text{ }^\circ\text{C}$ )

Remarkable difference in rheological properties of both polymers should be considered to explain the viscoelastic behavior of the investigated blends described above (Figures 20-22). PA6 proves  $\eta^*$  almost three times higher (taken at 240°C) than BioFlex, which has melting point at 160 °C. However, the results from rheological measurements show increased elasticity of the polymer melt at low  $\omega$  for PA6 rich samples. This is noticeable especially in Figure 20. The explanation of such enhancement could be consequence of droplet-matrix morphology (see Figures 15-16) of the samples, which is typical for immiscible polymer blends. It has been shown that this kind of morphology displays relaxation in long time range, mostly shape relaxation of the deformed droplets. This process is mostly driven by the interfacial tension [82, 127-131]. On the other hand, shape relaxation is less visible in case of co-continuous morphologies [132]. The reason of the observed phenomenon could be found in possible PA6 and BioFlex interface interactions, which is considerable at low concentrations of the biodegradable matrix (up to 25 wt. %). The parallel features of viscoelastic properties were also found in the dependences taken at 235 and 250 °C.

### **Composition dependence**

In order to clarify the influence of one of the components of the blend on the rheological properties, composition dependences of selected rheological properties are discussed below. The composition dependences of complex viscosity,  $\eta^*$ , observed at 240°C at various angular frequencies,  $\omega$  (0.373, 3.73 and 37.3 rad.s<sup>-1</sup>), are shown in semilogarithmic coordinate plot (Figure 23). As it can be seen both positive (PDB) and negative (NDB) deviation behaviour from the logarithmic additivity rule (expressed by dashed lines in the Figure 23) were observed for the studies of polymer blends over whole range of their compositions. While PDB is the characteristic for homogeneous polymer mixtures and heterogeneous,

emulsion-like immiscible blends, NDB is typical for the systems showing immiscibility and phase separation. The PDB-NDB phenomenon was noticeable especially for the measurements at low  $\omega$  and it was reduced with increasing  $\omega$ . PDB is typical for PA6 rich blends up to 25 wt. % of BioFlex content. Higher concentrations of biodegradable matrix lead to a change into NDB. It is also obvious that the PDB-NDB turning point is shifted towards higher BioFlex concentrations with rising  $\omega$ . Moreover, the curve corresponding to the results taken at low  $\omega$  shows even second turn into PDB for BioFlex rich blends (over 80 wt. %). According to the literature already published, the conversion from PBD to NDB at certain co-polyester concentration can be related to the phase inversion point [84].

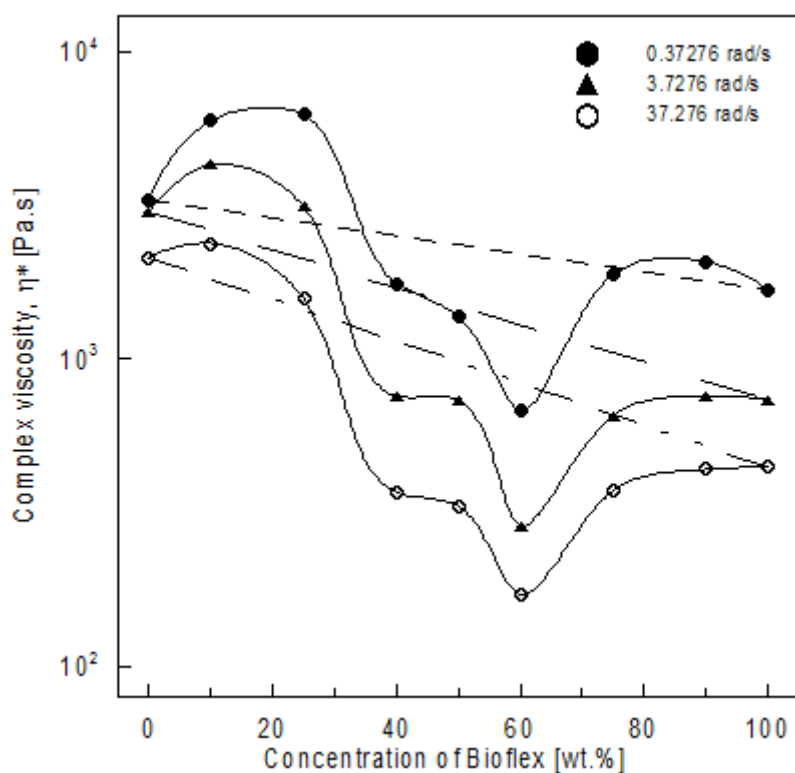


Figure 23: Complex viscosity versus BioFlex content in the blends

The enhanced elasticity of the PA6 rich blends is clearly visible in Figure 24, where  $G'$  versus BioFlex concentration for various  $\omega$  is depicted. The values of  $G'$  were above additivity rule over whole concentration range

of BioFlex at lowest  $\omega$ . Nevertheless, PDB-NDB effect occurs at higher  $\omega$  due to a possible vanishing of the interfacial interactions at higher shear strain rates. The minimal  $G'$  was observed for PA6/BioFlex 40/60 in all cases. This concentration can be considered as the point where interfacial area reaches its minimum and fully co-continuous interpenetrated phase morphology can be expected [126].

It should be repeated that similar trends were obtained for the measurements proceeded at 235 and 250 °C, which are not presented here. The total values of the studied viscoelastic characteristics were obviously shifted due to temperature effect.

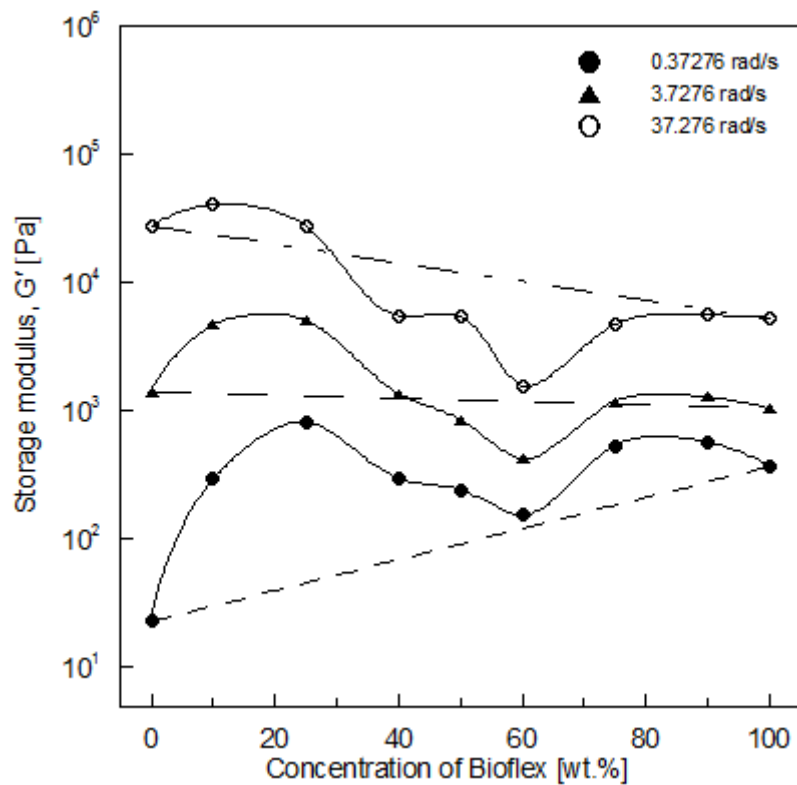


Figure 24: Storage modulus versus BioFlex content in the blends at various angular frequencies

The activation energy ( $E_a$ ) can validate the presented data. The values of  $E_a$  for various  $\omega$  were determined by using modified Arrhenius formula (Equation 27):

$$\ln \eta^* = \ln A - \left( \frac{E_a}{R} \right) \frac{1}{T} \quad (27)$$

where,  $\eta^*$  (Pa.s) is complex viscosity of the material taken given temperature, T (K), at  $\omega$  of 0.373, 3.73 and 37.3 rad.s<sup>-1</sup>, respectively. A is experimentally determined pre-exponential factor and R represents universal gas constant (8.314 J.K<sup>-1</sup>.mol<sup>-1</sup>). The concentration dependencies of  $E_a$  are shown in Figure 25. These results confirm the assumption of the effect of interfacial tension in case of PA6 rich samples. The slope of the linear fit extends the concentration effect of highly viscous BioFlex on rheological properties of the blends, which is strongly dependent on the level of mechanical energy applied to the systems expressed in form of oscillatory movement, which acts against possible polymer-polymer cohesive interactions in the blended material.

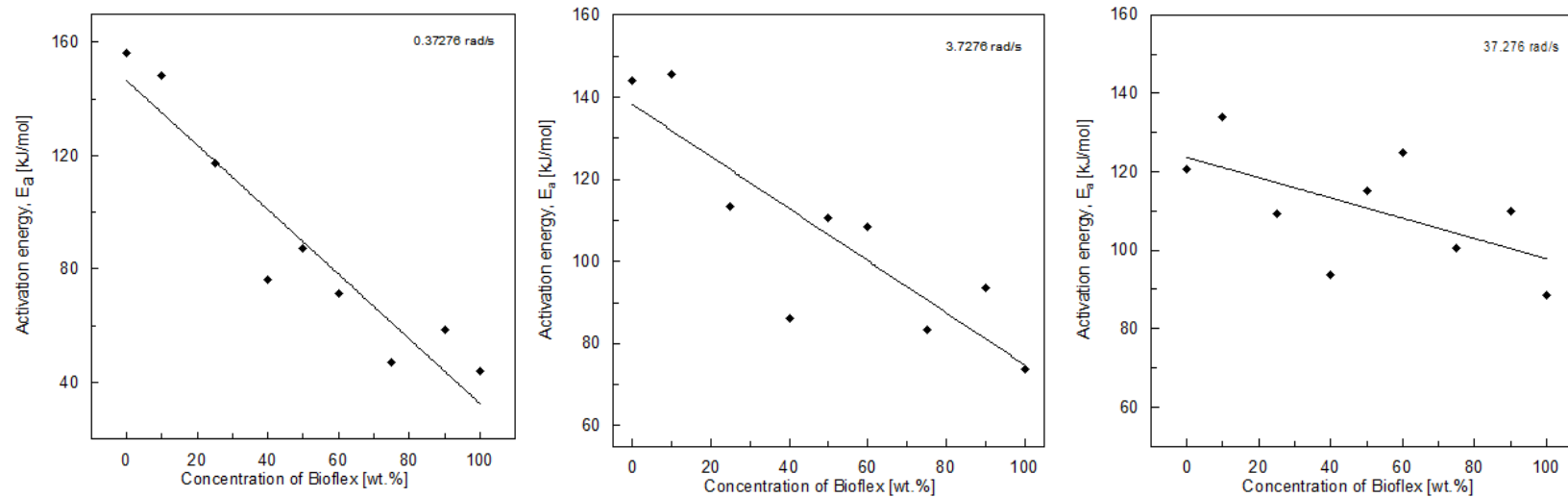


Figure 25: Activation energy calculated according the Equation 27 versus BioFlex concentration in the blend at various angular frequencies

### *Comparison of experimental data with some of the already reported models for phase inversion prediction*

As it has been presented by Tol et al. [132], the occurrence of phase inversion phenomenon and formation of co-continuous network structure was long time believed to be only possible in a narrow composition range. It led to the attempts to predict the phase inversion point. The following part of this work will compare some of the published methods of phase inversion prediction with our experimental data.

Many works have been published assuming an indication of co-continuous phase formation, which is connected with phase inversion of the immiscible components in the system. The principles of this phenomenon can be found in model of an emulsion. When a small amount of a liquid 1 is added to a liquid 2, droplet dispersion of the minor phase liquid is created. The matrix is formed by major phase of the liquid 2. At certain concentration of liquid 1/liquid 2 mixture the dispersed phase becomes matrix and vice versa. This concentration is known as the phase inversion concentration,  $\phi_I$ , and it is expressed by following equation:

$$\phi_{1I} = 1 - \phi_{2I} \quad (28)$$

where,  $\phi_{1I}$  and  $\phi_{2I}$  represents volume concentration at phase inversion point of the liquid 1 and 2, respectively [83].

The first expression for predicting the co-continuity formation we compare in this work was proposed by Paul and Barlow already in 1980 (Equation 9-10 which is already presented in chapter 1.2.3) [85]. It is based on viscosity ratio,  $\lambda$ , of the pure components. Viscosities of the polymer 1 ( $\eta_1$ ) and polymer 2 ( $\eta_2$ ) (in case of binary polymer blend) should be taken at the shear rate used for preparation of the blends. Some of the publications substitute viscosity by torque [121].



$$\frac{\phi_{1I}}{\phi_{2I}} = \frac{\eta_1}{\eta_2} \equiv \lambda$$

The effect of elasticity (i.e. contribution to interfacial tension) on the prediction of the phase inversion concentration was presented by Bourry and Favis and it is the modification of the Equation 9-10. The influence of elasticity factor on phase inversion point is considered here by using two measures; storage modulus,  $G'$  and phase angle  $\tan \delta$  [87] which is already displayed by the Equation 14-15 in the Chapter 1.2.3.

$$\frac{\phi_{1I}}{\phi_{2I}} = \frac{G'_2}{G'_1}$$

$$\frac{\phi_{1I}}{\phi_{2I}} = \frac{\tan \delta_1}{\tan \delta_2}$$

Following equation is displayed by Equation 12 in the first chapter and modified by Utracki [84]. It includes intrinsic viscosity  $[\eta]$  of the component. Its use is limited to:  $0.1 \leq \lambda \leq 10$ .

$$\phi_{2I} = \frac{1 - \log(\lambda/[\eta])}{2}$$

The phase inversion compositions calculated by the Equations 9, 12 and 14-15 are shown in Table 4. It is required to mention that indexes 1 and 2 stand for PA6 and BioFlex, respectively. The values of  $\eta$ ,  $G'$  and  $\tan \delta$  used for all calculations were taken at  $\omega = 100 \text{ rad.s}^{-1}$ . In case of Equations 9 and 12, the phase inversion concentration of BioFlex,  $\phi_{2I}$ , is also obtained by torque ratios of pure PA6 ( $\tau_{\text{PA6}}$ ) and BioFlex ( $\tau_{\text{BioFlex}}$ ) detected during blend preparation. Intrinsic viscosity of BioFlex,  $[\eta]$  (Equation 11), was determined by using Ubbelohde viscometer. The measurement was carried out in chlorophorm at  $30^\circ\text{C}$ . It was found that  $[\eta] = 1.30 \text{ dL.g}^{-1}$ .

The calculated values of  $\phi_{2I}$  differ significantly from the relatively low contents of BioFlex to the concentrations approaching almost 90 wt. %

(Table 4). The measurement temperature effect on the phase inversion prediction is not significant and the obtained values slightly increase with rising temperature of the rheological measurements.

Table 4: Phase inversion compositions of the PA6/Bioflex systems calculated on the basis of various models

Models	Phase inversion composition of PA/BioFlex system							
	235°C		240°C		250°C		Torque based calculation	
	vol. %	wt. %	vol. %	wt. %	vol. %	wt. %	vol. %	wt. %
$\frac{\phi_1}{\phi_2} = \frac{\eta_1}{\eta_2} = \lambda$	16.7	18.4	17.9	19.7	19.6	21.0	19.8	21.7
$\frac{\phi_1}{\phi_2} = \frac{G'_2}{G'_1}$	87.3	88.6	86.0	87.7	84.1	85.6	-	-
$\frac{\phi_1}{\phi_2} = \frac{\tan \delta_1}{\tan \delta_2}$	59.7	62.5	58.7	61.5	57.6	60.4	-	-
$\phi_2 = \frac{(1 - \log \lambda / [\eta])}{2}$ ; [ $\eta$ ] = 1.3	20.8	22.8	22.6	24.7	24.4	26.7	25.4	27.7

The calculation done on the basis of  $\tau_{PA6}$  and  $\tau_{BioFlex}$  ratio does not vary from the viscosity based calculations in Equations 9. However, it is closer to the values obtained at highest tested temperature (250°C). Similar discrepancies were reported by e.g. Omonov et al., who used several models for phase inversion predictions of polypropylene/polystyrene blends [82]. It could be assumed that synergism of polymer-polymer mutual interaction as well as their chemical structure and processing conditions are responsible for co-continuous morphology establishment. Thus, the individual models used

in this study can hardly consider all factors which are relevant here. On the other hand, comparison of these models with experimental data may reveal which factor is predominant in the given system.

In our case the model designated as Equation 15 here seems to correspond to the experimental data. Both SEM and rheological investigations reveal that there is relatively wide concentration range where co-continuous structure may exist (50-60 wt. % of Bioflex). It is not in discrepancies with the works reported during the last decade. The most of the semi-empirical equations used for inversion point calculation are related to viscosity ratio of the blend components i.e. the tendency of the lower viscous polymer to encapsulate the higher viscous component is considered. However, it has been proved that phase inversion is not dependent on viscosity ratio solely and co-continuous structure can be reached over wider interval of concentrations (co-continuity interval) [133-142].

Since the relatively good correlation of experimental data with model in Equation 15, the elasticity effect contributing to interfacial tension could be considered as significant in the studies PA6/BioFlex systems.

### **3.2 The effect of morphological organization on mechanical and thermal properties of the PA6/BioFlex polymeric blends**

#### **INTRODUCTION**

In recent years the study of the structure-property relationship of multicomponent polymer systems has gained a great deal of attention as a consequence of their wide technological applicability. Most of these systems are constituted by scarcely miscible polymers forming multiphase materials whose properties can be greatly affected by the mode of dispersion, size and orientation of the phases. Moreover, interface interactions between the components can often arise during the mixing of polymer melts and influence the nucleation and growth of the crystalline phases. Thus, mechanical properties of the polymer blends are known to be strongly dependent on morphological parameters of the systems. It means that resulting mechanical properties of a blend can be rarely correlated to the simple composition correlation [143].

The aim of this chapter is to determine the influence of morphological factors on mechanical and thermal properties of the resulting blend based on PA6 and BioFlex. Morphological studies have been already presented in previous chapter, so, the description of the mechanical properties investigation will be discussed further. In addition, structural analysis done by Fourier transform infrared spectroscopy followed by practical consequence on water uptake ability will be described here as well since this parameter has crucial effect on practical applicability of the developed material.

## **EXPERIMENTAL PART**

### **Testing of mechanical properties**

#### ***Static tensile measurements***

Mechanical properties of pure PA 6 and BioFlex as well as their blends, which were prevented from moisture absorption, were measured on INSTRON 8871 at 23 °C, 40% relative humidity. The initial length of samples was 50 mm, width 10 mm, and thickness about 150  $\mu\text{m}$ . The speed of the moving clamp was 20 and 200  $\text{mm}\cdot\text{min}^{-1}$ . Specimens were conditioned at 25 °C and 50 % RH for 1 week before testing. Each set of the sample consisted at least of 10 specimens.

#### ***Impact strength***

The impact strength (Charpy) of the blends was tested by using ZWICK 5113 testing machine equipped with 5J hammer. The dimensions of the specimens were approx. 80, 10 and 4 mm in length, height and width, respectively. The testing was carried out at 23 °C and 40 % RH. Five specimens from each mixture were tested minimally.

#### ***Dynamic mechanical analysis (DMA)***

Dynamic mechanical properties of PA/Bioflex composites in the form of rectangular bars with dimensions of 50X10X1 mm were investigated using DMA 242 analyzer (Netzsch, USA). The measurements were carried out in three point bending mode of the equipment and corresponding viscoelastic properties, storage modulus  $E'$ , loss modulus  $E''$  and  $\tan \delta$  were determined as a function of temperature. The temperature range used was at -20 to +120°C with the heating rate of 2 °C/min under liquid nitrogen flow. The samples were scanned at the frequency of 1 Hz with a static strain of 0.3% and dynamic strain of 0.1%.

## **Testing of thermal properties**

### ***Differential scanning calorimetry (DSC)***

The thermal properties of the blends were analyzed using a NETZSCH DSC 200 F3 under nitrogen flow 60 ml/min. Samples were tested by triple cycle heating- cooling-heating from 0 °C to 250 °C (10 °C/min). The value of  $T_g$  was determined in the second heating cycle at the midpoint stepwise increase of the specific heat associated with glass transition. Melting temperature ( $T_m$ ) was determined from the thermogram. Melting enthalpy ( $H_m$ ) of PLA matrix was gained after subtracting the enthalpy of cold-crystallization and subsequently divided by the weight fraction of PLA in the sample.

### ***Fourier transform infrared spectroscopy-Attenuated total reflectance (FTIR-ATR)***

To identify the physico-chemical structure of pure PA6, BioFlex and their blends FTIR spectroscopy analysis was carried out. The experiments were conducted on films by NICOLET 320 FTIR, equipped with attenuated total reflectance (ATR) accessory utilizing the Zn-Se crystal and software package OMNIC over the range of wave lengths 4000 – 750  $\text{cm}^{-1}$  at room temperature. The uniform resolution 2  $\text{cm}^{-1}$  was maintained in all cases.

### ***Water-uptake measurement***

The water-uptake measurements of the polymer blends were investigated by ASTM D 570. The specimen were pre-dried at 80 °C before using, and then were immersed in distilled water and incubated at 37 °C under static conditions. The specimens were removed, blotted and immediately weighted. They were then immersed again in the water until the last time point. WU (%) was calculated using the following equation:

$$WU = \frac{W_1 - W_0}{W_0} \times 100 \quad (29)$$

where,  $W_0$  is the initial weight of specimen after pre-drying,  $W_1$  is the wet mass of the specimen at certain times.

## RESULTS AND DISCUSSION

### Testing of mechanical properties

#### *Tensile testing*

The tensile properties of pure PA6, BioFlex and their blends are depicted as BioFlex concentration dependence on Young's modulus (E), tensile strength and tensile strain in Figures 26-28. The figures are filled in by additivity mixing rule information represented by dashed lines. In addition the effect of deformation rate expressed as a speed of the moving clamp (20 and 200 mm/min) is considered here.

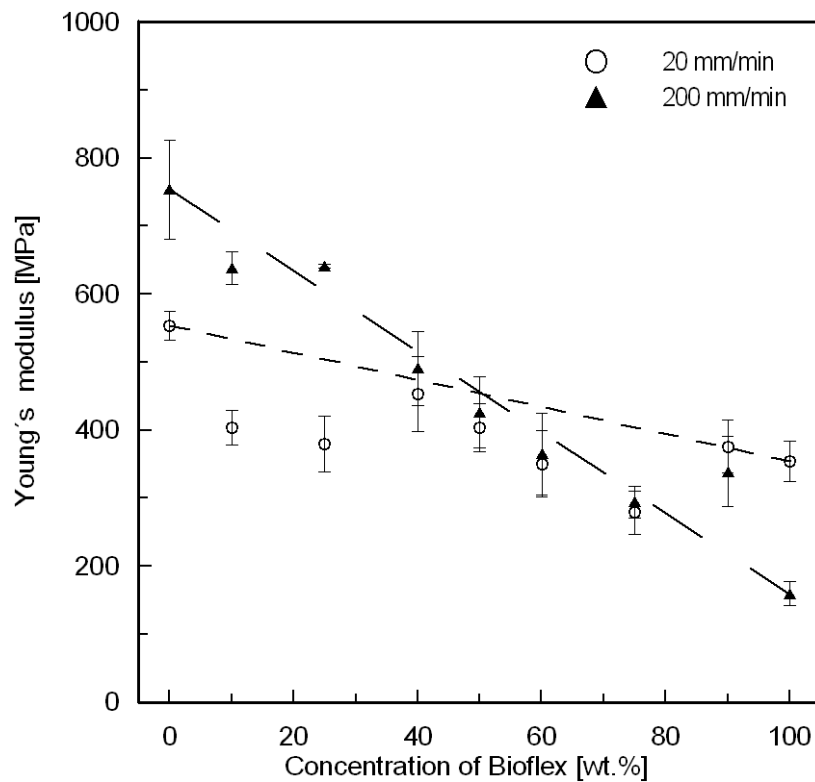


Figure 26: Dependence of Young's modulus on BioFlex concentration in the PA6/BioFlex blends

As it can be seen in Figure 26, the values of E are strongly dependent on the rate of tensile deformation in case of pure components. Generally, E decreases with increasing content of BioFlex. However, the decrease, which can be characterized by the line showing the course of the additivity mixing rule, is steeper for high deformation rate. The experimental data more or less follow this rule. On the other hand relatively significant negative deviation was observed in case of the results obtained at 20 mm/min in both PA6 and BioFlex rich blends. It reveals a weak interaction between matrix and domains of the dispersed polymer present in minor scale. The values of E, interestingly, correspond to additivity rule in the co-continuity interval (see previous chapter). Interestingly, positive deviation from additivity mixing rule was noticed for both PA6 and BioFlex rich blends.

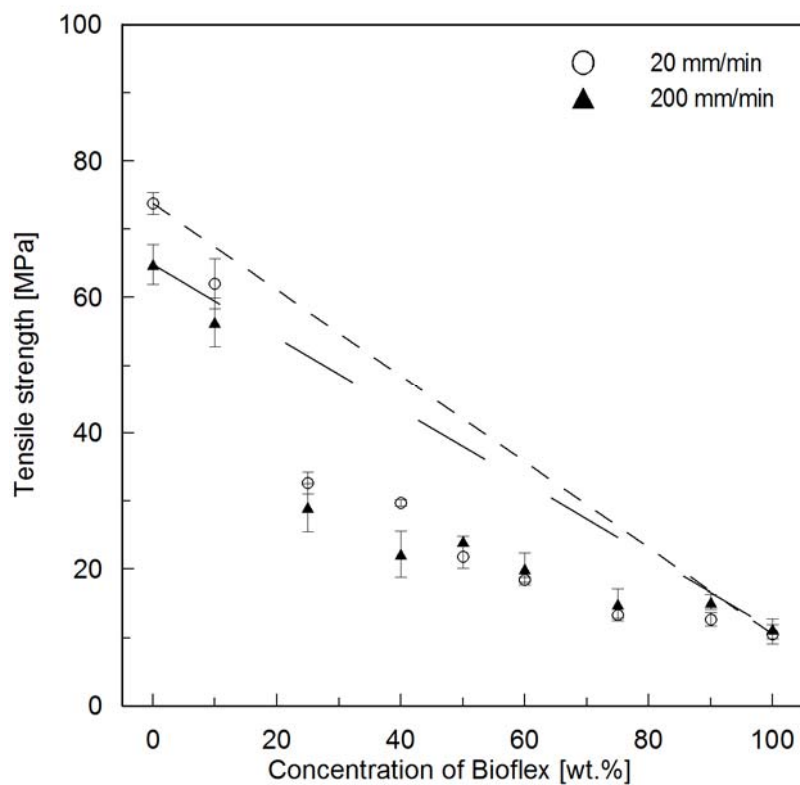


Figure 27: Dependence of tensile strength on BioFlex concentration in the PA6/BioFlex blends



The tensile strength vs. BioFlex concentration dependences of the blends shown in Figure 27 have similar trend in all cases. The increase in BioFlex content is followed by steep reduction of tensile strength of the blends. The BioFlex rich systems (above 75 wt. % of BioFlex) prove their mechanical properties similar to pure co-polyester. The only noticeable difference can be found in case of pure PA6. The lower deformation rate provides higher tensile strength values due to longer relaxation time given to polymer chains during tensile deformation. All blends are characteristic by highly negative deviation from the additivity mixing rule. It is caused by significantly different mechanical properties of the pure polymers. The specimens with co-continuous morphology do not show any special behaviour.

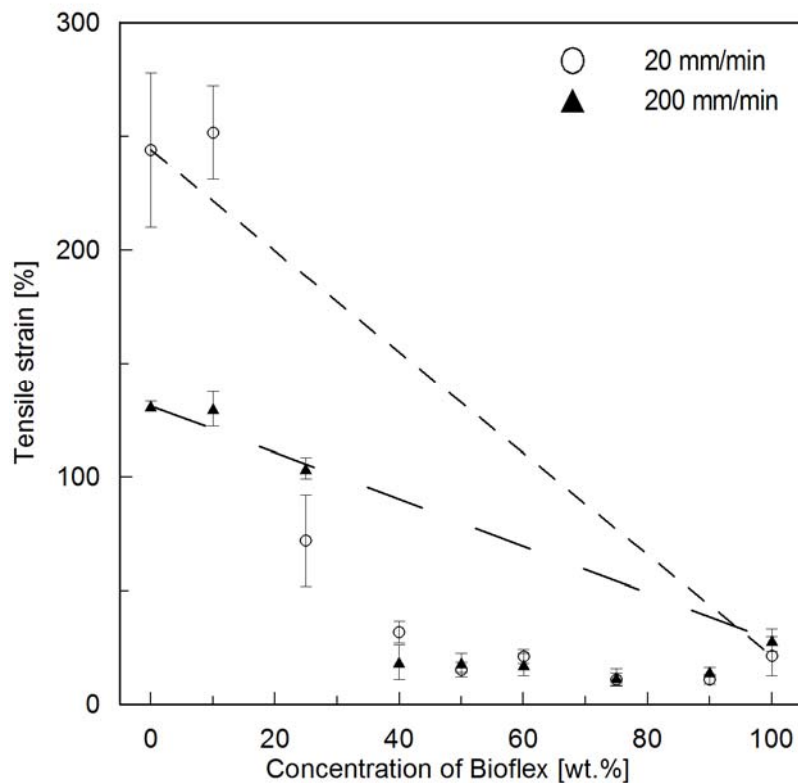


Figure 28: Dependence of tensile strain on BioFlex concentration in the PA6/BioFlex blends

Figure 28 shows maximal elongation of the samples in dependence of their composition. It is required to remind that all specimens were conditioned in a chamber at room temperature and 50 % RH. The

consequence of that can be noticed in high elongability of pure PA6, which is known to be moisture sensitive. The moisture effect on the mechanical properties of PA6 is apparent in case of PA6 rich blends as well. Pure BioFlex have tensile strain value below 50 % under both low and high deformation rate. The blends containing more than 25 wt. % of BioFlex have strongly negative deviation from additivity mixing rule and they are approaching the tensile strain value of the pure co-polyester when BioFlex concentration rises above 50 wt. %.

The behaviour of the samples described above shows mostly negative deviation from additivity mixing rule in case of tensile strength and tensile strain. An explanation of such phenomenon can be found partially in nature of individual components of the binary systems and in morphological organization of the blends (see chapter 1). There is huge difference in mechanical properties of PA6 and biodegradable co-polyester. While pure PA6 has tensile strength over 270 MPa, BioFlex shows almost ten times lower values. The similar situation can be observed for tensile strain. However, moisture effect on maximal tensibility of PA6 must be considered here. Young's modulus,  $E$ , of both matrixes does not differ as noticeably as for tensile strength and tensile strain. Nevertheless, PA6 has several times higher  $E$  than co-polyester. The results presented in Figures 25-28 reveal the significant drop in mechanical properties (tensile strength and tensile strain) already at the lowest additions of BioFlex. It means that mechanical properties are affected by poor cohesiveness of the matrixes at high deformations. On the contrary, small deformation represented by  $E$  allows the application of morphological factors discussed in previous chapter. The size of the domains and their distribution play considerable role here. The co-continuity interval observed around 40-60 wt. % of BioFlex presence is characteristic by correspondence with additivity mixing rule, probably, due to higher compactness of the both PA6 and co-polyester matrix.

### ***Impact strength***

The results from the comparative testing of the polymer blends toughness determined by impact strength measurements (Charpy method) are introduced in Table 5. The amount of absorbed energy during specimens fracture is decreasing with increasing content of BioFlex in the blends. The only exception is created by the blend containing 25 wt. % of the biodegradable component. Its impact resistance rises even above the value for pure PA6. This toughness improvement can be observed in Young's modulus vs. BioFlex concentration dependence for the rate 200 mm/min (Figure 26). This concentration seems to be optimal from the mechanical properties point of view.

Table 5: Impact strength of the PA6 and selected PA6/BioFlex blends

Sample	Impact resistance AK (kJ/m <sup>2</sup> )
PA6	15.40 ± 1.74
PA/Bioflex 90/10	16.59 ± 1.59
PA/Bioflex 75/25	18.68 ± 1.11
PA/Bioflex 50/50	12.02 ± 1.34
PA/Bioflex 25/75	9.25 ± 1.41
PA/Bioflex 10/90	*
BioFlex	*

\*not broken (too flexible)

### ***Dynamic mechanical analysis (DMA)***

The viscoelastic properties of the pure PA6, BioFlex and PA6/BioFlex 50/50 blend observed by DMA are presented in Figures 29-31 as temperature dependences of storage modulus ( $E'$ ), loss modulus ( $E''$ ) and phase angle ( $\tan\delta$ ), respectively. As can be noticed in Figure 29, pure PA6 provides relatively strong response to applied strain. The inflection point (IP) of the

curve showing its storage modulus dependence on temperature can be found at 20 °C. It is connected with glass transition phenomenon. BioFlex, on the contrary, has low signal and its IP is located more or less in the same temperature interval. The blend containing 50 wt. % of BioFlex lies more or less in the middle of the  $E'$  range defined by the dependences of the pure matrixes.

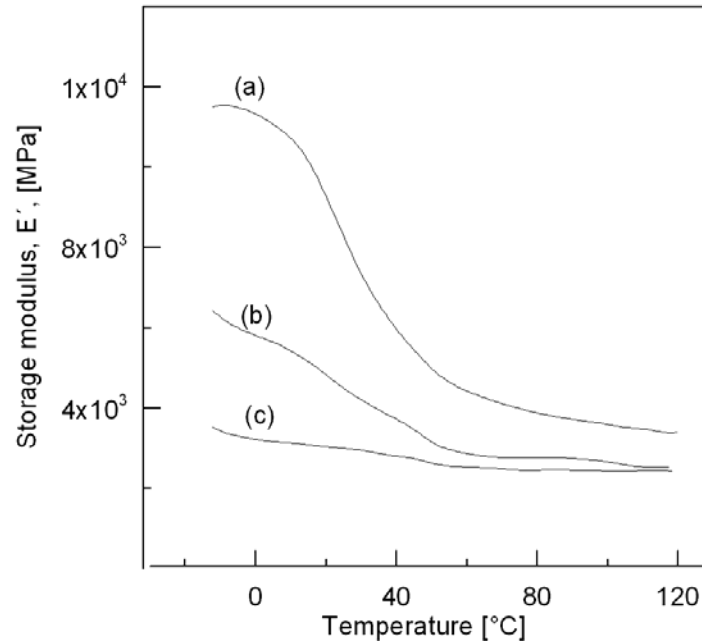


Figure 29: Storage modulus as a function temperature for PA6 (a), PA6/BioFlex 50/50 (b) and BioFlex (c)

The loss modulus,  $E''$ , as a function of temperature for the same samples as presented above is shown in Figure 30 as well as phase angle,  $\tan \delta$ , temperature dependence, which can be found in Figure 31. In both cases PA6 is characterized by the highest response, which is decreasing with increasing BioFlex concentration. It is in accordance with tensile testing measurements presented above. The glass transition temperature ( $T_g$ ) can be read from the shown dependences for PA6 rich blends. Unfortunately it is rarely possible to estimate  $T_g$  for the samples with higher (over 25 wt. %) due to their softness, which makes the reproducible measurements in three point bending mode impossible. On the other and, the results prove the

existence of two  $T_g$  points of the blends, which correspond to the glass transitions of individual components of the investigated binary systems. It can be noticed especially in Figure 30 and Figure 31.

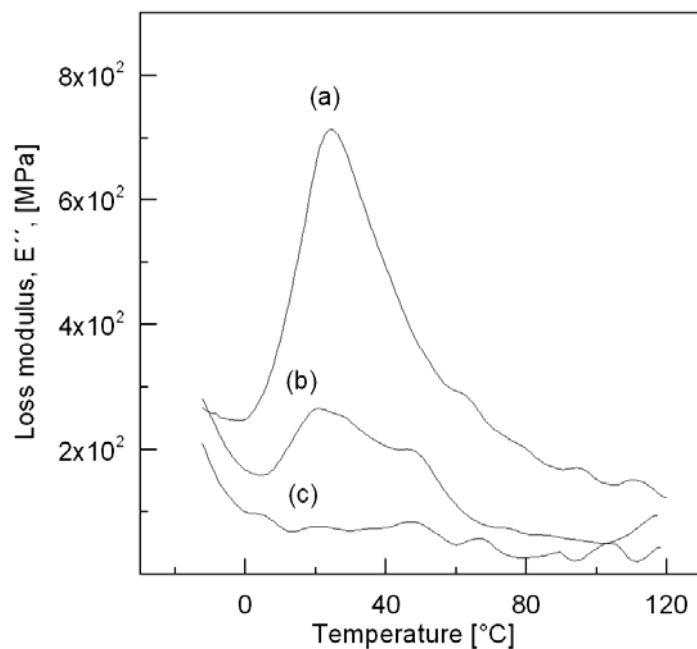


Figure 30: Loss modulus as a function temperature for PA6 (a), PA6/BioFlex 50/50 (b) and BioFlex (c)

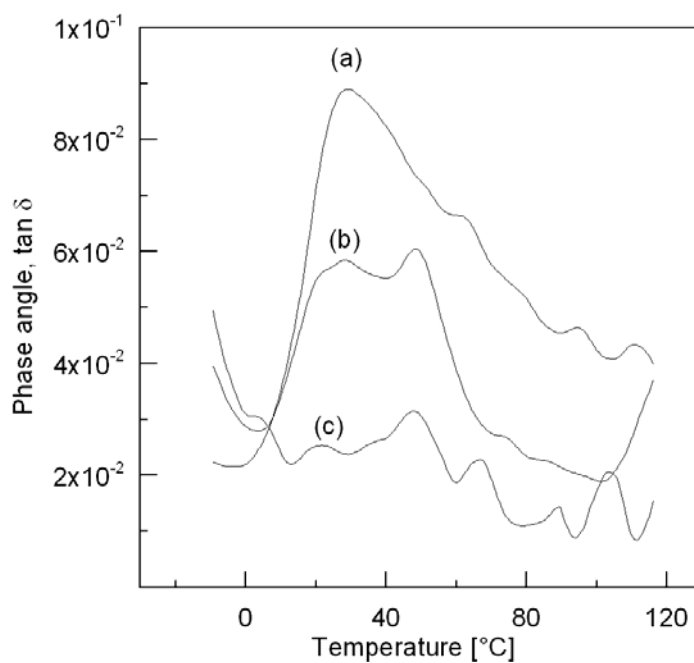


Figure 31: Phase angle as a function temperature for PA6 (a), PA6/BioFlex 50/50 (b) and BioFlex (c)

## Testing of thermal properties

### *Differential scanning calorimetry (DSC)*

The results from DSC measurements are summarized in Table 6. The DSC spectra of pure polymers shows melting point of PA6 at 222.9 °C. Pure BioFlex is characteristic by two melting peaks situated at 144.9 and 152.5°C. A broad cold crystallization revealing peak was found at 106.6 °C. Glass transition,  $T_g$ , was detected at 57.3 °C. The blends of PA6 and BioFlex show increased  $T_g$  value with increasing content of BioFlex in the system. It is in accordance with the expectation since  $T_g$  of pure polyamide is reported to be close to room temperature [144]. The shift of  $T_g$  (Table 6) may reveal the possible polymer-polymer interactions in the interface regions. The glass transition was not observed for pure and PA6 rich blends (0–25 wt, % BioFlex). The increasing amount of biodegradable component is also detectable by occurrence of typical double melting peaks, which become more intensive with rising concentration of BioFlex. On the contrary, these results fully correspond to mechanical properties data (tensile strength and strain), where the blends containing over 40 wt. % of BioFlex show the behavior similar to those observed in case of pure co-polyester.

The values of detected changes of melting ( $\Delta H_m$ ) and cold crystallization enthalpy ( $\Delta H_c$ ) were used for relative comparison of sample crystallinity. PA6 is known to have high crystallization tendency [144]. It is proved by the experimental results presented in Table 6. On the other hand, PLA based co-polyester shows low crystalline fraction ratio.

The dependences of melting crystallization reduced by enthalpy of cold crystallization ( $\Sigma\Delta H_{mi}-\Sigma\Delta H_{ci}$ ) on BioFlex content are shown in Figure 32 (taken from 2<sup>nd</sup> heating scan, full symbols).

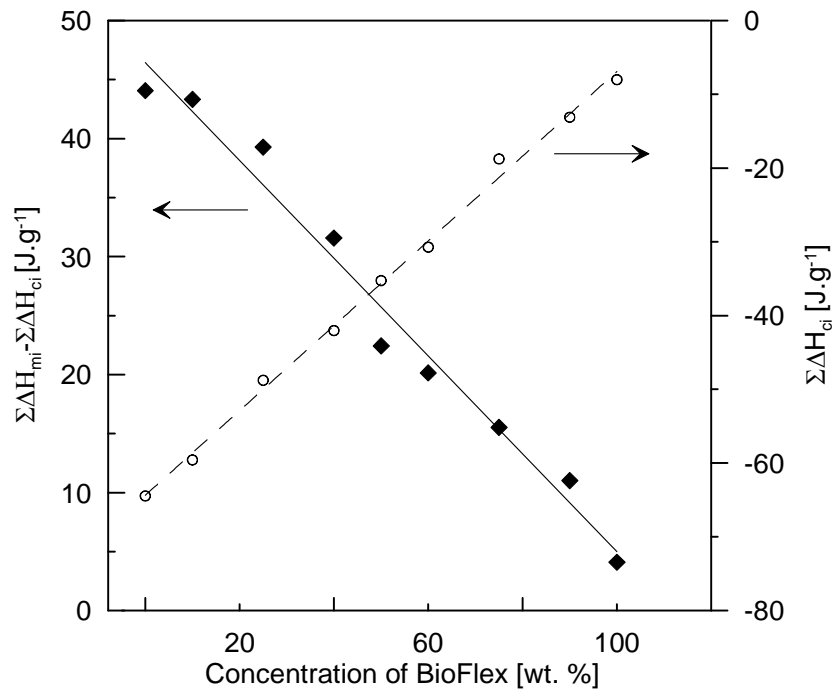


Figure 32: Relative crystallinity comparison of PA6, BioFlex and their blends (full symbols – 2<sup>nd</sup> heating scan, empty symbols – cooling scan)

The same figure also presents  $\Sigma\Delta H_{ci}$  versus BioFlex concentration, which was obtained from cooling DSC scan (empty symbols). It can be noticed that crystalline phase ratio decreases linearly with BioFlex content increase. The formation of co-continuity does not seem to affect the crystallization process.

Table 6: Thermal properties of PA6/Bioflex blends

PA6/Bioflex blends	First heating scan									Cooling scan					Second heating scan
	T <sub>m1</sub>	T <sub>m2</sub>	T <sub>m3</sub>	ΔH <sub>m1</sub>	ΔH <sub>m2</sub>	ΔH <sub>m3</sub>	T <sub>c</sub>	ΔH <sub>c</sub>	ΣΔH <sub>mi</sub> -ΣΔH <sub>ci</sub>	T <sub>c1</sub>	T <sub>c2</sub>	ΔH <sub>c1</sub>	ΔH <sub>c2</sub>	ΣΔH <sub>ci</sub>	T <sub>g</sub>
	(°C)	(°C)	(°C)	(J/g)	(J/g)	(J/g)	(°C)	(J/g)	(J/g)	(°C)	(°C)	(J/g)	(J/g)	(J/g)	(°C)
100/0	-	-	222.9	-	-	44.07	-	-	44.07	-	189.2	-	-64.46	-64.46	*
90/10	-	-	223.5	-	-	43.34	-	-	43.34	-	189.4	-	-59.58	-59.58	*
75/25	-	151	223.9	-	1.46	37.83	-	-	39.29	-	190.6	-	-48.78	-48.78	*
60/40	143.5	151.4	222.9	0.08	1.88	29.62	-	-	31.58	-	190.4	-	-42.04	-42.04	57
50/50	145.4	153.6	223.3	1.43	3.21	21.61	109.5	2.81	23.44	81.8	191.1	-3.40	-31.86	-35.26	57.8
40/60	145.5	152.9	221.6	1.89	5.06	16.06	110.4	2.86	20.15	82.3	191.3	-4.17	-26.56	-30.73	58.7
25/75	146.2	152.6	221.3	1.81	5.51	8.89	111.5	0.68	15.54	86.1	191.5	-5.79	-12.97	-18.76	58.4
10/90	146.9	153.9	220.8	0.87	7.03	4.78	113.1	1.66	11.03	86.8	190.3	-7.55	-5.56	-13.11	58.3
0/100	144.9	152.5	-	0.97	6.85	-	106.6	3.7	4.12	93.8	-	-8.02	-	-8.02	57.3

\*-not detected



***Fourier transform infrared spectroscopy-Attenuated total reflectance (FTIR-ATR)***

FTIR-ATR spectra of pure PA6, BioFlex and their blends are presented in Figure 33. The characteristic absorption peaks of the pure matrixes and their assignment to the polymer structure are shown in Tables 7 and 8. The obtained spectra clearly show the composition response in form of the characteristic peaks intensity. These results do not reveal a chemical interaction between PA6 and BioFlex, which can be detected by used method. On the other hand, the composition information and its semi-quantitative correlation is could be proceeded on the basis of obtained data.

Table 7: Assigning of the absorption peaks to chemical band for pure PA6

Absorbance peak position – wavenumber [ $\text{cm}^{-1}$ ]	Explanation
3300	N-H stretching
3075	O-H stretching, moisture
2978	C-H stretching
2860	C-H stretching, $-\text{CH}_2-$
1632	C=O stretching
1539	N-H deformation
1463	$-\text{CH}_2-$ scissoring
1412	C-H rocking
1374	C-H symmetric deformations, rocking
1260	N-H deformation
1201	C-H bending
1163	C-H bending
1147	C-C stretching
1100	C-H bending
724	N-H bending
682	N-C=O bending

Table 8: Assigning of the absorption peaks to chemical band for pure BioFlex

Absorbance peak position – wavenumber [ $\text{cm}^{-1}$ ]	Explanation
2957	C-H asymmetric stretching
2864	C-H stretching
1712	C=O stretching
1455	-CH <sub>2</sub> - scissoring
1412	C-H rocking, C-O stretching
1378	C-H rocking, deformations
1273	C-O-C and C-O stretching
1428	C-H rocking, C-O stretching
1163	C-O stretching
1117	C-O-C symmetric stretching
1104	C-O-C asymmetric stretching
1016	C-H bending
931	C-H out of plane bending
867	C-H bending
729	C-H bending

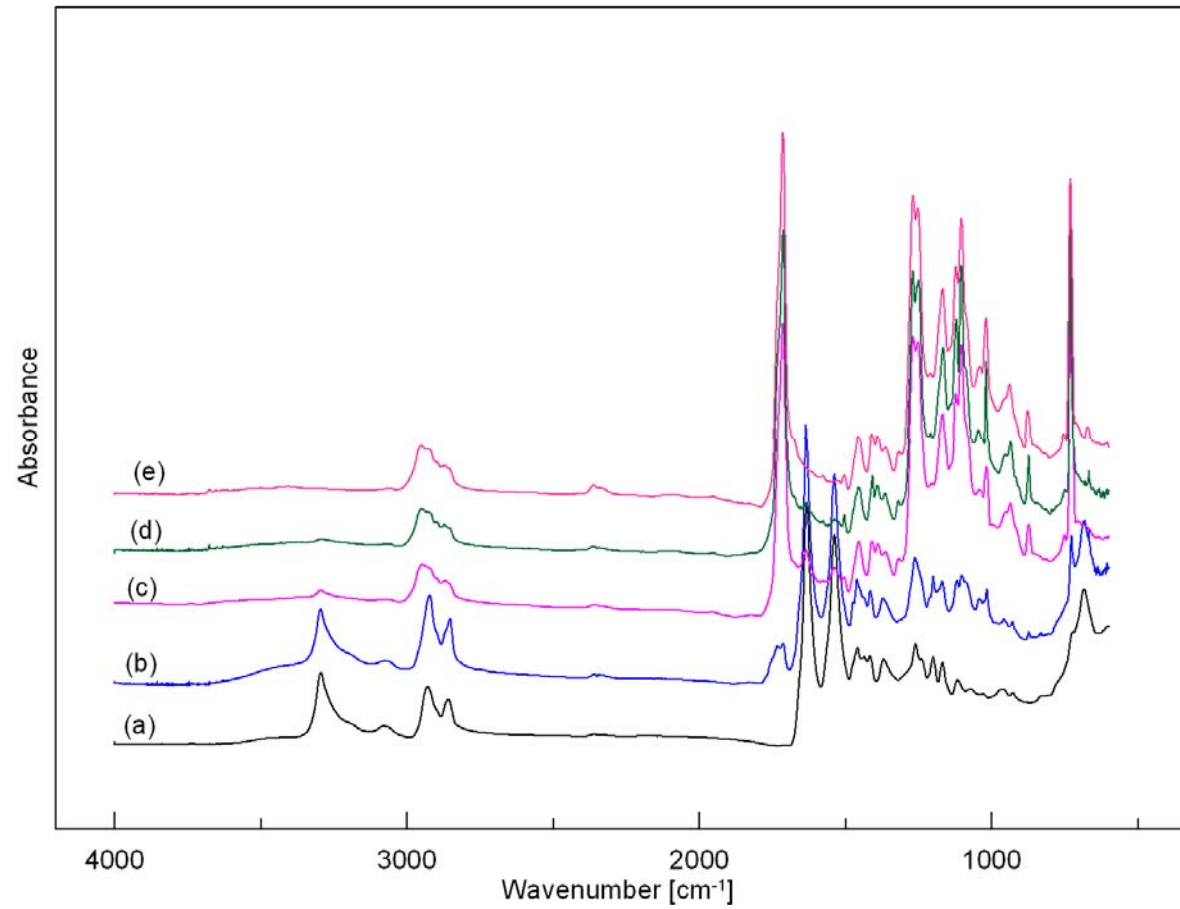


Figure 33: FTIR-ATR spectra of pure PA6 (a), BioFlex (e) and their blends PA6/BioFlex (wt./wt.) 75/25 (b), 50/50 (c) and 25/75 (d)

### *Water-uptake measurement*

It has been known that polyamide based materials are extremely sensitive to water absorption even in form of the atmospherically present moisture. The data obtained from water uptake experiment confirm this fact. As it can be noticed in Figure 34, pure PA6 shows the highest water absorption – almost 9 wt. % after 3 days of the experiment. On the other hand, BioFlex proves water uptake below 1 wt. % during whole experiment time (5 days). The behaviour of the blends of PA6 and BioFlex corresponds to their compositions i.e. with increasing content of PA6 in the system the water uptake grows almost linearly. The amount of the absorbed water became constant after 72 hours of the experiment duration in all cases.

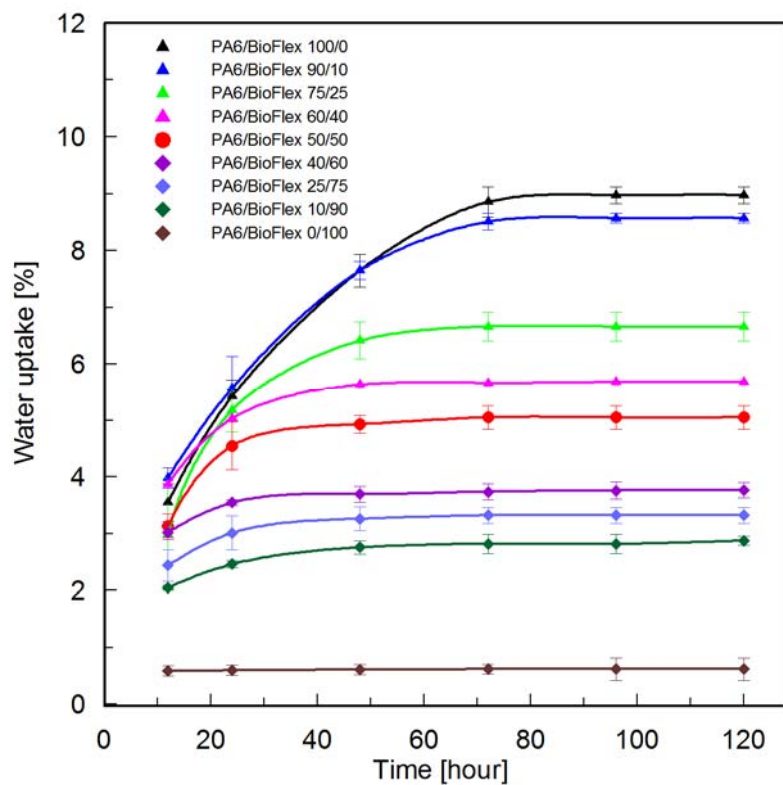


Figure 34: Water uptake of the pure matrixes and polymer blends versus time of the soaking experiment

### **3.3 Time dependent release of model bioactive component from the PA6/BioFlex polymeric blends with various morphology**

#### **INTRODUCTION**

The final chapter presenting experimental data obtained during assigning of this PhD study is focused on the describing and proving controlled release ability of the developed polymer blends with co-continuous morphology. The blends will be compared to pure polymeric matrixes ability to controlled release the model bioactive agent in relation to pure matrixes modified with the same compound and under same conditions. More concretely, the aim chapter is to correlate the release ability of the incorporated model compound from the PA6/BioFlex polymer blends. Crystal violet (CV) was used as a model compound in this study. CV is also known as gentian violet. It is commonly applied as a bactericide and an antifungal agent. In medical care it is effectively used for the treatment of serious heat burns, radiation-induced wound and other injuries to the skin and gums because of its antifungal and antiseptic effects [145]. For wound treatment, it can be useful to non-adherent type of wound dressing. Another advantage of CV is an easy detectability by common analytical methods such as UV-VIS spectrometry.

#### **EXPERIMENTAL PART**

##### ***Sample preparation for release studies***

The PA6/Bioflex blends were prepared by using Brabender Plasti-coder kneader. The volume of chamber was 50 cm<sup>3</sup>. The blending was carried out at 230 °C and 25 rpm for 8 min. The resulting products of mixing were pulverized and moulded into the thin plate (thickness 1mm) in a manual press at 235°C for 10 min and subsequently cooled under pressure 10 MPa. The blends of

PA6/Bioflex were prepared in ratios 100/0, 90/10, 75/25, 60/40, 50/50, 40/60, 25/75, 10/90 and 0/100 wt. %. The concentration of CV was kept at 1 wt. % in all cases (related to total mass of polymer components).

### ***Release study setting***

Piece of samples (diameter 14 mm) were cut out from the prepared polymer sheets. The specimens were dried up to the constant weight and introduced into the reactor containing releasing medium. Four types of releasing media were used in this study to describe the releasing profile of CV from the polymer matrix:

- Distilled water (**M1**)
- Physiological solution (0.9 wt. % NaCl water solution) (**M2**)
- Carbonate buffer, pH=9 (**M3**)
- Hydrochloric acid solution, pH=2 (**M4**)

Total volume of the release medium in the reactor was 10 ml. The reactors containing specimen were kept in conditioned chamber under continuous shaking (140 rpm) at 37 °C. The specimens were taken out in predetermined intervals, dried carefully by paper napkin and put into another reactor containing fresh release medium. The amount of release CV was determined spectrometrically by Helios  $\gamma$  (ThermoFischer, USA) spectrometer at 579 nm (M1-M3) and 585 nm (M4) against blank (releasing medium without specimen). The calibration absorbance versus CV concentration in given released medium dependences were prepared and verified before each measurement. The observed data of the cumulative mass of the released CV related to 1 g of the sample material were evaluated by using first-order kinetics (Equation 30) and regression processed by the least squared method, applying the Solver subprogram of Microsoft Excel 2003.

$$C_{REL} = C_{MAX} \times (1 - e^{-kt}) \quad (30)$$

where,  $C_{REL}$  (mg/g) is the experimental concentration of CV that was released at time  $t$ ,  $C_{MAX}$  (mg/g), means the maximal theoretical concentration of CV released from 1 g of the sample, and  $-k$  ( $h^{-1}$ ) represents the rate constant i.e. time needed to reach  $C_{MAX}$  [146-147].

## RESULTS AND DISCUSSION

The release profiles of CV from the polymer matrix containing from 0 to 100 wt. % into four types of release media (M1-4) of BioFlex are shown in Figures 35-38 as the time dependencies of cumulative released CV mass related to 1 g of the sample material.

The release into all media have similar trend, which shows low release activity for pure components (PA6 and BioFlex). The increasing amount of the biodegradable component leads to increase of the CV release activity (CVRA). It is followed by CVRA drop towards to the values of pure BioFlex. However, the CVRA drop occurrence varies in dependence on release medium. This critical BioFlex content in the blend was observed at 75, 75, 60 and 60 wt. % for the media M1, M2, M3 and M4, respectively. It is clearly visible in Figure 39, where total amount of released CV versus BioFlex concentration is depicted after 383 hour of the experiment (maximal time investigated).

The strong pH and ionic strength dependence on amount of released CV can be noticed in Figure 39 as well. While the highest CV cumulative concentrations were observed for medium M4 (HCl solution, pH=2), physiological solution designated as M2 (NaCl solution 0.9 wt. %) reveals the lowest affinity to CV. The moderate values were obtained for DW (M1) and carbonate buffer (M3).

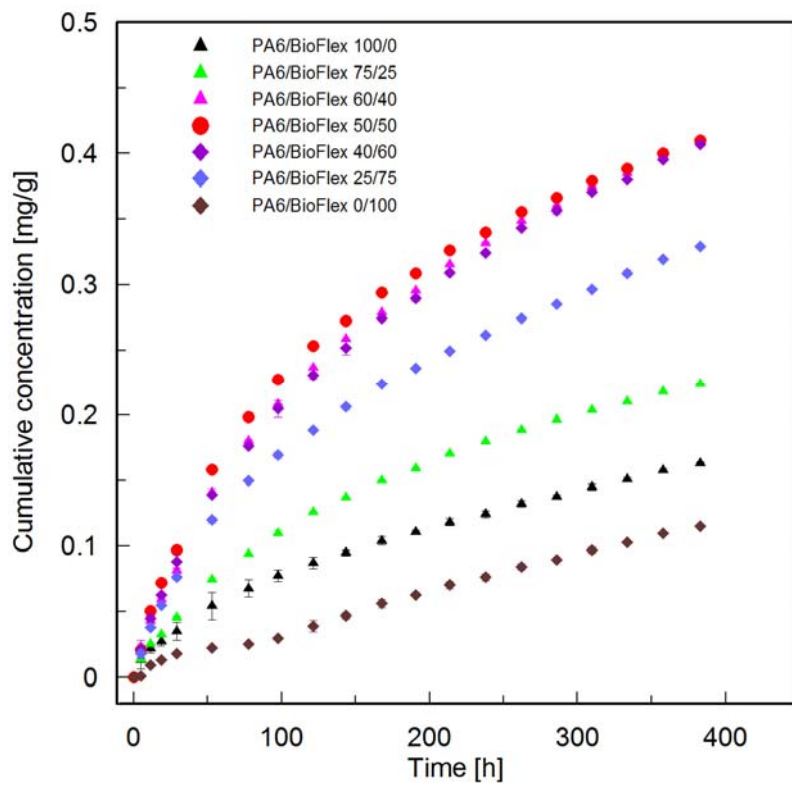


Figure 35: Release profile of crystal violet into distilled water

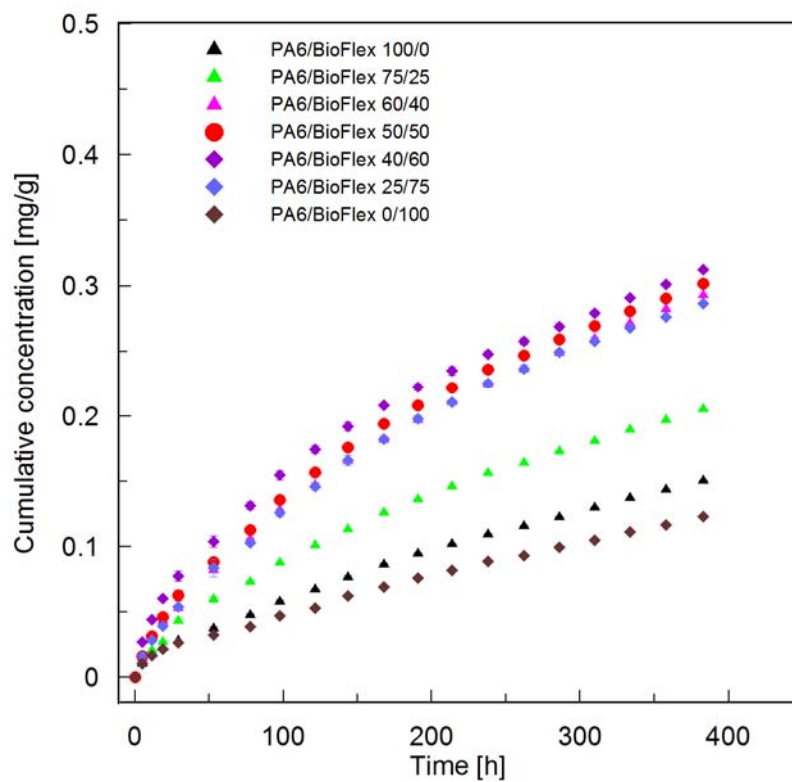


Figure 36: Release profile of crystal violet into physiological solution



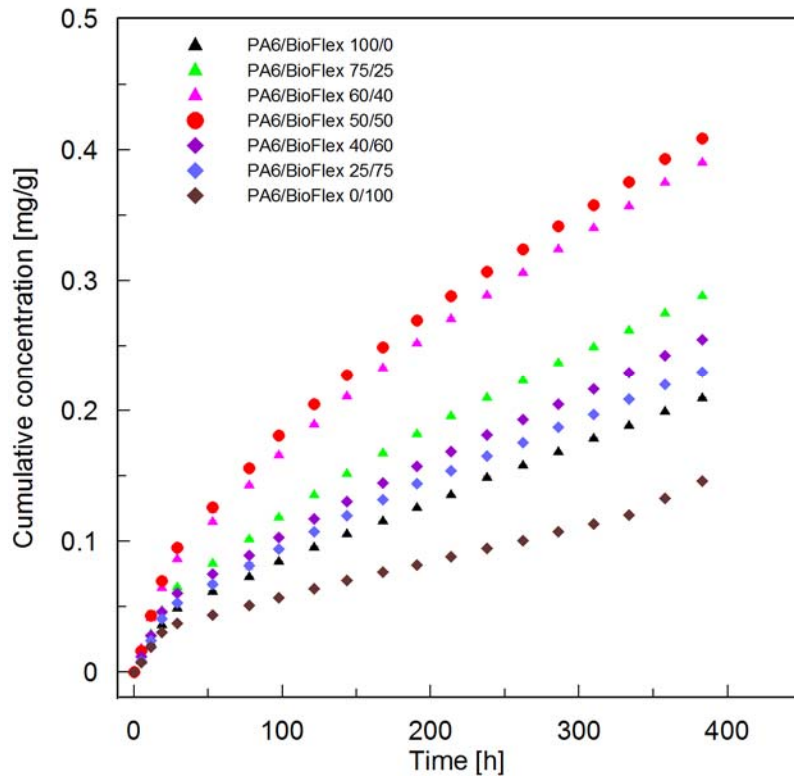


Figure 37: Release profile of crystal violet into carbonate buffer

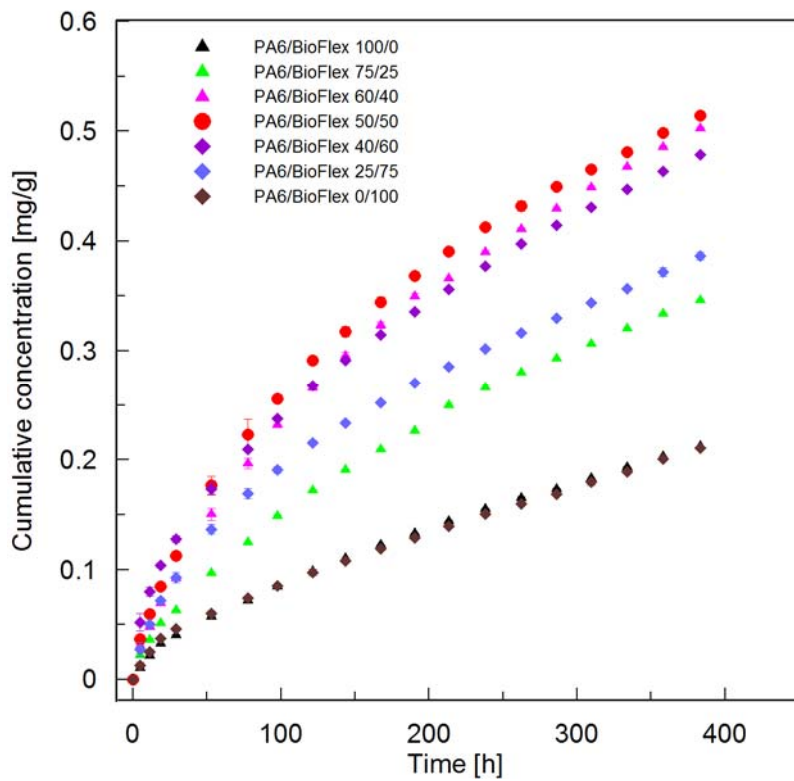


Figure 38: Release profile of crystal violet into hydrochloric acid solution

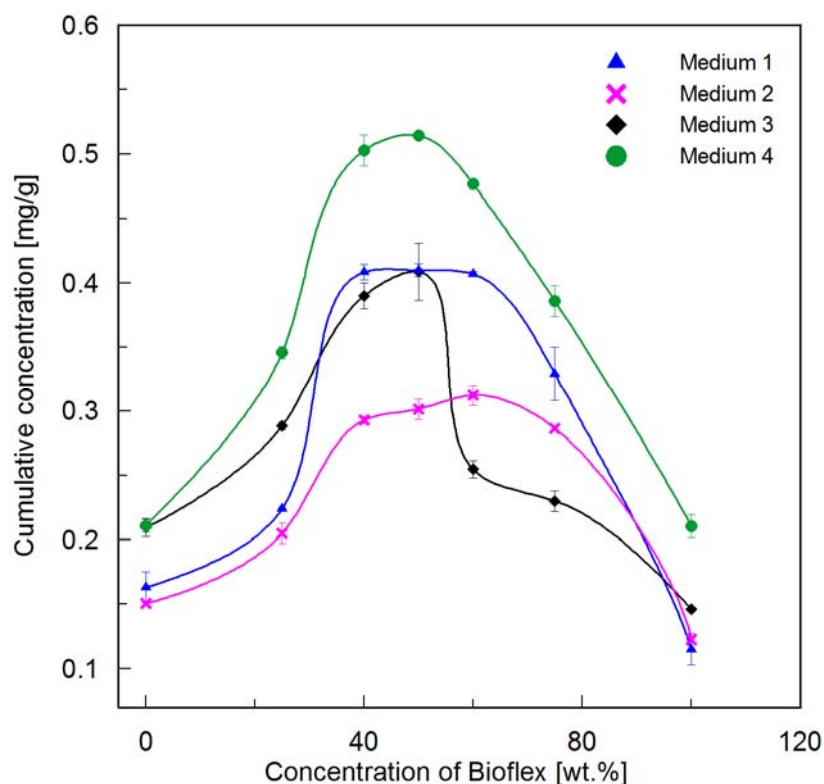


Figure 39: Comparison of the total amount of released CV in four media

Despite the experiment was carried out maximally for 383 hours the statistical analysis mediated by using of suitable mathematical model can allow predicting the CVRA for longer time periods. The kinetic constants calculated on the basis of Equation 30 are shown in Table 9-12.

Table 9: The constants of Equation 30 describing release kinetics of CV from polymer blends in medium M1 (distilled water)

Sample	$C_{MAX}$ [ $mg \cdot g^{-1}$ ]	$-k \cdot 10^{-2}$ [ $g \cdot mg^{-1}$ ]	$r^2$
PA6/BioFlex 100/0	0.1739	0.5802	0.9929
PA6/BioFlex 75/25	0.2352	0.6355	0.9971
PA6/BioFlex 60/40	0.4227	0.6783	0.9967
PA6/BioFlex 50/50	0.4056	0.8246	0.9948
PA6/BioFlex 40/60	0.4186	0.6700	0.9951
PA6/BioFlex 25/75	0.3580	0.5800	0.9944
PA6/BioFlex 0/100	0.3681	0.0984	0.9948

Table 10: The constants of Equation 30 describing release kinetics of CV from polymer blends in medium M2 (physiological solution)

Sample	$C_{MAX}$ [mg.g <sup>-1</sup> ]	$-k \cdot 10^{-2}$ [g.mg <sup>-1</sup> ]	$r^2$
PA6/BioFlex 100/0	0.1985	0.3482	0.9954
PA6/BioFlex 75/25	0.2403	0.4575	0.9967
PA6/BioFlex 60/40	0.3421	0.4660	0.9974
PA6/BioFlex 50/50	0.3395	0.5175	0.9970
PA6/BioFlex 40/60	0.3235	0.6542	0.9921
PA6/BioFlex 25/75	0.3326	0.4859	0.9998
PA6/BioFlex 0/100	0.1598	0.3522	0.9899

Table 11: The constants of Equation 30 describing release kinetics of CV from polymer blends in medium M3 (carbonate buffer)

Sample	$C_{MAX}$ [mg.g <sup>-1</sup> ]	$-k \cdot 10^{-2}$ [g.mg <sup>-1</sup> ]	$r^2$
PA6/BioFlex 100/0	0.2606	0.3767	0.9874
PA6/BioFlex 75/25	0.3473	0.4131	0.9924
PA6/BioFlex 60/40	0.4556	0.4490	0.9922
PA6/BioFlex 50/50	0.4589	0.4965	0.9914
PA6/BioFlex 40/60	0.3066	0.4043	0.9867
PA6/BioFlex 25/75	0.2771	0.4095	0.9884
PA6/BioFlex 0/100	0.1659	0.3989	0.9656

Table 12: The constants of Equation 30 describing release kinetics of CV from polymer blends in medium M4 (hydrochloric acid solution)

Sample	$C_{MAX}$ [mg.g <sup>-1</sup> ]	$-k \cdot 10^{-2}$ [g.mg <sup>-1</sup> ]	$r^2$
PA6/BioFlex 100/0	0.2671	0.3804	0.9955
PA6/BioFlex 75/25	0.4114	0.4467	0.9972
PA6/BioFlex 60/40	0.5601	0.5287	0.9974
PA6/BioFlex 50/50	0.5399	0.6442	0.9956
PA6/BioFlex 40/60	0.4890	0.6802	0.9858
PA6/BioFlex 25/75	0.3965	0.6569	0.9907
PA6/BioFlex 0/100	0.2564	0.3956	0.9886

The results presented above in Tables 9-12 reveal highest CV release characteristic for the medium M4. It means that CV proves the highest affinity towards low pH medium unlike distilled water (M1) or even the medium with high ionic strength (M2), where the release characteristics were the lowest. On

the other hand, there is not a significant difference from the other media. The statistical analysis shows relatively good correlation of the experimental results with the used model (Equation 30). It is obvious that CVRA is dependent on medium type as well as blend composition and its morphological arrangements. The blends with co-continuous morphology show the highest release profiles despite the pure matrixes lies on the bottom of the tested samples list. The reason of such behaviour may be connected with possible CV availability on the interface PA6-BioFlex. However, this hypothesis must be confirmed or confuted by further experimental work.

## Conclusions

The polymeric systems with co-continuous morphology are promising for various applications where controlled release of a bioactive agent (special packaging, medical devices) provided that one of the phase is created by a polymer, which can allow the transport of either the incorporated bioactive substance from the polymer matrix or, vice versa, surrounding medium into polymer matrix and interact with the compound consequently (e.g. biodegradable polymer, matrix with significantly various diffusion characteristics or solubility in the surrounding medium).

In this view, a partially biodegradable polymeric blend based on polyamide 6 (PA6) and commercially available co-polyester of polylactide (BioFlex) were studied in this work. The aim was to determine the co-continuity morphology composition. It was observed by using scanning electron microscopy (SEM) and archeological measurements in dynamic mode. The results were compared by solvent extraction method and semi-empirical models developed for phase inversion concentration prediction, which is connected to co-continuous morphology formation.

The results from SEM shown formation of co-continuity for the blends containing 50-60 wt. % of BioFlex. However, rheological measurements reveal occurrence of certain broader co-continuity interval which could be possible to consider already for the blends with BioFlex content over 25 wt. %. Solvent extraction method corresponds, on the other hand, to SEM results.

The comparison of several semi-empirical models showed relatively high variance of the predictions. Nevertheless, the best fit with our experimental data was found for the model considering the elasticity effect contributing to interfacial tension between PA6 and BioFlex.

An influence of morphological factors on mechanical and thermal properties structure of the resulting blend based on PA6 and BioFlex was determined by investigation of mechanical properties (tensile and impact strength testing, dynamic mechanical analysis (DMA)). Thermal properties were studied by using Differential scanning calorimetry (DSC). Structural characteristics were observed by Fourier transform infrared spectroscopy (FTIR). In addition, water uptake properties were also investigated.

The testing of tensile properties was carried out at two various deformation rates (20 and 200 mm.min<sup>-1</sup>). The dependences of Young's modulus on BioFlex concentration show the higher correspondence of the results to additivity mixing rule, which consider the mechanical properties of the pure polymeric matrixes. The lower deformation rate is characteristic by negative deviation from additivity mixing rule. The samples with co-continuous structure (50 and 60 wt. % of BioFlex) have Young's modulus values similar to the theoretical ones (based on additivity mixing rule calculations). Other observed parameters (tensile strength and tensile strain) show significantly negative deviation from this rule in all cases. The blends with BioFlex presence above 40 wt. % prove similar behavior to those observed for the pure BioFlex.

The impact strength testing (Charpy method) show enhancement of sample toughness at 25 wt. % of BioFlex presence. The amount of absorbed impact energy decreases with further additions of biodegradable co-polyester.

Dynamic mechanical analysis spectra show typical trend, which can be found in case of immiscible binary systems. The similar observations were presented by DSC, where individual components of the blend were identified through their endothermic response corresponding to melting process. Since glass transition temperature ( $T_g$ ) of PA6 can be rather detected,  $T_g$  of BioFlex was detected solely. However, it is known that PA6 has its  $T_g$  located around room

temperature. The observed  $T_g$  versus BioFlex concentration dependence is in accordance with tensile properties results. The effect of blending process on crystalline phase formation follows linear behavior. The higher PA6 content the higher crystallinity of the samples.

The structural characterizations done by FTIR spectroscopy does not prove arise of new chemical bonds between PA6 and BioFlex. Obtained FTIR spectra correspond to the structure of the individual components as well as their polymer blends.

It has been known that polyamide based materials are extremely sensitive to water absorption even in form of the atmospherically present moisture. The data obtained from water uptake experiment confirms this fact. As can be noticed in Figure 34, pure PA6 shows the highest water absorption – almost 9 wt. % after 3 day of the experiment. BioFlex proves water uptake bellow 1 wt. % during whole experiment time (5 days). The behaviour of the blends of PA6 and BioFlex corresponds to their compositions i.e. with increasing content of PA6 in the system the water uptake grows almost linearly. The amount of the absorbed water became constant after 72 hours of the experiment duration in all cases.

The correlation of the release ability of an incorporated model compound from the PA6/BioFlex polymer blends in dependence on the morphological arrangement in the blend was investigated finally. Crystal violet (CV) was used as a model compound in this study. The release profiles of CV from the polymer matrix containing from 0 to 100 wt. % into four types of release media (distilled water (M1), physiological solution (M2), carbonate buffer (M3) and hydrochloric acid solution (M4)). The release kinetics profiles show the higher release activity for the medium with pH=2 (M4). On the contrary, distilled water proved the lowest affinity to CV during release studies. Despite generally low release ability of the pure matrixes (PA6 and BioFlex), their blends,

interestingly, have significantly higher releasing ability. The highest values of CV released from the blend were observed for the blends with co-continuous morphology. The statistical data treatment by using first order kinetics model was used for the characterization of the releasing profiles and possible long-term prediction of the release behaviour.



## **Contribution to science and practice**

The presented thesis brings complex review of the area of bioactive packaging materials, which has predicted high applicability in practice. All methods used during assigning of the tasks of the given PhD topic were adopted or more often developed on the basis of current scientific works published in reputed impacted journals. In addition, most of the results are under preparation (or have been already submitted) for publication in impacted scientific journals.

The factual contribution of this work can be summarized in the following points:

- Preparation of wide review in the area of bioactive packaging
- Development and description of new partially biodegradable polymeric blend for potential use in packaging (food, pharmaceutical), medical device production
- Detailed description of co-continuity phenomenon and its correlation with experimental data
- Transfer of the obtained knowledge
- Establishment of international research teams within projects carried out at TBU

The practical contribution is not significant due to relatively innovative ideas which have been developed during this work. Some developed procedures are under consideration for protection from the intellectual property point of view. However, relatively active interest of the private companies from food packaging as well as biochemistry area could prove a tenability of the proposed work.

## References

1. MARSH, K., BUGUSU, B. Food Packaging -Roles, Materials and Environmental Issue, *Journal of Food Science* , vol.72, 2007, Nr.3.
2. BROWN, H., WILLIAMS, J. Packaged product quality and shelf life. In R. Coles, D. McDowell, & M. J. Kirwan. *Food Packaging Technology* London: Blackwell Publishing, 2003, p. 65-94, Electronic ISBN: 978-1-4051-4771-2
3. STEVEN, D. M., HOTCHKISS, J. M. Non-migratory bioactive polymers in food packaging. In Ahvenainen, R., *Novel Food Packaging Techniques*. Cambridge: Woodhead Publishing, 2003, ISBN: 978-1-85573-675-7
4. LOPEZ-RUBIO, A., GAVARA, R., LAGARON, J. M. Bioactive Packaging: Turning foods into healthier foods through biomaterials, *Trends in Food Science and Technology*, vol.17, 2006, p. 567-575
5. SINGH, R. K., SINGH, N. Quality of the packaged food, *Innovations in Food Packaging* , doi:10.1016/B978-012311632-1/50035-8, 2003
6. KILCAST, D., SUBRAMANIAM, P. Introduction. In D. Kilcast, & P. Subramaniam, *The stability and shelf-life of food 2000*, Cambridge: Woodhead Publishing p. 1-18, ISBN: 1 85573 500 8
7. HELEN, B., JAMES, W. Packaged product quality and shelf-life. In *Food Packaging Technology*, 2003, Electronic ISBN: 978-1-4051-4771-2
8. TUCKER, G. S. Food biodeterioration and methods of preservation. In *Food Packaging Technology*, 2003, p. 32-64
9. HAN, J. H. Antimicrobial Packaging Systems, *Innovations in Food Packaging*, doi: 10.1016/B978-012311632-1/50038-3, p. 20-107, 2005
10. BILLINGHAM, N. Environmentally-Friendly Plastics-What are the options? *MoDeSt 2008*, Liege, Belgium: CERTECH., 2008, p. 28
11. KIRWAN, M. J., STRAWBRIDGE, J. W. Plastics in Food Packaging. In R. Coles, D. McDowell, & M. J. Kirwan, *Food Packaging Technology*. Blackwell Publishing, 2003, Electronic ISBN: 978-1-4051-4771-2
12. LIU, L. S., FINKENSTADT, V. L., LIU, C. K., JIN, T., FISHMAN, M. L., HICKS, K. B. Preparation of Polylactic acid and Pectin Composite Films Intended for Applications in Antimicrobial Packaging. *Jour of Appl Pol Sci*, vol.106, 2007, p-801-810
13. AHVENAINEN, R. *Novel Food Packaging*. Woodhead Publishing, 2003, ISBN: 978-1-85573-675-7
14. RUSSO, P., ACIERNO, D. Thermal and Mechanical Characterization of Films from Nylon 6/EVOH blends. *European Polymer Journal* , vol.35, 1999, p-1261-1268.
15. IFT . (2007). Retrieved from <http://www.ift.org>
16. DHIRENDRA, K. S., CATO, L. T. Synthetic Biomedical Polymers for Tissue Engineering and Drug Delivery . In S. O. Gabriel, & A. G. Suresh,

- Advanced Polymeric Materials*. CRC Press, 2003, p. 479-527, ISBN: 1-58716-047-1
17. KRESSLING, L. L., STRONG, L. E. (1999). *Bioactive Polymers*. Springer Berlin/Heidelberg.
  18. CAO, W., HENCH, L. L. Bioactive Materials. *Ceramics International* , vol.22, 1996, p. 493-507.
  19. KOTHAPALLI, M., MORGAN, M., SADLER, G. UV Polymerization Based Surface Modification Techniques for the Production of Bioactive Packaging. *Jour of Appl Pol Sci* , vol. 107, 2008, p. 1647-1654.
  20. KOTHAPALLI, A., Comparison of Kinetic Profile of Free and Immobilized Glucose Oxidase, Immobilized on Low-Density Polyethylene Using UV Polymerization. *Journal of Food Science* , vol. 72, 2007, p. C478-C482
  21. DAINELLI, D., GONTARD, N. Active and intelligent food packaging: Legal aspects and safety concerns. *Trends in Food Sci & Tech* , vol. 19, 2008, p. S103-S112
  22. MISTRY, Y. Development of LDPE-based Antimicrobial Films for Food Packaging, Master thesis, Victoria University, 2006
  23. SEBASTEIN, F., STEPHANE, G., COPINET, A., COMA, V. Novel Biodegradable Films Made from Chitosan and Poly(lactic acid) with antifungal properties against mycotoxinogen strains. *Carbohydrate Polymers* , vol.65, 2006, p. 185-193
  24. CLARINVAL, A. M., CRIF, H. J. Classification of Biodegradable Polymers. In S. Ray, *Biodegradable Polymers for Industrial Applications*, Cambridge: Woodhead Publishing, 2005, p. 3-29, ISBN: 1 85573 934 8
  25. FAROOQAHMED, K. S., KONERIPATTI, K. R., THRANATHAN, R. N. Functional Packaging Properties of Chitosan Films. *Z Lebensm. Unters. Forsch. A* , vol. 206, 1998, p. 44-47
  26. HELANDER, I. M., NURMIAHO-LASSILA, E. L., AHVENAINEN, R., RHOADES, J., ROLLER, S. Chitosan disrupts the barrier properties of the outer membrane of Gram-negative bacteria. *International Journal of Food Microbiology* , vol. 71, 2001, p. 235-244
  27. FERNANDEZ-SAIZ, P. Characterization of antimicrobial properties on the growth of *S. aureus* of novel renewable blends of gladins and chitosan of interest in food packaging and coating applications. *International Journal of Food Microbiology* , vol.124, 2008, p. 13-20
  28. TRIPATHI, S., MEHROTRA, G. K., DUTTA, P. K. Chitosan based antimicrobial films for food packaging applications. *e-Polymers*, 093, 2008, <http://www.e-polymers.org> ISSN 1618-7229
  29. PARK, S. I., DAESCHEL, M. A., ZHAO, Y. Functional Properties of Antimicrobial Lysozyme-Chitosan Composite Films. *Food Microbiology and Safety, JFS*, vol. 69, 2006, p. 215-221

30. RAO, V., JOHNS, J. Thermal Behavior of Chitosan/Natural Rubber Latex Blends: TG and DSC Analysis. *Journal of Thermal Analysis and Calorimetry*, vol. 92, 2008, p. 801-806
31. VERMEIREN, L., DEVLIEGHERE, F., van BEEST, M., de KRUIJF, N., DEBEVERE, J. Development in the active packaging of foods. *Trends in Food Sci & Techn*, vol. 10, 1999, p. 77-86
32. TEW, G. N. De Novo Design of Biomimetic Antimicrobial Polymers. *Polymer Science and Engineering*, vol. 99, 2002, p. 5110-5114
33. GODDARD, J. M., HOTCHKISS, J. H. Polymer Surface Modification for the Attachment of Bioactive Compounds. *Progress in Polymer Science*, vol. 32, 2007, p. 698-725
34. PAVLOVIC, E. Spatially Controlled Covalent Immobilization of Biomolecules on Silicon Surfaces. Thesis, Uppsala, Sweden, 2003
35. GODDARD, J. M., TALBERT, J. N., HOTCHKISS, J. H. Covalent Attachment of Lactase to Low-Density Polyethylene Films. *Journal of Food Science*, vol. 72, 2007, p. 36-41
36. CIGDEM, M., AHMET, Y. Incorporation of partially purified hen egg white lysozyme into zein films for antibacterial packaging. *Food Research International*, vol. 39, 2006, p. 12-21
37. CONTE, A., DEL NOBILE, M. A. Development of immobilized lysozyme based active film. *Journal of Food Engineering*, vol. 78, 2007, p. 741-745
38. APPENDINI, P., HOTCHKISS, J. H. Immobilization of Lysozyme on Food Contact Polymers as Potential Antimicrobial Films. *Packaging Technology Science*, vol. 10, 1997, p. 271-279
39. PLATT, D. K. *Biodegradable Polymers*. Smithers Rapra Limited, UK, 2006
40. SOARES, N. F., HOTCHKISS, J. H. Naringinase Immobilization in Packaging Films for Reducing Naringin Concentration in Grapefruit Juice. *Journal of Food Science*, vol. 63, 1998, p. 61-65.
41. KOTWAL, S. M., SHANKAR, V. (2009). Immobilized invertase. *Biotechnology Advances*, doi:10.1016/j.biotechadv.2009.01.009.
42. HAN, J. H. (2003). Antimicrobial Food Packaging. In R. Ahvenainen, *Novel Food Packaging Techniques*. Cambridge: Woodhead Publishing Limited.
43. HAN, J. H., SCANLON, M. G. Mass transfer of gas and solute through packaging materials. *Innovations in Food Packaging*, doi:10.1016/B978-012311632-1/50034-6, 2005
44. BAJPAI, A. K., SANDEEP, S. K., BHANU, S., KANKANE, S. Responsive polymers in controlled drug delivery. *Progress in Polymer Science*, vol. 33, 2008, p. 1088-1118
45. MOUSAVI, S. M., DESOBRY, S., HARDY, J. Mathematical modelling of migration of volatile compounds into packaged food via package free

- space. Part II: Spherical shaped food. *Journal of Food Engineering*, vol. 36, 1998, p. 453-472
46. AVEROUS, L. Polylactic acid: synthesis, properties and applications. *Monomers, Polymers and Composites from Renewable Resources*, doi:10.1016/B978-0-08-045316-3.00021-1, 2008
  47. SIRACUSA, V., ROCCULI, P., ROMANI, S., ROSA, M. D. Biodegradable polymers for food packaging: a review. *Trends in Food Science and Technology*, vol. 19, 2008, p. 634-643
  48. MATSUMURA, S. Mechanism of biodegradation. In R. Smith, *Biodegradable polymers for industrial applications*, Cambridge: Woodhead Publishing, 2005, p. 357-394, ISBN: 1 85573 934 8
  49. SINGH, B., SHARMA, N. Mechanistic implications of plastic degradation. *Polymer Degradation and Stability*, vol. 93, 2008, p. 561-584
  50. LAKSHMI, N. S., CATO, L. T. Biodegradable polymers as biomaterials. *Progress in Polymer Science*, vol. 32, 2007, p. 762-798
  51. VASANT, R. V., MANNFRED, H. A. *Drug delivery systems*. 2-nd edition, CRC Press, Boca Raton, 2003
  52. BRANNON-PEPPES, L. Polymers in controlled drug delivery, Biomaterials, *Medical plastics and Biomaterials*, 1997
  53. DEL NOBLE, M. A., CONTE, A., BUONOCORE, G. G., INCORONATO, A. L., MASSARO, A., PANZA, O. Active packaging extrusion processing of recyclable and biodegradable polymers. *Journal of Food Engineering*, vol 93, 2009, p. 1-6
  54. SUPPAKUL, P. Active Packaging Technologies with an Emphasis on Antimicrobial Packaging and its Applications. *Journal of Food Science*, vol. 68, 2003, p. 408-420
  55. RAI, M., YADAV, A., GADE, A. Silver nanoparticles as a new generation of antimicrobials. *Biotechnology Advances*, vol. 27, 2009, p. 76-83
  56. AKBAS, M. Y., OZDEMIR, M. Application of gaseous ozone to control population of Escherichia coli, Basillus cereus and Basillus cereus spores in dried figs. *Food Microbiology*, vol. 25, 2008, p. 386-391.
  57. LEE, D. S. Packaging containing natural antimicrobial or antioxidative agents. In *Innovations in Food Packaging*, doi:10.1016/B978-012311632-1/50039-5, 2005, p. 108-122
  58. COMA, V. Bioactive packaging technologies for extended shelf life of meat-based products. *Meat Science*, vol. 78, 2008, p. 90-103
  59. SOBRIN-LOPEZ, A., MARTIN-BELLOSO, O. Use of nisin and other bacteriocins for preservation of dairy products. *International Dairy Journal*, vol. 18, 2008, p. 329-343

60. BRODY, A. L., BUDNY, J. A. Enzymes as active packaging agents. In M. L. Rooney, *Active Food Packaging*. Glasgow: Blackie Academic Professional, 2007, p. 174-192, Electronic ISBN: 978-1-60119-356-8
61. WellnessWest, Packaging Technology, vol.4, 2008, [http://www.wellnesswest.ca/index.php?option=com\\_content&task=view&id=17&Itemid=4](http://www.wellnesswest.ca/index.php?option=com_content&task=view&id=17&Itemid=4)
62. HAN, J. H., HO, C. H. L., RODRIGUES, E. T. Intelligent packaging, *Innovations in Food Packaging*, doi:10.1016/B978-012311632-1/50041-3, 2005, p-138-155
63. BRODY, A. L., BUGUSU, B., HAN, J. H., SAND, C. K., McHUGH, T. H. Innovative food packaging solutions, *Jour of Food Sci*, vol. 73, 2008, p. 107-116
64. UTRACKI, L. A. Polymer blends handbook, Verlag: Springer, 2002
65. SHONAIKE, G. O. SIMON, P., Polymer blends and alloys, Marsel Dekker Ink, 1999
66. HE, Y., ZHU, B., INOUE, Y. Hydrogen bonds in polymer blends. *Prog in Polym Sci*, vol. 29, 2004, p. 1021-1051
67. UTRACKI, L. A. Polymer blend, Verlag: Springer, 2000
68. ROBENSON, L. M. Polymer blend. *A comprehensive review*, Munich: Hanser Publishing, 2007, ISBN: 978-1-56990-408-4
69. VASILE, C., KULSHRESTHA, A. K. Handbook of polymer blends and composites, Rapra technology, 2003, ISBN: 1-85957-303-7
70. SALEM, D. R. Structure formation in polymeric fibers, Hanser Publishing, 2000
71. KULSHRESHTHA, A. K. Handbook of polymer blend , Rapra Technology, 2003
72. WARFIELD, R. W., HARTMAN, B. Corresponding states relationship for resistivity of glassy polymers. *Polymer*, vol. 21 , 31-34
73. UTRACKI, L. A. Polymer Alloys and Blends. Munich: Hanser, 1989
74. BAKER, W. E., SCOTT, C. E., HU, G. H. Reactive polymer blending. Munich: Hanser, 2003
75. UTRACKI, L. A. Commercial Polymer Blend. Verlag: Springer, 1998
76. LIU, N. C., HUANG, H. Types of ractive polymers used in blending. In W. E. Baker, & G. Hu, *Reactive polymer blending*, 2001
77. HAN, C. D. Rheology and Processing of Polymeric Materials. NewYork: Oxford, 2007
78. WILLEMSE, R. C., POSTHUMA de BOER, A., van DAM, J., GOTSIS, D. Co-continuous morphologies in polymer blends: the influence of the interfacial tension. *Polymer* , vol. 40, 1999, p. 827-834
79. LI, Y., SHIMIZU, H. Novel morphologies of poly(phenylene oxide) (PPO)/polyamide 6 (PA6) blend nanocomposites. *Polymer Communication*, vol. 45, 2004, p. 7381-7388

80. CHAREF, H., SABU, T., GABRIEL, G. *Micro- and nanostructured multiphase polymer blend system*. CRC, 2005
81. MOHAMMAD, B. R., ALI, Y. A., MOHAMMAD, Z. E., AHMAD, R., DENIS, R. Rheology of co-continuous phase in physical thermoplastic elastomer. *Polymer International*, vo. 53, 2004, p. 1448-1455
82. OMONOV, T. S., HARRATS, C., MOLDENAERS, P., GROENINCKX, G. Phase continuity detection and phase inversion phenomena in immiscible polypropylene/polystyrene blends with different viscosity ratios. *Polymer*, vol. 48, 2007, p. 5917-5927
83. PAUL, D. R., BARLOW, J. W. Polymer blends. *J Macromol Sci, Polymer Reviews* 1980;18:109-168
84. UTRACKI, L. A., On the viscosity-concentration dependence of immiscible polymer blends. *J Rheol* 1991;35(8):1615-1637
85. KRIGIER, I. M., DOUGHERTY, T. J. A Mechanism for Non-Newtonian Flow in Suspensions of Rigid Spheres. *Trans. Soc. Rheol* 1959;3:137-152
86. STEINMANN, S., GRONSKI, W. Cocontinuous polymer blends: influence of viscosity and elasticity ratios of the constituent on phase inversion. *Polymer*, vol. 42, 2001, p. 6619-6629
87. BOURRY, D., FAVIS, B. D. Co-continuity and phase inversion in HDPE/PS blends: Influence of interfacial modification and elasticity. *Journal of Polymer Science*, vol. 36, 1998, p. 1889-1899
88. WILLEMSE, R. C., SPEIJER, A., LANGERAAR, A. E., POSTHUNA de BOER, A. Tensile moduli of co-continuous blends. *Polymer*, vol. 40, 1999, p. 6645-6650
89. GALLOWAY, J. A., MACOSKO, C. V. Comparison of methods for the detection of co-continuity in poly/polystyrene blends, *Polymer Engineering and Science*, 2004,  
[http://findarticles.com/p/articles/mi\\_hb3367/is\\_4\\_44/ai\\_n29099619/](http://findarticles.com/p/articles/mi_hb3367/is_4_44/ai_n29099619/)
90. PAGE, I. B. Polyamides as engineering thermoplastic materials, *Review Reports*, Rapra Technology, 2000
91. GUPTA, A. P., KUMAR, V. New emerging trends in synthetic biodegradable polymers-poly(lactide): A critique, *European Polymer Journal*, 2007, 43, 4053-4074
92. SEBASTIEN, F., STEPHAN, G., COPINET, A., COMA, V, Novel biodegradable films made from chitosan and poly(lactic acid) with antifungal properties against mycotoxinogen strains, *Carbohydrate Polymers*, 65, 185-193
93. DAVID K. PLATT, *Biodegradable Polymers*, Market report, Smithers Rapra Limited, UK, 2006
94. <http://www.ultraflexx.com/PDFs/BIOflex.pdf>
95. AURAS, R., HARTE, B., SELKE, S. An overview of polylactides as packaging materials. *Macromol Biosci*, 2004; 4: 835-864



96. SEDLARİK, V, SAHA, N, SEDLARIKOVA, J, SAHA, P. Biodegradation of Blown Films Based on Poly (lactic acid) under Natural Conditions. *Macromolecular Symposia* 2008;272:100-103
97. COLES, R., McDOWELL, D., J. KIRWAN, M, *Food packaging technology*, Blackwell Publishing LLC, USA, 2003
98. WHITE, J. L., CORAN, A. Y., MOET, A., *Polymer mixing*. Carl Hanser Verlag, Munich, 2001. ISBN: 3-446-18495-3
99. SAWYER, L. C., GRUBB, D. T., MEYERS, G. F. *Polymer Microscopy*. New York: Springer, 2008, e-ISBN: 978-0-387-72628-1.
100. ITO, S., AOKI, H. Nano-Imaging of Polymers by Optical Microscopy. *Adv Polym Sci* 2005, 182:131-169.
101. STUART, B. H. *Polymer Analysis*. New York: Wiley, 2005
102. NIELSEN, L. E., LANDEL, R. F. *Mechanical properties of polymers and composites*. New York: Marcel Dekker, Inc, 1994
103. CAMPO, F. A. *Selection of Polymeric Materials-How to select design properties from different standards*. William Andrew Publishing, 2008
104. HAINES, P. J. *Thermal Methods of Analysis: Principles, Applications and Problems*. London: Blackie, 1995
105. MENCZEL, J. D., PRIME, R. B. *Thermal analysis of polymers. Fundamentals and applications*. New Jersey: Wiley, 2009
106. NARANJO, A., NOREIGA, M., OSSWALD, T., ROLDAN-ALZATE, A., SIERRA, J. D. *Plastic testing and characterization. Industrial applications*, Hanser Verlag, Munich, 2008
107. D'SOUZA, S. S., DeLUCA, P. P., Methods to assess in vitro drug release from injectable polymeric particulate systems. *Pharm. Res*, 2006, vol.23
108. [http://www.ptli.com/testlopedia/tests/water\\_absorption-D570.asp](http://www.ptli.com/testlopedia/tests/water_absorption-D570.asp)
109. RAUWENDAAL, C., *Polymer mixing. A self-study guide*. Hanser Publishers, Munich, 1998, ISBN: 3-446-18784-7
110. ROTHS, T., FRIEDRICH, C., MARTH, M., HONERKAMP, J. Dynamics and rheology of the morphology of immiscible polymer blends – on modeling and simulation. *Rheol Acta* , 2002;41:211-222
111. KIMBER, R. G. E., WALKER, A. B., SCHRODER-TURK, G. E., CLEAVER, D. J. Bicontinuous minimal surface nanostructures for polymer blend solar cells. *Phys Chem Chem Phys* 2010;12(4):844-851
112. SVOBODA, P., SVOBODOVA, D., SLOBODIAN, P., MERINSKA, D., IIZUKA, Y., OUGIZAWA, T., INOUE, T. Phase separation and phase dissolution in poly (epsilon-caprolactone)/poly(styrene-co-acrylonitrile) blend. *Eur Poly J* 2009;45(8):2434-2432
113. BARZEGARI, M. R, YOUSEFI, A. A, ZEYNALI, M. E., RABII, A., RODRIGUE, D. Rheology of co-continuous phase in physical thermoplastic elastomers. *Polym Int* 2004;53:1448-1455



- 114.HAN, M. S., LIM, B. H, JUNG, H. C., HUYN, J. J. C., KIM, S. R., KIM, W. N. Reactive blends of poly(butylenes terephthalate)/polyamide-6 with ethylene glycidyl methacrylate. *Korea-Aust Rheo J* 2001;13(4) 169-177
- 115.SARAZIN, P., ROY, X., FAVIS, B. D. Controlled preparation and properties of porous poly (L-lactide) obtained from a co-continuous blend of two biodegradable polymers. *Biomaterials* 2004;25:5965-5978
- 116.MAQUET, V., JEROME, R., Design of macroporous biodegradable polymer scaffolds for cell transplantation. *Mater Sci Forum* 1997;250:15-42
- 117.FINK, J. K., High performance polymers. In: Fink JK, editor: William Andrew 2008. p. 403-410
- 118.TODO, M., PARK, S. D., TAKAYAMA, T., ARAKAWA, K. Fracture micromechanisms of bioabsorbable PLLA/PCL polymer blends. *Eng Fract Mech* 2007;74(12):1872-1883
- 119.SCHWACH, E., SIX, J. L, AVEROUS, L. Biodegradable Blends Based on Starch and Poly(Lactic Acid): Comparison of Different Strategies and Estimate of Compatibilization. *J Polym Environ* 2008;16(4): 286-297
- 120.WANG, Y. B, HILLMYER, M. A. Polyethylene-poly (L-lactide) diblock copolymers: Synthesis and compatibilization of poly(L-lactide)/polyethylene blends. *J Polym Sci Pol Chem* 2001;39(16):2755-2766
- 121.RETOLAZA, A, EGUIAZABAL, J. I., NAZABAL, J. Structure and mechanical properties of polyamide 6,6/polyethylene terephthalate) blends. *Polym Eng Sci* 2004;44(8):1405-1413
- 122.DEYRA, MIGHRI, F, BOUSMINA, M., KALIAQUINE, S. Polyamide/polystyrene blend compatibilization by montmorillonite nanoclay and its effect on macroporosity of gas diffusion layers for proton exchange membrane fuel cells. *Fuel Cells* 2007;7(6):447-452
- 123.XIONG, C. X., LU, S. J., WANG, T., HONG, Y., CHEN, T., ZHOU, Z. Y. Study on morphology of compatibilized poly (vinyl chloride)/ultrafine polyamide-6 blends by styrene-maleic anhydride. *J Appl Polym Sci* 2005;97(3):850-854
- 124.ZHANG, W., LIU, S. P., LIU, J., ZHANG, Y. Miscibility and Mechanical Properties of Polylactide/Polyamide Elastomer Blends. 2008 International symposium on fiber based scaffolds for tissue engineering, proceedings. 2008:165-167
- 125.LACROIX, C., BOUSMINA, M., CARREAU, P. J., FAVIS, B. D., MICHEL, A. Properties of PETG/EVA blends: 2. Study of reactive compatibilization by n.m.r. spectroscopy and linear viscoelastic properties. *Polymer* 1996; 37(14):2939-2947.

126. BOUSMINA, M., MULLER, R. J. Linear viscoelasticity in the melt of impact PMMA. Influence of concentration and aggregation of dispersed rubber particles. *Jour Rheol* 1993;37(4):663-679.
127. FRIEDRICH, C., GLEINSER, W., KORAT, E., MAIER, D., WEESE, J. Comparison of sphere-size distributions obtained from rheology and transmission electron microscopy in PMMA/PS blends. *Jour Rheol* 1995;39(6):1411-1425.
128. VINCKIER, I., MOLDENAERS, P., MEWIS, J. Relationship between rheology and morphology of model blends in steady shear flow. *Jour Rheol* 1996; 40(4):613-631.
129. WORK, W. J., HORIE, K., HESS, M., STEPTO, R. F. T. Definitions of terms related to polymer blends, composites, and multiphase polymeric materials. *Pure Appl Chem* 2004;76(11):1985-2007
130. PALIERNE, J. F. Linear rheology of viscoelastic emulsions with interfacial tension. *Rheol Acta* 1991; 29(3):204-214.
131. UTRACKI, L. A. Viscoelastic behavior of polymer blends. *Polym Eng Sci* 1998;28(21):1401-1404
132. TOL, R. T., GROENINCKX, G., VINCKIER, I., MOLDENAERS, P., MEWIS, J. Phase morphology and stability of co-continuous (PPE/PS)/PA6 and PA/PA6 blends: effect of rheology and reactive compatibilization. *Polymer* 2004;45:2587-2601
133. VEENSTRA, H., van DAM, J., POUSTHUMA de BOER, A. Formation and stability of co-continuous blends with a poly (ether-ester) block copolymer around its order-disorder temperature. *Polymer* 1999;40:1119-1130
134. VENSTRA, H., NORDER, B., van DAM, J., POSTHUMA de BOER, A. Stability of co-continuous polystyrene/poly (ether-ester) blends in shear flow. *Polymer* 1999;40:5223-5226
135. HE, J., BU, W., Zeng, J. Co-continuity in immiscible binary polymer blends. *Polymer* 1997; 38:6347-6353.
136. VERHOOGT, H., van DAM, J., POSTHUMA de BOER, A. Morphology-Processing relationship in interpenetrating polymer blends. *Adv Chem Ser* 1994; 239:333-351.
137. DEDECKER, K., GROENINCKX, G. Reactive compatibilization of A/(B/C) polymer blends. Part 2. Analysis of the phase inversion region and the co-continuous phase morphology. *Polymer* 1998; 39:4993-5000.
138. FAVIS, B. D., CHALIFOUX, J. P. Influence of composition on the morphology of polypropylene/polycarbonate blends. *Polymer* 1988; 29:1761-1767.
139. MEKHILEF, N., VERHOOGT, H. Phase inversion and dual-phase continuity in polymer blends: theoretical predictions and experimental results. *Polymer* 1996; 37:4069-4077.

140. KITAYAMA, N., KESKKULA, H., PAUL, D. R. Reactive compatibilization of nylon 6/styrene-acrylonitrile copolymer blends. Part 1. Phase inversion behaviour. *Polymer* 2000; 41:8041.
141. LI, J. M., FAVIS, B. D. The role of the blend interface type on morphology in co-continuous polymer blends. *Macromolecules* 2002;35:2005-2016.
142. CHUAI, C. Z., ALMDAL, K., LYGAAE-JORGENSEN, J. Phase continuity and inversion in polystyrene/poly (methyl methacrylate) blends. *Polymer* 2003; 44:481-493.
143. PRACELLA, M., PETRIS, S. D., BUTTA, E. Polycarbonate-linear low density polyethylene blends: thermal and dynamic-mechanical properties *Journal of Materials Science*, 1990, 25, 3693-33700
144. AVRAMOV, I., AVRAMOVA, N., FACIROV, S. An attempt to obtain amorphous polyamide 6, *Macromol. Chem. Rapid Commun*, 1990:11:135-140
145. MAK, S.S.S. Efficacy of non-adherent dressing versus gentian violet for treatment of radiation-induced moist desquamation wounds in patients with nasopharyngeal carcinoma. *Hong Kong Med J*. 2007: 13. 8-12
146. MERCHAN, M., SEDLARIKOVA, J., SEDLARIK, V., MACHOVSKY, M., SVOBODOVA, J., SAHA, P. Antibacterial polyvinyl chloride/ antibiotic films: The effect of solvent on morphology, antibacterial activity and release kinetics, accepted for publication in *Journal of Applied Polymer Science*
147. SEDLARIK, V., GALYA, T., SEDLARIKOVA, J., VALASEK, P., SAHA, P. The effect of preparation temperature on the mechanical and antibacterial properties of poly (vinyl alcohol)/silver nitrate films. *Polym Degrad Stabil* 2010, 95, 399-404

## LIST OF FIGURES

Figure 1: Schematic models of polymer systems with bioactive agents.

Figure 2: Concept of biological surface modification

Figure 3: A schematic drawing illustrating the three mechanisms for controlled drug release from a polymer matrix.

Figure 4: Mass transfer phenomena and their characteristic coefficients

Figure 5: Classification of biodegradable polymers

Figure 6: Classification of hydrolytic degradation of hydrolysable polymers

Figure 7: Generalized illustration of effect of compatibilizer methods on the particle size

Figure 8: Schematic showing the roles of reactive compatibilizing agent when melt blended with two immiscible homopolymers

Figure 9: Types of blend morphologies

Figure 10: Ring-opening polymerization of the lactide to polylactide

Figure 11: Chemical structure of polyamide 6

Figure 12: Chemical structure of crystal violet

Figure 13: Tensile stress-strain curve of thermoplastic resin

Figure 14: Typical DSC curve obtained for semicrystalline polymer sample

Figure 15: SEM picture of the cold fractured specimens of PA6/BioFlex blends (a) 90/10, (b) 75/25, (c) 60/40, (d) 50/50, (e) 40/60 and 25/75 (wt./wt.) before chloroform treatment

Figure 16: SEM picture of the cold fractured specimens of PA6/BioFlex blends (a) 90/10, (b) 75/25, (c) 60/40, (d) 50/50, (e) 40/60 and 25/75 (wt./wt.) after chloroform treatment

Figure 17: Particle size (diameters) distribution of the PA6/BioFlex blends

Figure 18: SEM picture of the cold fractured specimens of PA6/BioFlex blends (a) 50/50, (b) 40/60, (c) 40/60 (lower magnification) after chloroform treatment

Figure 19: Co-continuity index versus BioFlex concentration

Figure 20: Storage modulus as a function of angular frequency (at 240°C)

Figure 21: Loss modulus as a function of angular frequency (at 240 °C)

Figure 22: Complex viscosity as a function of angular frequency (at 240 °C)

Figure 23: Complex viscosity versus BioFlex content in the blends

Figure 24: Storage modulus versus BioFlex content in the blends

Figure 25: Activation energy calculated according the Equation 27 versus BioFlex concentration in the blend

Figure 26: Dependence of Young's modulus on BioFlex concentration in the PA6/BioFlex blends

Figure 27: Dependence of tensile strength on BioFlex concentration in the PA6/BioFlex blends

Figure 28: Dependence of tensile strain on BioFlex concentration in the PA6/BioFlex blends

Figure 29: Storage modulus as a function temperature for PA6 (a), PA6/BioFlex 50/50 (b) and BioFlex (c)

Figure 30: Loss modulus as a function temperature for PA6 (a), PA6/BioFlex 50/50 (b) and BioFlex (c)

Figure 31: Phase angle as a function temperature for PA6 (a), PA6/BioFlex 50/50 (b) and BioFlex (c)

Figure 32: Relative crystallinity comparison of PA6, BioFlex and their blends

Figure 33: FTIR-ATR spectra of pure PA6 (a), BioFlex (e) and their blends PA6/BioFlex (wt./wt.)75/25 (b), 50/50 (c) and 25/75 (d)

Figure 34: Water uptake of the pure matrixes and polymer blends versus time of the soaking experiment

Figure 35: Release profile of crystal violet into distilled water

Figure 36: Release profile of crystal violet into physiological solution

Figure 37: Release profile of crystal violet into carbonate buffer

Figure 38: Release profile of crystal violet into hydrochloric acid solution

Figure 39: Comparison of the total amount of released CV in four media

## LIST OF TABLES

Table 1: Definitions of the various polymer blends

Table 2: Approaches for achieving miscible blends or compatible phase separated blends

Table 3: Characteristics of the BioFlex domains dispersed within PA6 matrix

Table 4: Phase inversion compositions of the PA6/Bioflex systems calculated on the basis of various models

Table 5: Impact strength of the PA6 and selected PA6/BioFlex blends

Table 6: Thermal properties of PA6/Bioflex blends

Table 7: Assigning of the absorption peaks to chemical band for pure PA6

Table 8: Assigning of the absorption peaks to chemical band for pure BioFlex

Table 9: The constants of Equation 30 describing release kinetics of CV from polymer blends in medium M1 (distilled water)

Table 10: The constants of Equation 30 describing release kinetics of CV from polymer blends in medium M2 (physiological solution)

Table 11: The constants of Equation 30 describing release kinetics of CV from polymer blends in medium M3 (carbonate buffer)

Table 12: The constants of Equation 30 describing release kinetics of CV from polymer blends in medium M4 (hydrochloric acid solution)

## LIST OF ABBREVIATIONS

BA	Bioactive agent
BPS	Bioactive polymer systems
CI	Co-continuity index
CTA	cellulose triacetate
CV	Crystal violet
DMA	Dynamical mechanical analysis
DSC	Differential scanning calorimetry
EVA	Ethylene vinyl alcohol
FTIR	Fourier transform infrared spectroscopy
IP	Inflection point
LDPE	Low density polyethylene
MBPS	Migratory bioactive polymer systems
NDB	negative deviation behaviour
NMBPS	Non-migratory bioactive polymer systems
PA6	Polyamide 6
PHA	polyhydroxyalkanoates
PHB	polyhydroxybutyrate
PLA	Polylactic acid
PVC	Polyvinyl chloride
PVOH	polyvinyl alcohol
SEM	Scanning electron microscopy
$T_c$	Crystallization temperature
$T_g$	Glass transition temperature
$T_m$	Melting temperature
WU	Water uptake

## **Curriculum vitae**

**Onon Otgonzul**                      \*1980 in Arkhangai, Mongolia

2006-present                      Ph.D. student at Polymer Centre, Faculty of  
Technology, Tomas Bata University in Zlin

2001-2004                      Master in Food Science, Mongolian University of  
Science and Technology, Ulaanbaatar, Mongolia

1997-2001                      Bachelor in Food Science, Mongolian University of  
Science and Technology, Ulaanbaatar, Mongolia

### **Presentations at international conferences**

- OTGONZUL, O. –MACHOVSKY, M. –SEDLARIK, V. –KITANO, T. – SAHA, P.: Structure properties of partially biodegradable polyamide/polyester polymer blend, 22nd International Symposium on Polymer Analysis and Characterization, June 22-24, 2009, Zlin, Czech Republic
- SEDLARIK, V. –KITANO, T. –OTGONZUL, O. – SAHA, P.: Viscoelastic properties of partially biodegradable polymer blend, Proceeding of Fifth International Conference on Polymer Modification Degradation and Stability, September 07-11, 2008, Liege, Belgium